JPE Journal of Photonics for Energy

PERSPECTIVE

Status report on emerging photovoltaics

Annick Anctil,[a] Meghan N. Beattie,[b] Christopher Case,[c] Aditya Chaudhary,[d] Benjamin D. Chrysler,[e] Michael G. Debije,[f] Stephanie Essig,[d] David K. Ferry,[g] Vivian E. Ferry,[h] Marina Freitag,[i] Isaac Gould,[j] Karin Hinzer,[b] Harald Hoppe,[k,l] Olle Inganäs,[m,n] Lethy Krishnan Jagadamma,[o] Min Hun Jee,[p] Raymond K. Kostuk,[q,r] Daniel Kirk,[c] Stephan Kube,[s] Minyoung Lim,[p] Joseph M. Luther,[t] Lorelle Mansfield,[t] Michael D. McGehee,[u,v] Duong Nguyen Minh,[t] Preeti Nain,[a] Matthew O. Reese,[t] Angèle Reinders,[w] Ifor D. W. Samuel,[x,*] Wilfried van Sark,[y] Hele Savin,[z] Ian R. Sellers,[aa] Sean E. Shaheen,[v,ab,ac,*] Zheng Tang,[ad] Fatima Toor,[ae,*] Ville Vähänissi,[z] Ella Wassweiler,[af] Emily L. Warren,[t] Vincent R. Whiteside,[ag] Han Young Woo,[p] Gang Xiong,[af] and Xitong Zhu[w]

[a]Michigan State University, Department of Civil and Environmental Engineering, East Lansing, Michigan, United States
[b]University of Ottawa, School of Electrical Engineering and Computer Science, SUNLAB, Ottawa, Ontario, Canada
[c]Oxford Photovoltaics Ltd., Kidlington, United Kingdom
[d]University of Stuttgart, Institute for Photovoltaics (IPV), Stuttgart, Germany
[e]Amazon Lab, Sunnyvale, California, United States
[f]Eindhoven University of Technology, Department of Chemical Engineering and Chemistry, Eindhoven, The Netherlands
[g]Arizona State University, School of Electrical, Computer & Energy Engineering, Tempe, Arizona, United States
[h]University of Minnesota, Department of Chemical Engineering and Materials Science, Minneapolis, Minnesota, United States
[i]Newcastle University, School of Natural and Environmental Sciences, Newcastle upon Tyne, United Kingdom
[j]University of Colorado, Department of Materials Science and Engineering, Boulder, Colorado, United States
[k]Friedrich Schiller University Jena, Laboratory of Organic and Macromolecular Chemistry (IOMC), Jena, Germany
[l]Friedrich Schiller University Jena, Center for Energy and Environmental Chemistry Jena (CEEC Jena), Jena, Germany
[m]Linköping University, Department of Biomolecular and Organic Electronics, Linköping, Sweden
[n]Linköping University, Department of Physics, Chemistry and Biology, Linköping, Sweden
[o]University of St Andrews, School of Physics and Astronomy, St Andrews, United Kingdom
[p]Korea University, Department of Chemistry, Seoul, Republic of Korea
[q]University of Arizona, Electrical and Computer Engineering Department, Tucson, Arizona, United States
[r]University of Arizona, The Wyant College of Optical Sciences, Tucson, Arizona, United States
[s]Heliatek GmbH, Dresden, Germany
[t]National Renewable Energy Laboratory, Golden, Colorado, United States
[u]University of Colorado, College of Engineering and Applied Science, Materials Science and Engineering Program, Department of Chemical and Biological Engineering, Boulder, Colorado, United States
[v]Renewable and Sustainable Energy Institute (RASEI), Boulder, Colorado, United States
[w]Eindhoven University of Technology, Energy Technology Group, Eindhoven, The Netherlands
[x]University of St Andrews, School of Physics and Astronomy, Organic Semiconductor Centre, St Andrews, United Kingdom
[y]Utrecht University, Copernicus Institute of Sustainable Development, Utrecht, The Netherlands
[z]Aalto University, Department of Electronics and Nanoengineering, Espoo, Finland
[aa]University at Buffalo, Department of Electrical Engineering, Buffalo, New York, United States
[ab]University of Colorado Boulder, Department of Electrical, Computer and Energy Engineering, Boulder, Colorado, United States
[ac]University of Colorado Boulder, Department of Physics, Boulder, Colorado, United States
[ad]Donghua University, Center for Advanced Low-dimension Materials, State Key Laboratory for Modification of Chemical Fibers and Polymer Materials, Shanghai, China
[ae]University of Iowa, Department of Electrical and Computer Engineering, Iowa City, Iowa, United States
[af]First Solar, California Technology Center, Santa Clara, California, United States
[ag]University of Oklahoma, Department of Physics and Astronomy, Norman, Oklahoma, United States

*Address all correspondence to Ifor D. W. Samuel, idws@st-andrews.ac.uk; Sean E. Shaheen, sean.shaheen@colorado.edu; Fatima Toor, fatima-toor@uiowa.edu

ABSTRACT. This report provides a snapshot of emerging photovoltaic (PV) technologies. It consists of concise contributions from experts in a wide range of fields including silicon, thin film, III-V, perovskite, organic, and dye-sensitized PVs. Strategies for exceeding the detailed balance limit and for light managing are presented, followed by a section detailing key applications and commercialization pathways. A section on sustainability then discusses the need for minimization of the environmental footprint in PV manufacturing and recycling. The report concludes with a perspective based on broad survey questions presented to the contributing authors regarding the needs and future evolution of PV.

Keywords: photovoltaics; solar cells; tandem PV; light management; detailed balance; indoor PV; agrivoltaics; sustainable manufacturing; recycling

1 Introduction

The field of photovoltaic (PV) solar power generation has grown to become a significant component of the global energy landscape, with ∼4.5% of the world's electricity being generated and ∼240 GW of new installations in 2022.[1,2] However, further acceleration of PV and other renewable energy sources is urgently required to mitigate the impacts of global greenhouse gas emissions. A recent analysis has concluded that PV needs to grow at ∼25% annually with a target of 75 TW of global installations by 2050, a ∼75x increase from current installed capacity.[3] While the existing PV landscape is largely dominated by silicon (crystalline and polycrystalline) and CdTe, achieving these long-term goals can be greatly aided by the development of new materials, device concepts, and light management strategies that enable higher efficiencies and more scalable and sustainable manufacturing.

This article is intended to provide a snapshot of the current status of emerging PV approaches that show potential in helping to achieve the above goals. It is intended to be a convenient resource for people within and outside the field, including new researchers, students, technology managers, and program managers, who can play a role in accelerating the global effort. The article is structured in sections covering silicon (Sec. 2), thin film (Sec. 3), III-V (Sec. 4), perovskite (Sec. 5), organic (Sec. 6), and dye-sensitized solar cells (Sec. 7). Each section provides background, a technology status update, and challenges towards commercialization/scalability. Subsequent sections provide an overview of the applications and commercialization of emerging PV (Sec. 8), strategies for exceeding the detailed balance limit (Sec. 9), and concepts in light management (Sec. 10). A final section describes sustainability and environmental impact issues that apply to all the above technologies (Sec. 11). The article concludes with a perspectives section (Sec. 12) that first discusses common themes that appear throughout the article, and then also presents and draws conclusions from a survey of emerging PV, which was completed anonymously by contributing authors.

2 Silicon Photovoltaics

2.1 Bifacial Silicon PV

Section Author: Fatima Toor (University of Iowa)

In recent years, bifacial silicon (Si) photovoltaics (PV) technology has been growing in commercial PV systems because it results in higher performance yield and lower levelized cost of energy (LCOE) compared with conventional monofacial PV technology.[4] Figure 1 illustrates the difference between monofacial and bifacial solar cell architectures. While traditional monofacial Si cells have an aluminum (Al)-based back surface field (BSF) that covers the entire backside of the cell precluding any light absorption on the backside, bifacial Si cells have point contacts that allow for backside light collection and absorption in the cells.

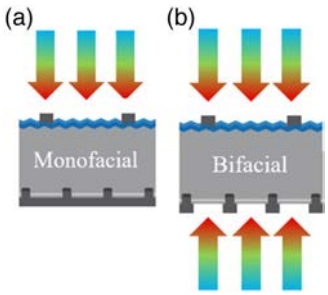

Fig. 1 Schematic of (a) monofacial and (b) bifacial solar cells.

The latest International Technology Roadmap for Photovoltaic (ITRPV) report[5] suggests that Al BSF cell concept is expected to be phased out within 2023. The report predicts that mature concepts of diffused and passivated pn junction Si solar cells will be further used in the mainstream commercial PV panels with different rear side passivation technologies, such as passivated emitter and rear cell (PERC),[6] passivated emitter, rear locally-diffused (PERL),[7] passivated emitter, rear totally diffused (PERT),[8] and tunnel oxide passivated contact (TOPCon).[9] The ITRPV report suggests that in 2022 the market share of PERC p-type mono-Si was 80%, however the share of p-type mono-Si PERC will decrease to about 10% within the next ten years since upcoming, promising new cell technologies are using n-type material. TOPCon on n-material, using tunnel oxide passivation stacks at the rear side, will gain market share from about 10% in 2022 up to 60% within the next ten years. Based on our analysis, TOPCon on n-type is expected to become the dominant cell concept after 2025.

All these cell architectures (PERC/PERL/PERT/TOPCon) support bifacial PV cell and module architecture. Therefore, not surprisingly, given the trends in advanced Si solar cell architectures, the ITRPV report predicts that by 2033, bifacial cells will make up 90% of the Si PV installations. Another notable trend presented in the ITRPV report is that, while in 2023, about 65% of modules are monofacial modules, the share of bifacial modules will grow to about 70% within the next years as shown in Fig. 2. This is because bifacial Si solar cells can be used in bifacial modules as well as in conventional, monofacial modules.

The bifacial PV project supported by the US Department of Energy (DOE)[10] performed and published extensive optical modeling based on RADIANCE[11] to determine the performance gains of bifacial modules installed at various tilt angles, with different row spacing, and ground

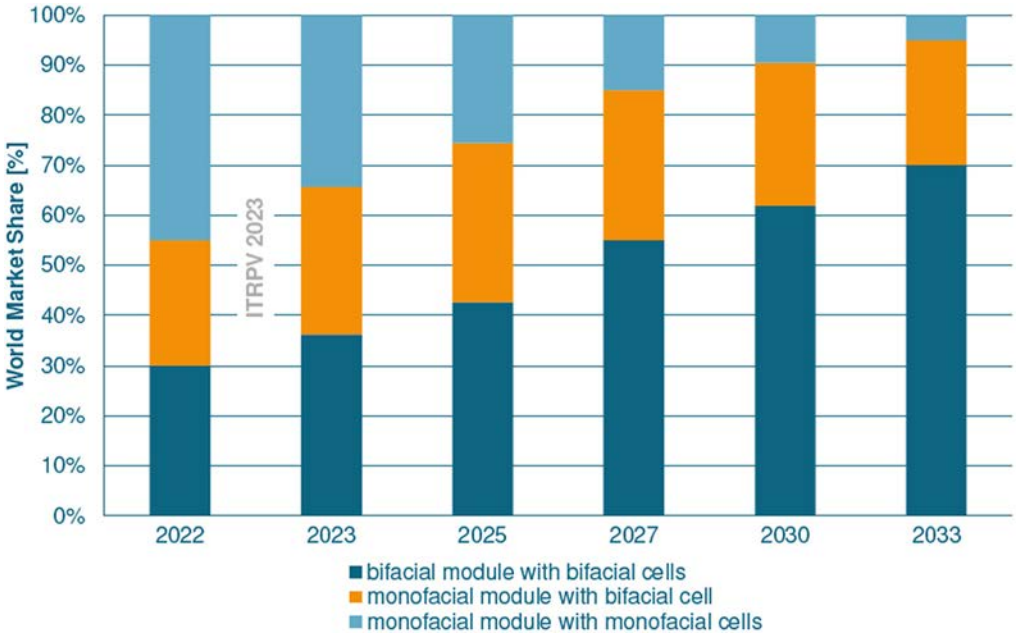

Fig. 2 ITRPV 2022-2033 predicted trends for monofacial and bifacial modules with bifacial Si solar cells.

albedo.[12–20] The team showed the effect of installation parameters on bifacial gain in energy (BGE) defined as: BGE $= (E_b/E_m) - 1$, where E_b and E_m are the energy yield of the bifacial and monofacial module, respectively. This value shows the energy gain in using bifacial PV system over the equivalent monofacial system (with the same installation parameters). The study's results indicate that bifacial PV arrays generate lower energy than expected due to horizon blocking and large shadowing area cast by the modules on the ground. For albedo of 21%, the center module in a large array generates up to 7% less energy than a single bifacial module – this single bifacial module is typically utilized for lab certification of BGE of bifacial modules. The team also proposed draft recommendations for IEC 60904 to include bifacial PV module testing so that bifacial PV gain measurements can be standardized.[21] The standard has since been formalized and adopted by the international community as IEC TS 60904-1-2:2019. As of 2023, the standard has gone through a further revision with added modifications for dual-simulator measurements to be re-published by the end of the year.

2.2 Black Silicon

Section Authors: Ville Vähänissi (Aalto University) and Hele Savin (Aalto University)

Nanostructured silicon, often called black silicon due to its dark appearance, eliminates surface reflectance over a wide wavelength range [Fig. 3(a)] due to gradual change in refractive index[23–25] and increases the absorption of long wavelengths due to extended optical path.[26–29] Therefore, black silicon is a promising alternative to minimize optical losses in PV applications. However, due to the rough nanoscale morphology, electrical passivation of such surfaces has been considered challenging. In 2012 this problem was tackled with atomic layer deposited Al_2O_3 that provides a conformal coating [Fig. 3(b)] combined with a high-quality interface with silicon.[30,31] Indeed, it was demonstrated that surface passivation was equally good in black silicon as in the planar counterparts.[32,33] The successful surface passivation of black silicon was also proven later in actual solar cells (IBC) resulting in an external quantum efficiency (EQE) close to unity in a broad wavelength range (300 nm-1000 nm) and a conversion efficiency well above 20%.[34]

In PERC and TOPCON cells (or any front contact cell type) emitter formation brings an additional challenge as it needs to be made on the nanostructured surface. The dopant profile is difficult to control via a conventional diffusion process. Consequently, dopant diffusion on enhanced surface areas often results in too heavy Auger and SRH recombination inside the nanostructures.[35–42] This problem has recently been overcome via a more controlled doping method, i.e. using ion-implantation, which has resulted in emitter saturation currents less than 20 fA/cm^2 [43] combined with EQEs even above 100% in UV.[44]

While the original motivation to use black silicon in PV has been the improved optics, other benefits have been discovered later on. Firstly, the nanotexturing does not seem to have any substrate crystallinity related limitations,[33] e.g., it works well also for the diamond-wire cut multicrystalline wafers that are difficult to texturize with conventional acidic solutions. This benefit is valid for all commonly known black silicon fabrication methods, i.e., dry etching,[45–47] metal

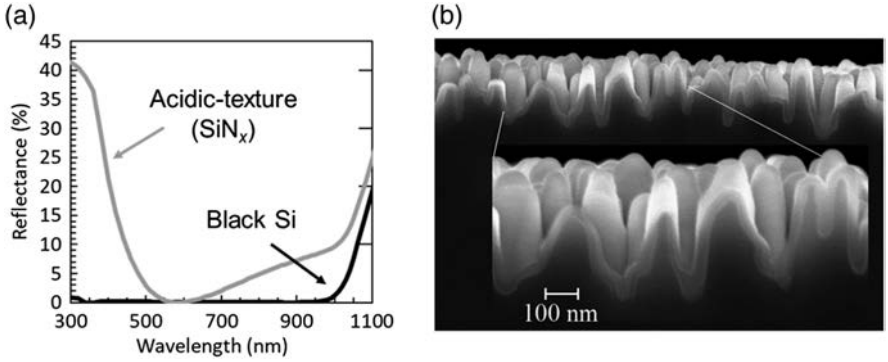

Fig. 3 (a) Reflectance of black silicon and acidic-textured silicon with SiN_x ARC as a function of wavelength.[22] (b) Scanning electron microscope image of black silicon surface coated with a 50 nm atomic layer deposited Al_2O_3 surface passivation layer using Beneq TFS-500 system.

Fig. 4 Dry-etched black silicon IBC solar panel without any antireflection coating fabricated in Naps Solar Systems, Finland. The energy conversion efficiency of 18.1% and 19.9% of the whole IBC module and the best individual cell of the module, respectively, demonstrate that fragile nanostructures can withstand standard module fabrication steps.[65]

assisted chemical etching,[48–55] and laser processing.[56–61] Another benefit is related to metal impurity gettering, i.e., black silicon has been shown to have a higher gettering efficiency for iron as compared to planar surfaces.[62] The same phenomenon is expected to take place for other mobile impurities as well. Quite surprisingly, black Si can also reduce the harmful light-induced degradation although the exact mechanism is still under debate.[63,64]

While the aforementioned fundamental limitations regarding integration of black silicon into solar cells have been overcome in the laboratory environment, industrial viability raises other challenges. These include possibly harsh handling of the nanostructured surfaces in the production line, potential contact resistance issues when using nonconformal screen printing, as well as preserving excellent optics during module encapsulation. There are preliminary results showing that all these issues can be tackled efficiently in industrial production (Fig. 4).[22] However, more extensive cost and lifecycle analysis would be required for black silicon to become the mainstream technology in PV. Fortunately, there are pioneers in the field who are already mass-producing black silicon solar cells. At the moment, metal assisted chemical etching seems to be the most viable fabrication method for the commercial cells as it requires fewer changes to the existing manufacturing lines.

3 Thin Film PV

3.1 $Cu(In,Ga)Se_2$ PV: Fundamentals and Efficiency Limits

Section Author: Lorelle Mansfield (National Renewable Energy Laboratory)

$Cu(In, Ga)Se_2$ (CIGS) solar cells have the highest record efficiency among commercialized thin-film PV technologies at 23.6%.[66] CIGS has the benefits of thin films,[67] such as low materials costs, low embodied carbon, and varied form factors. The substrate design of most cells (Fig. 5) allows fabrication on flexible plastics and metal foils, which leads to a multitude of potential applications. It is suitable for architectural solar, military deployment, space power, and consumer applications. Flexible substrates also allow for roll-to-roll fabrication enabling rapid manufacturing of high-efficiency devices.

CIGS technology has experienced several technological advances in recent history. One of the most impactful has been post-deposition treatments (PDT) with alkali metal fluorides, such as potassium fluoride (KF), rubidium fluoride (RbF), and cesium fluoride (CsF) which have significantly improved open-circuit voltage (V_{OC}) and efficiency of devices, even those fabricated at lower temperatures. Lower temperature processing can be further enhanced through alloying CIGS with small amounts of silver (Ag), which also results in smoother surfaces, improved crystallinity, and increased carrier concentrations. Traditionally, chemical-bath deposited cadmium sulfide (CdS) was used as a buffer layer, whereas now zinc oxysulfide (Zn(O,S)) and other more transparent and more manufacturable (e.g. sputtered) layers are being employed. Research directions being explored include CIGS for tandem solar cells. Bandgap variations are key to efficient tandems, and the CIGS-based material system can be tuned from 1 eV to around 2.5 eV by alloying in the form of $(Ag, Cu)(In, Ga)(Se, S)_2$ (Fig. 6). Existing high-efficiency low-

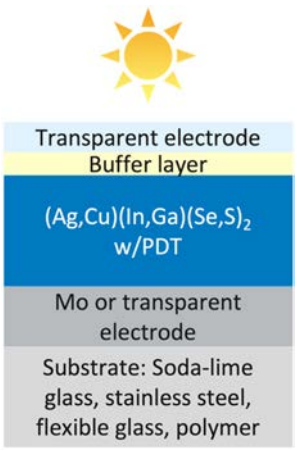

Fig. 5 Cross-section of a typical CIGS-based device.

Ag	Cu	In	Ga	Se	S	Ternary	Bandgap
	X	X		X		$CuInSe_2$	1.00
X		X		X		$AgInSe_2$	1.24
	X	X			X	$CuInS_2$	1.54
	X		X	X		$CuGaSe_2$	1.68
X			X	X		$AgGaSe_2$	1.84
X		X			X	$AgInS_2$	1.98
	X		X		X	$CuGaS_2$	2.43
X			X		X	$AgGaS_2$	2.51

Fig. 6 $(Ag, Cu)(In, Ga)(Se, S)_2$ material system with bandgaps of ternary compounds.

bandgap CIGS cells are excellent bottom cells for perovskite and CdTe top cells, and improved wide-bandgap CIGS top cells could even be paired with Si bottom cells.

Although CIGS-based PV are efficient and stable, several challenges have delayed their ubiquitous adoption. As could be expected, initial CIGS installations were not as robust as subsequent generations, which led to an incorrect assumption that CIGS products were inherently inferior solar cells. Unfortunately, some potential investors still hold those views, and CIGS research and development funding has decreased compared to other thin-film technologies, particularly in the US. To date, CIGS technology has suffered from a greater gap in efficiency between record cells (23.6%) and record modules (19.2%) than other commercialized PV technologies. Closing this gap could be accomplished through using wider bandgap absorbers, designing new ways to assemble cells into modules, and developing better transparent conductive contacts.[68] Unlike silicon technology, CIGS has yet to experience the full benefit of economies of scale. With the complexity of processing required to fabricate the absorber material, most companies have proprietary manufacturing equipment. That relegates the technology to smaller markets where premium prices are accepted for products with specific requirements such as flexibility and high specific power. Lower-cost processing methods and equipment designs have the potential to revolutionize the industry and bring CIGS to multi-GW scale.

3.2 CdTe PV: Fundamentals and Efficiency Limits

Section Author: Matthew O. Reese (National Renewable Energy Laboratory)

CdTe is the most scaled thin-film PV technology. This is enabled by low material costs, high-throughput deposition, robust process space, low degradation, and low embodied energy. While CdTe is directly competing at utility-scale with Si, it has done so with relatively low

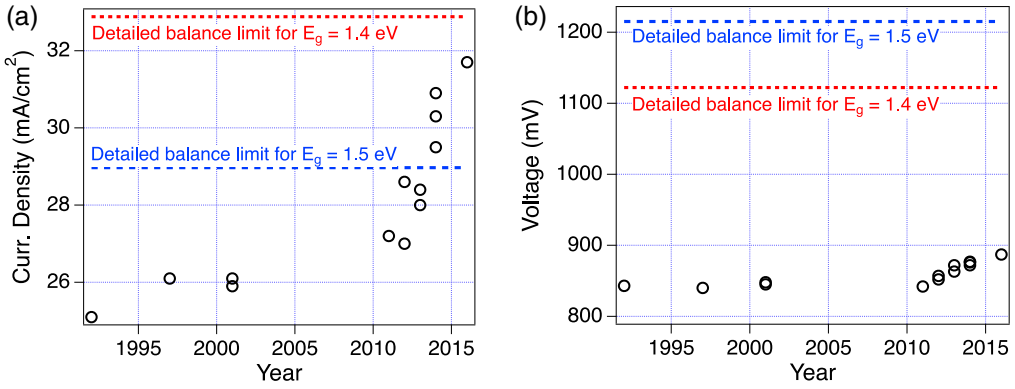

Fig. 7 (a) CdTe PV certified record cell current densities and (b) open-circuit voltages, relative to the detailed balance limit for the bandgap of CdTe (1.5 eV) and a bandgap of 1.4 eV, which is typical of Se-alloyed material. Data from the semi-annual publication up to Version 61 of "Solar cell efficiency tables" (Ref. 70).

demonstrated cell record efficiency, having only achieved ~2/3 of its detailed balance limit. The current collection has been well-engineered, such that it is near the theoretical limit. Further monofacial improvements will largely stem from advances enabling improved photovoltage.

CdTe devices have eliminated the parasitically-absorbing CdS emitter with a deleterious "cliff" in its band conduction band offset (CBO), replacing it with a wider bandgap oxide, such as the tunable $Mg_xZn_{1-x}O$ enabling a small "spike" in CBO with reduced recombination.[69] Furthermore, the absorber transitioned from the congruently-sublimating, binary CdTe absorber to a graded ternary Cd(Se,Te). This has changed the effective device bandgap from 1.5 eV in pure CdTe (which is present now at the back) to ~1.4 eV at the front. This increases the theoretical and effective current density in devices [Fig. 7(a)], while raising the overall theoretical efficiency limit by ~1% absolute. These changes have dramatically improved achievable minority carrier lifetimes from a few ns to >100 ns.[71,72] Due to this increase in lifetime, device photovoltage has seen a modest increase even though the bandgap has decreased ~100 mV [Fig. 7(b)].

While CdTe has demonstrated scalability and low cost, it must demonstrate continued efficiency improvement. Over the past several years, work has revolved around changing the defect (doping) chemistry to achieve this. Initial demonstrations with single crystals demonstrated an improvement in stable carrier concentration of ~100x using a group V (GrV) dopant to replace traditional Cu to explicitly improve V_{OC}.[73] While GrV dopants have improved stability over Cu due to much lower diffusion and a reduction in complexing with Cl,[74,75] much improved V_{OC} and efficiency over Cu-doped polycrystalline thin-film devices have yet to be realized. This is for a few reasons. First, the large increase in absorber carrier concentration collapses the space charge region, making devices more sensitive to front interface recombination.[76] Second, long lifetime from Se incorporation makes devices more sensitive to back interface recombination. Third, GrV-doped polycrystalline absorbers, while capable of high carrier concentration, have low activation, leading to significant losses from voltage fluctuations.[77] Increasing V_{OC} requires simultaneous improvements on multiple fronts. However, in less than eight years, insight from single crystals is influencing GW-scale decisions. GrV-doped CdTe PV promises increased energy yield due to its increased stability over its Cu-doped predecessor, with demonstrated similar initial efficiencies that are poised to increase over the next few years as these challenges are overcome.

3.3 CdTe PV: Commercial Perspective

Section Authors: Ella Wassweiler (First Solar) and Gang Xiong (First Solar)

CdTe is the most commercially successful thin film PV technology. In 2022, CdTe module production capacity has exceeded 9 GW annually and is expected to reach 21 GW by 2025. At the start of 2023, First Solar, the largest CdTe solar module manufacturer, reached a milestone of

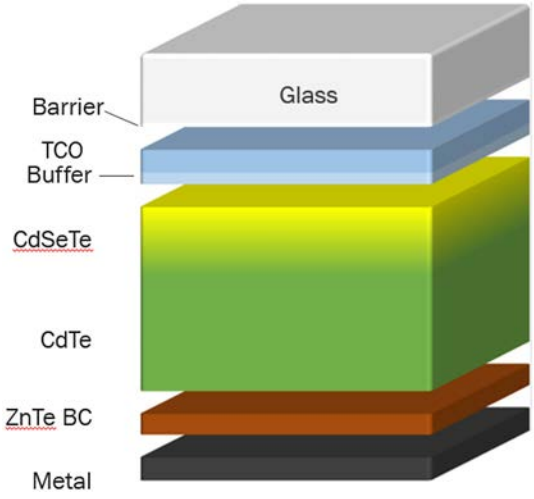

Fig. 8 State-of-art CdTe solar cell structure.

50GW accumulated production. Thin film CdTe manufacturing has an inherently better cost structure compared to Si. In addition, CdTe has an energy yield advantage due to its lower temperature coefficient, better spectra response, and slower long term degradation rate. These advantages allow CdTe to compete with Si in utility-scale markets. Roughly 40% of the US utility-scale PV market was served by CdTe in 2019.

Currently the record CdTe solar cell efficiency is 22.3%.[78] Module efficiency has exceeded 19%. The state-of-art CdTe solar cell structure is outlined in Fig. 8. The absorber typically consists of a graded $CdSe_xTe_{1-x}$ alloy. A buffer layer such as $Zn_{1-x}Mg_xO$ can be inserted between the transparent conducting oxide (TCO) and absorber. With a small positive conduction band offset between $Zn_{1-x}Mg_xO$ and absorber, carrier recombination at the front interface can be suppressed. ZnTe is a good back contact to CdTe with relatively low barrier height (~0.2 eV).[79]

The absorber is typically p-type, traditionally doped by Cu with carrier concentration between 10^{14} and 10^{15} cm^{-3}. Increasing carrier concentration is a major pathway to further boost CdTe solar cell efficiency.

Carrier concentrations greater than 10^{16} cm^{-3} have been demonstrated with group-V dopants such as As or P. For example, 22% As-doped CdTe devices have been reported.[80] Compared to Cu-doped devices, As doping has additional energy yield advantages including even lower long-term degradation rate and lower temperature coefficients.[81] The paradigm shift from Cu to As-doping, provided a new platform and opportunities to further improve CdTe solar cell performance. In order to do so, it is suggested that the reduction of non-radiative recombination in the device stack, as well as reduction of potential fluctuation in the absorber are of critical importance.[77,80]

First Solar's Series 7 module is 2.8 m^2 in size and has total area efficiency of up to 19.3%. CdTe modules are fabricated using a fully integrated inline process, with glass-in and module-out within 4 hours. Compared to Si, CdTe solar module has lower energy payback time and lower environmental footprint.

Improving module efficiency is the most effective way to reduce the cost per watt for manufacturing and levelized cost of electricity of a PV system. Bifacial CdTe solar cells have also been demonstrated.[82] There is great synergy between cell efficiency and bifaciality improvement, as both require further reduction of back contact recombination loss. With less back contact recombination, absorber thickness can also be effectively reduced.

4 III-V Tandem PV

4.1 III-V Tandem PV

Section Authors: Meghan N. Beattie (University of Ottawa) and Karin Hinzer (University of Ottawa)

Bandgap engineering of III-V materials and vertical integration of multiple subcells in tandem devices has resulted in the highest efficiency PV. III-V semiconductors have high absorption, and many compositions have direct bandgaps. Multiple pn junction subcells absorb a larger portion of the solar spectrum and reduce thermalization losses compared to single junction devices. The higher energy photons from the solar spectrum are absorbed by the largest bandgap subcells at the top of the tandem stack, while the lower energy photons are transmitted through the top subcells to be absorbed by the smaller bandgap subcells below. Figure 9 displays common approaches.

The standard approach uses lattice-matched materials for the entire device, minimizing dislocations in the crystal lattice. Lattice-matched subcells are interconnected using transparent tunnel diodes [Fig. 9(a)]. In this series-connected configuration, the device current is limited by the smallest subcell current. The current generated in each subcell is maximized by tuning layer thicknesses and bandgaps so that each subcell absorbs the same amount of light. The lattice-matching requirement leads to the use of a variety of materials from Ge for the bottom subcell to ternary and quaternary III-V alloys or nanostructures[83,84] for upper layers.

With limited semiconductor substrates to choose from, the lattice-matched approach has a limited material design space, which caps the efficiency. Several advanced strategies have been developed to overcome the lattice-matching constraint, enabling the development of all-III-V and III-V hybrid tandems. One such approach is wafer bonding, wherein subcells are grown on different substrates and directly bonded without an intermediate layer[85–87] [Fig. 9(b)]. A four-junction GaInP/GaInAs//GaInAsP/GaInAs wafer bonded device demonstrated the highest recorded solar cell efficiency to date: 47.6% under an irradiance of 665 suns.[70,86]

Another approach uses a graded metamorphic buffer to increment the lattice constant from that of the substrate to that of the subcell material[84,88–90] [Fig. 9(c)]. Excellent crystal quality can be achieved for III-V semiconductors grown on metamorphic buffer layers. An example is this six-junction AlGaInP/AlGaAs/GaAs/GaInAs(3) inverted metamorphic cell with a peak efficiency of 47.1% under 143 suns.[89,91]

A third technique to overcome lattice-matching involves mechanical stacking of fabricated subcells grown on different substrates using a transparent adhesive to join the upper and lower subcells[92–94] [Fig. 9(d)]. This technique allows for electrical configurations with two, three, or four terminals, overcoming current-matching constraints. This approach was used to fabricate a four terminal, three-junction mechanically stacked GaInP/GaAs//Si device having 35.9% efficiency under 1-sun illumination.[94,95]

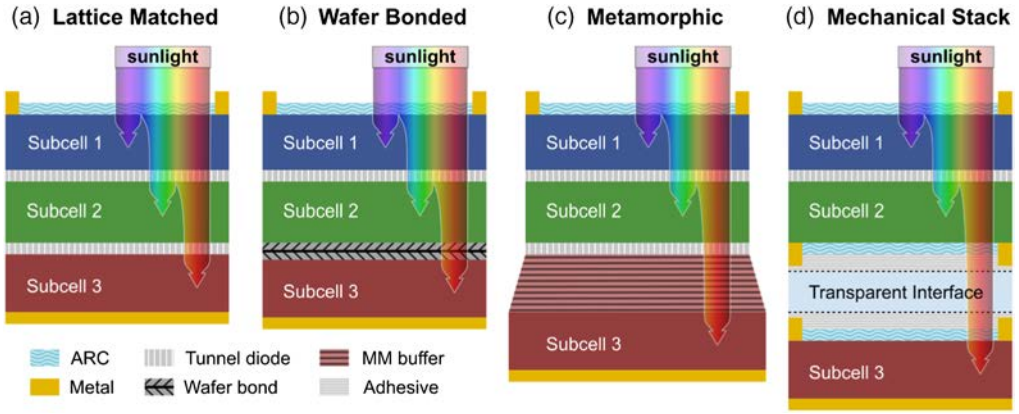

Fig. 9 Schematic showing four different design architectures for III-V tandem solar cells. ARC, antireflection coating; MM, metamorphic.

Table 1 Selected III-V tandem cells and efficiencies from solar cell efficiency tables (version 63).[70]

Design	Efficiency (%)	Intensity (suns)	Category	Group(s)
2J GaAsP/Si	23.4	1	MM, Si	OSU/UNSW/SolAero[88]
3J GaInP/GaAs/Si	25.9	1	MM, Si	Fraunhofer ISE[101]
3J GaInP/AlGaAs/CIGS	28.1	1	MS, CIGS	AIST/Fraunhofer ISE[93]
2J GaInP/GaAs	32.8	1	LM	LG Electronics[102]
2J GaAs//Si (4-terminal)	32.8	1	MS	NREL/CSEM/EPFL[102]
2J GaInP/mqw-GaAs	32.9	1	mqw	NREL/UNSW[103]
3J GaInP/GaAs//Si	35.9	1	MS, Si	NREL/CSEM/EPFL[94]
3J GaInP/GaInAsP//Si	36.1	1	WB, Si	Fraunhofer ISE/AMOLF[85]
3J GaInP/GaAs/GaInAs (ELO)	37.8	1	MM, ELO	Microlink[104]
6J AlGaInP/AlGaAs/GaAs/GaInAs(3)	39.2	1	MM	NREL[89]
3J GaInP/mqw-GaAs/GaInAs	39.5	1	MM, mqw	NREL[84]
2J GaInAsP/GaInAs	35.5	38	MM	NREL[102]
3J GaInP/GaAs/GaInAs	44.4	302	MM	Sharp[105]
4J GaInP/GaAs/GaInAs/GaInAs	45.7	234	MM	NREL[106]
6J AlGaInP/AlGaAs/GaAs/GaInAs(3)	47.1	143	MM	NREL[89]
4J GaInP/GaInAs//GaInAsP/GaInAs	47.6	665	WB	Fraunhofer ISE[86]

LM, lattice-matched; WB, wafer-bonded; MM, metamorphic; MS, mechanical stack; Si, III-V/silicon tandem; CIGS, III-V/CIGS tandem; mqw, multiquantum well; ELO, epitaxial lift-off.

These architectures can be combined with subcell segmentation to further enhance efficiencies.[96] This design technique enables near-perfect current-matching using non-ideal absorber bandgaps by dividing each subcell into semitransparent pn junction segments. It is used in vertically segmented III-V photonic power converters (PPCs) that convert monochromatic laser light to electricity. Multijunction III-V PPCs with up to 30 absorbing segments have been demonstrated with efficiencies up to 66%.[97–100]

Due to their highest efficiencies, long-lifetimes, radiation hardness, and low resistances, III-V multijunction PV power satellites, unmanned vehicles and concentrated solar systems. Table 1 lists selected III-V tandem cells of note with corresponding efficiencies from Green et al.[70]

4.2 III-V/Si Tandem Junction Solar Cells

Section Authors: Stephanie Essig (ipv, University of Stuttgart) and Emily L. Warren (National Renewable Energy Laboratory)

Research and development of III-V/Si tandem solar cells is motivated by the efficiency enhancement achievable with multijunction architectures and the low cost and current market dominance of Si. Theoretically, the detailed balance efficiency of Si-based two (2J) and three-junction (3J) solar cells reaches 45% and almost 50%, respectively.[107] From a detailed balance perspective, the ideal III-V top cell material for a Si-based 2J device is GaInP with a bandgap of 1.8 eV and record 1-sun single-junction efficiency of 22.0%.[70] Fabrication of III-V solar cells is based on epitaxy, yet the direct growth of III-Vs with suitable bandgap energies on Si is challenging due to a mismatch in lattice constant and thermal expansion.[108] Therefore, high threading dislocation densities occur, causing significant non-radiative recombination losses in the top cell, which limit the

tandem cell performance.[90] To overcome this difficulty, alternative manufacturing methods, including mechanical stacking[109–112] and wafer-bonding,[85,113,114] of the III-V and Si cells, have been investigated.

The efficiency of monolithic III-V/Si dual-junction solar cells fabricated by metal organic vapor phase epitaxy (MOCVD) or molecular beam epitaxy (MBE) on Si has so far been limited to 25.0%.[115] This record device comprises a 1.7 eV wide-bandgap GaAsP top cell on a graded GaAsP buffer, that effectively reduces the dislocation density. In comparison, 3J cells realized by direct epitaxy on Si have reached higher efficiencies up to 25.9%,[101] but have not surpassed the record values for Si single-junction devices. Other possible ways to reduce the dislocation density and cost of polished surfaces include use of nanopatterned substrates, and dislocation filtering approaches such as strained superlattices and thermal cycle annealing.[116–118]

In contrast, mechanically stacked and wafer-bonded III-V/Si tandems push the efficiency of Si-based PV beyond 30%. Their few-μm thick III-V top cells are grown lattice-matched on GaAs parent wafers and transferred to independently fabricated Si bottom cells. Hence, both the Si and III-V cells are manufactured using the optimum processes. Subsequent integration by wafer-bonding requires extremely clean, mirror-polished surfaces to allow atomic bond formation across the heterogeneous semiconductor interface.[119] Improved current-matching of the subcells has recently raised the record efficiency of wafer-bonded GaInP/GaInAsP/Si 3J solar cells to 35.9%.[85] The comparably easier integration by mechanical stacking involves typically an adhesive or glue between the III-V and Si cell that can level out interface irregularities. When applying front and rear contacts on each subcell, the tandem device can also be operated in 4-Terminal (4T) configuration. Compared to the commonly used 2-Terminal configuration, 4T offer the advantage that top and bottom cells are operated independently. Hence no current-matching is needed, a wider range of top cell bandgap energies can be used, and the energy output depends less on the temperature and solar spectrum.[120] Mechanically stacked 4T devices reached record efficiencies of 32.8% for 2J (GaAs/Si; see Fig. 10) and 35.9% for 3J (GaInP/GaAs/Si) using both-sides contacted Si heterojuction cells.[94] Similar 3J efficiency of 35.4% was achieved when using a rear-contacted Si bottom cell.[121] Devices have also been stacked using transparent conductive adhesives or metal nanoparticles, often with the goal of forming 3T tandems, and these devices have reached efficiencies of 27.3%[7] (2J,TCA) and 30.8%[122] (3J, Pd nanoparticles).

Despite the high efficiencies and good scalability of III-V/Si multijunction solar cells, they will only be successful if their costs on a US$/Watt level will approach those of commercial Si single-junction technology.[92] Main cost drivers are the MOCVD deposition of the III-V top cell, and the III-V growth substrate.[123] Therefore, extensive research on cost reduction strategies like the use of hydride vapor phase epitaxy (HVPE)[123] instead of MOCVD and advanced lift-off[124] and substrate reuse[125] approaches are needed.[126]

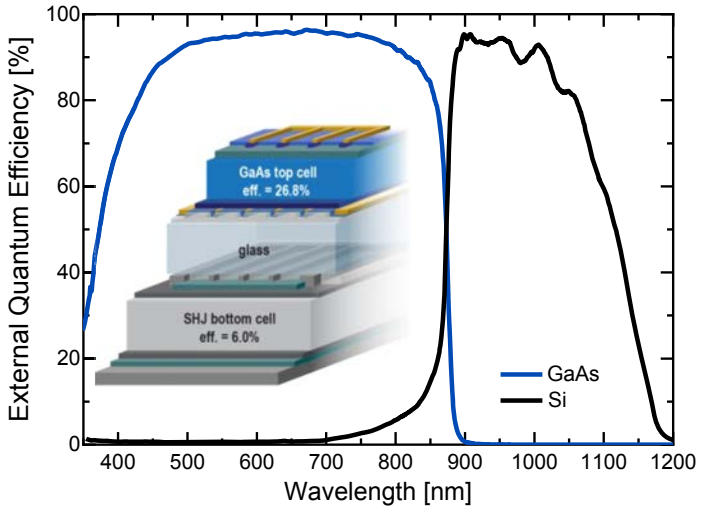

Fig. 10 External Quantum Efficiency and sketch of a 4T GaAs/Si tandem solar cell with 32.8% efficiency.[94]

5 Perovskite PV and Tandems

5.1 Stability of Perovskite Solar Panels with Partial Shading

Section Authors: Isaac Gould (University of Colorado Boulder) and Michael D. McGehee (University of Colorado Boulder and RASEI)

In a solar panel, partial shading prevents only some of the cells from generating photocurrent. Since all cells must pass the same amount of current for the panel to generate power and the cells are in series with each other, the cells that are illuminated put the shaded cells into whatever reverse bias is needed for current matching to occur. Several research groups have tested perovskite cells in reverse bias and observed both short-term reversible and irreversible degradation problems.[127–131]

Several interesting observations have been made on the reverse bias behavior of perovskite solar cells. When metal electrodes are used the current typically increases very suddenly and localized heating is observed with thermal imaging.[127,132] This behavior is attributed to the formation of a shunt caused by the metal penetrating through the perovskite. The extreme heating at the shunt causes permanent damage to most layers of the cell. In contrast, this behavior is not seen when transparent conducting oxides and carbon electrodes are used. In these cells there is an exponential increase in current that starts typically between -2 V and -6 V when sweeping the voltage to increasing negative voltages.[127–131] This current is enabled by tunneling of holes from the electron transport layer due to strong band bending associated with mobile ions redistributing to screen the applied field. After passing current through a cell in reverse bias for as little as one minute, the efficiency can be reduced by more than 50 %.[129,133] Much, but not all, of this efficiency recovers if the cell is exposed to one sun at a positive voltage for approximately 30 minutes.[129,133,134] The rapid degradation most likely occurs because holes oxidize iodide on the octahedral corners to form smaller neutral iodine species that can move to interstitial sites, creating a vacancy in the process.[135,136] With few electrons being present in reverse bias, the reverse reaction is slow. The iodine interstitials act as recombination centers, which dramatically reduces the efficiency of the cell. During the recovery process at positive voltage, the iodine interstitials are reduced and return to the octahedral corners. The recovery only occurs, however, if the iodine species stay in the perovskite film.[129,137,138] For this reason, internal barriers that confine the iodine to the perovskite are critically important.

There has been some progress towards improving reverse bias stability by using carbon electrodes.

If strategies for preventing degradation in reverse bias are not found, then engineering solutions for preventing degradation due to partial shading will be needed. Wolf *et al*. have analyzed different panel designs and suggested that perovskite-silicon tandems can more readily be protected with bypass diodes because the high breakdown strength of silicon enables many tandems to be protected with one bypass diode.[139] It is not clear how the current could be routed from the electrodes in a monolithically integrated panel (made with scribes) to a bypass diode on the side. The voltage drop would be quite large if current had to travel the length of a panel through a transparent conducting oxide. In contrast, it is easy to run current from silicon or perovskite-silicon tandem cells with metal ribbon to bypass diodes, which are typically incorporated into the junction box.

It is likely that bypass diodes can be used to protect perovskite-silicon tandems. Research will be needed to find ways to protect other types of perovskite solar cells to prevent degradation due to partial shading.

5.2 Perovskite/Silicon Tandem Solar Cells

Section Authors: Aditya Chaudhary (ipv, University of Stuttgart) and Stephanie Essig (ipv, University of Stuttgart)

Since crystalline silicon (c-Si) solar cells approach their theoretical efficiency limit, there is an increasing interest in c-Si-based tandem PV. Stacking a wider bandgap metal-halide perovskite (ABX_3) cell onto a c-Si cell offers the potential to reach conversion efficiency over 30%, and to reduce levelized costs of electricity.[140,141] There are three architectures (Fig. 11) in which a tandem cell can be realized, i.e., 2-terminal (2T), 3-terminal (3T) and 4-terminal (4T). All these architectures

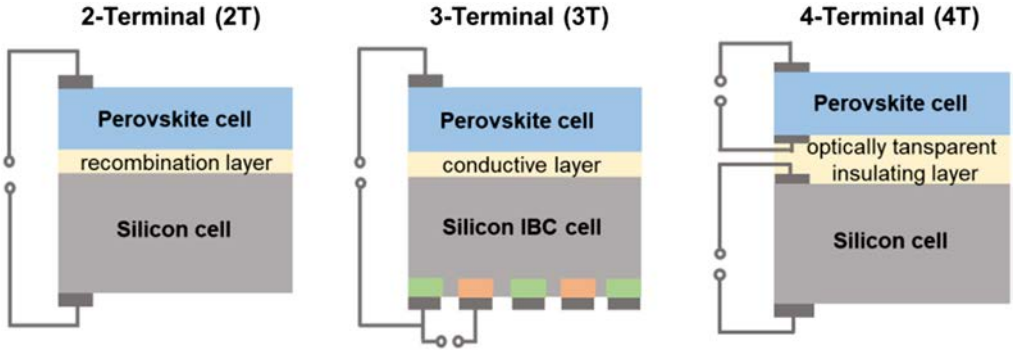

Fig. 11 Comparison of perovskite/c-Si tandem solar cells with 2-,3- and 4-terminal configuration.

have their own advantages as well as limitations. Owing to the easy industrial realization and lower requirements on the balance of system, 2T architecture is touted to be the most promising.[142]

The first results of 2T perovskite/c-Si tandem cells, in which the top and bottom cells are connected in series, were published in 2015.[143] From then on research has focused on the optimum device architecture, stability improvement and the defect-free large-area deposition of the top perovskite cell on c-Si.[144–146]

To reach efficiencies over 30% with 2T tandem cells for operation temperatures between 20 and 100°C, a perovskite top cell with bandgap energy in the range of 1.65-1.73 eV is needed,[147] which can be realized by varying the ABX_3 composition.[148] Furthermore, maximum energy yield requires that the perovskite cell coats the textured c-Si bottom cell conformally[149,150] which poses a challenge for solution-based deposition methods of the perovskite layers. In recent time, strategies have been developed to circumvent this issue, such as reducing the c-Si cell pyramid size or using innovative surface textures, increasing the thickness of perovskite film or application of self-assembled monolayers (SAM).[151–153]

Recently, record efficiencies of 33.7% and 33.9% were reported for 2T perovskite/c-Si tandem cells by a group from KAUST, Saudi Arabia, and LONGi, China, respectively.[154] For the 4T architecture, a record tandem cell efficiency of 30.3% was demonstrated in early 2023 by the group from The Australian National University.[155] In contrast to the monolithic 2T devices, the top and bottom cells of 4T tandems are manufactured separately and then mechanically stacked.[150] This decouples the cells electrically, and hence there is no need for current matching of the sub-cells. Efficiencies of 3T tandem cells are still below 20%, nevertheless this architecture has great potential as the third contact allows the excess photo current of a subcell to be used, which would be lost in a 2T configuration.[156,157]

Current world records for perovskite/c-Si tandem cells have been achieved with small cell areas ($\leq$4 cm^2), almost a factor of 50 less than commercial c-Si solar cells. Upscaling to an area as large as c-Si cells without losses in efficiency is the foremost challenge. Current research suggests that the most scalable production techniques for the perovskite cells are CVD and solution-based methods, such as slot-die coating, blade coating, inkjet printing and screen printing.[158–160]

Apart from upscaling, degradation of the perovskite top cells[161] is considered the major obstacle to commercialization of perovskite/c-Si tandem cells. To be competitive with the established c-Si single-junction modules, stable operation for a minimum of 20-25 years is needed. Yet, a recent study by a group from KAUST showed, that employing 2D/3D perovskite heterojunctions significantly improves the damp heat-stability and allows to pass industrial test protocols for PV modules.[162]

5.3 Perovskite Silicon Tandem Cells and Modules

Section Authors: Daniel Kirk (Oxford Photovoltaics Ltd.) and Christopher Case (Oxford Photovoltaics Ltd.)

Mainstream solar cell technology (or technologies) has developed rapidly in terms of efficiency[163] concomitant with a huge increase in scale; global PV installations in 2022 were above 250GW and year-on-year growth is expected for decades to come. However, the giant

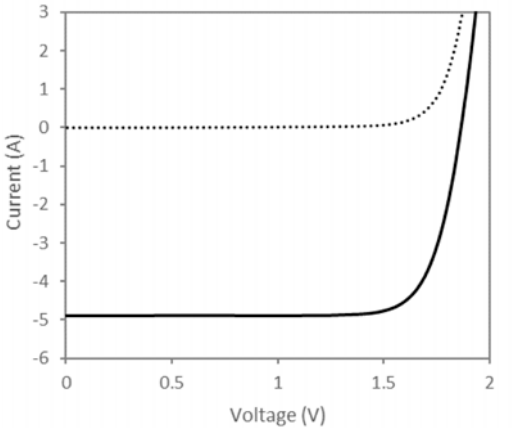

Sample No.	219165
Efficiency (%)	28.2
Power (W)	7.29
Area (cm^2)	258.15
I_{sc} (A)	4.905
V_{oc} (V)	1.868

Fig. 12 Light-IV (solid line) and Dark-IV (dotted line) of >28% tandem cell. Image courtesy of Oxford PV.

strides taken in silicon technology development mean that it is now approaching its efficiency limit—perovskite-silicon tandem technology opens up huge new possibilities for higher efficiency devices and have become the subject of intense academic and industrial interest.

The majority of the high efficiency devices reported in the literature have been at small area[142] with very few examples of commercially viable cell formats. Oxford PV has recently measured efficiency of > 28% on full area tandem cells with >250 cm^2 area; the IV curve and details are shown in Fig. 12. This fundamentally proves there is no issue with transferring high performance from small area cells to large area, mass production. Moreover, the assembly of high efficiency cells into industrial scale modules has also been demonstrated, with module efficiency of >23% already shown.[164] Albeit there is still clearly work to do to increase the cell and module efficiency in line with small cell records, it is already true that perovskite-based tandem technology is class-leading in this area.

As mentioned, more than 250GW of solar was installed in 2022—Oxford PV capacity for tandem cells is roughly 0.01% of this; the biggest challenge towards commercialization is to move towards production volumes where real economies of scale can be realised. The biggest barrier to this movement is procurement of tools capable suited for tandem cell application with very high throughput and short lead times. Concerted global effort on equipment provision will greatly accelerate progress towards multi-GW tandem production.

In the short term, one area of challenge is around measurement and certification of PVSK-Si tandem products. The technology for accurate measurement of full-size tandems exists but is not widely available. Work to define appropriate measurement systems and standards is active and has made much progress but adoption of steady-state lamps with advanced spectral control is a prerequisite for classifying such modules ready for sale. Furthermore, such measurement is essential for certification of the modules as compliant with international standards. The most appropriate standards for tandem modules are the current silicon-oriented ones (IEC 61215 & IEC 61730) and conformity to these requirements is currently being tested, however there is a need for the community to scrutinize such standards and determine if further or different tests are required for this new technology. To ensure these standards are appropriate also requires a growing understanding of long-term performance of tandem devices in operation; deploying significant quantities of tandem modules in appropriate climatic zones is therefore of utmost importance.

6 Organic PV

6.1 Nonfullerene Acceptors: Progress, Challenges, and Perspectives

Section Authors: Min Hun Jee (Korea University), Minyoung Lim (Korea University), and Han Young Woo (Korea University)

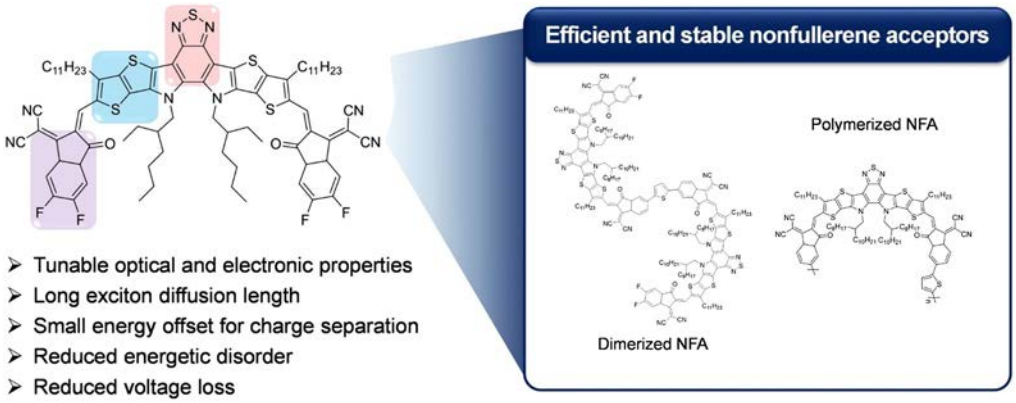

Fig. 13 Design strategies and advantages of non-fullerene acceptors.

Over the past decade, significant progress has been achieved in organic photovoltaics (OPV), leading to the successful demonstration of power conversion efficiencies (PCEs) reaching nearly 20%,[165–167] which was benefitted from the development of the outstanding non-fullerene acceptor (NFA) of Y6 in 2019.[168] Numerous derivatives of Y6 and other NFAs have been reported, employing innovative strategies such as chlorination, conjugation-extension, and symmetry-breaking, etc.[169–172] Compared to fullerene acceptors, NFAs offer several distinct advantages, including facilely tunable optical and electronic structures, longer exciton diffusion length, smaller energy offsets for charge separation and reduced energetic disorder, leading to lower energy losses (Fig. 13). He et al.[166] reported an NFA of BTP-H2 to have a near-zero highest occupied molecular orbital (HOMO) offset with the polymer donor PM6, showing efficient hole transfer and small voltage loss to achieve PCEs of 18.5% for binary PM6:BTP-H2 and 19.2% for ternary PM6:BTP-H2:L8-BO blends. To address thermal, mechanical, and long-term stability for small molecular NFA-based OSCs, Yu et al. developed a vinylene-linker-based polymer NFA (PY-V-γ) featuring a coplanar and rigid molecular conformation with high mobility and reduced energetic disorder, achieving a 17.1% PCE with PM6 as a donor.[173] To combine the advantages of small molecular and polymerized NFA systems, Sun et al. reported a dimerized Y6-derived NFA with an electron-donating benzodithiophene linker (DYBO), successfully demonstrating both high efficiency (PCE > 18%) and excellent stability ($t_{80\%}$ > 6,000 hours).[174]

For real industrialization of OPVs, some remaining challenges need to be carefully considered. To realize large-area OPV devices using high-throughput roll-to-roll printing processes,[175] it is essential to develop organic materials that can be processed using non-spin coating methods, utilizing environmentally friendly and green solvents. In the case of semi-transparent OPVs, there is a need to improve both PV performance and average visible transmittance by incorporating near-infrared absorbing materials into the active layer.[173,175–177] Additionally, the use of flexible linkers can be explored to enhance both the PV efficiency and mechanical properties of the stretchable devices.[178,179] Moreover, it is crucial to develop cost-effective synthesis for mass production of NFAs. It is also crucial to address the issue of stability in OPVs in order to achieve commercial viability for large-area applications. While encapsulation can help mitigate extrinsic degradation of OPVs, there is a need for a fundamental solution to address the problem of low stability resulting from intrinsic factors such as thermal degradation and photoreaction. Therefore, when developing new high-performance NFAs, it is imperative to conduct extensive research on the impact of their chemical structures on the long-term stability of OPV devices under various conditions, including thermal stress and exposure to light in ambient air. By addressing these challenges, significant progress can be made towards making OPV commercially feasible.

6.2 Optical Incoupling in Thin Film Organic PV Devices

Section Authors: Zheng Tang (Donghua University) and Olle Inganäs (Linköping University)

Organic photovoltaic (OPV) materials have poor transport properties for charge carriers, compared to classical inorganic PV materials. Thin active layers (<< 1 micrometer) are therefore

necessary for OPV devices. This leads to optical losses due to reflection and parasitic absorption. OPV devices are thus easy targets for light trapping and optical incoupling.[180–182] With the recent OPV materials of high performance, increasing exciton diffusion lengths[183] and cost, stability is improved with thinner absorbers[184]; thus optical incoupling is also relevant here to enable extremely thin film devices.

Strategies for improving light incoupling in the thin OPV devices include both macro- and mesoscale geometry modifications of device architecture, as well as micro- and nanopatterning of materials and devices, using physical effects from microcavity optics in multilayer structures, diffraction or scattering of light, and modification of incoming light with plasmonics. As a transparent electrode is necessary for light incoupling, a considerable effort has gone into making transparent anodes (cathodes), with decreased power dissipation or decreased reflection in the electrode facing incoming light, but not covered in this overview.

6.2.1 *Mode structure of light in multilayer devices*

Solutions to Maxwell's equation in the one dimensional device model of a stack of materials with different dielectric functions are now a standard tool for simulation of devices.[185] This transfer matrix method was used also to shape the electromagnetic power dissipation into the optical absorber in the stack, and used to design optical cavity structures.[186] Thin organic layers were also used simultaneously for exciton blocking and optical cavities.[187]

When the active layers are thinner than optimal, cavity optimization become beneficial.[188] A sizable absorption enhancement over a wide wavelength range was realized for PV devices by designing new cavities, with the enhancement more pronounced for the absorption tail;[189] see Fig. 14.

When tandem devices are built, the distribution of different wavelengths of exciting light between the active materials is critical, and with series connected devices, the balance of photocurrents from these must sometimes be found; here the microcavity structure is also of importance.[190,191]

While optical cavity structures are often useful for narrowband organic photodiodes,[192] they have smaller relevance for PV devices where the overriding aim is power generation, and with one cavity but many wavelengths of light.[188]

6.2.2 *Meso- and microscopic geometry design for light incoupling*

By modifying the mesoscopic and macroscopic geometry of the thin OPV films reflected light from opaque devices can generate higher photocurrent. This was demonstrated in folded single junction and tandem junction devices,[193–195] where a macroscopic V-shaped cell geometry was used, in which adjacent OPV devices were located at an angle, with subsequent reflection and possible absorption in the adjacent device. This deviation from the standard planar geometry comes at the price of use of more absorber material.

Microstructures using V-shaped light traps[196] were demonstrated enhancing the incoupling of light. With another light trap based on microlenses covering a surface and focusing light into aligned apertures in a highly reflective metal mirror in front of the device, effective light trapping was demonstrated.[197] An reflective echelle grating at the back of a semitransparent solar cell can also be used to trap transmitted light, and bring it back for absorption.[198]

Micro- and nanopatterning of the OPV film was first used in soft embossed optical gratings[199] where light incoupling was demonstrated. Subsequent work has used periodic or nonperiodic patterning of a flexible substrate for the OPV to guide light into the active layer.[186,200] This has also been done with extremely thin film polymer substrates.[200]

Microstructured light couplers may also be formed as external elements,[201–204] in the form of periodic textures, diffraction gratings or aperiodic diffractive elements.[205,206] Colloidal photonic crystals have been used for large area printed OPV modules.[207]

6.2.3 *Plasmons and light scattering*

Coupling of light to plasmons in metallic nanostructures have been demonstrated, both with metal gratings coupling light into surface polariton modes at the interface between metal

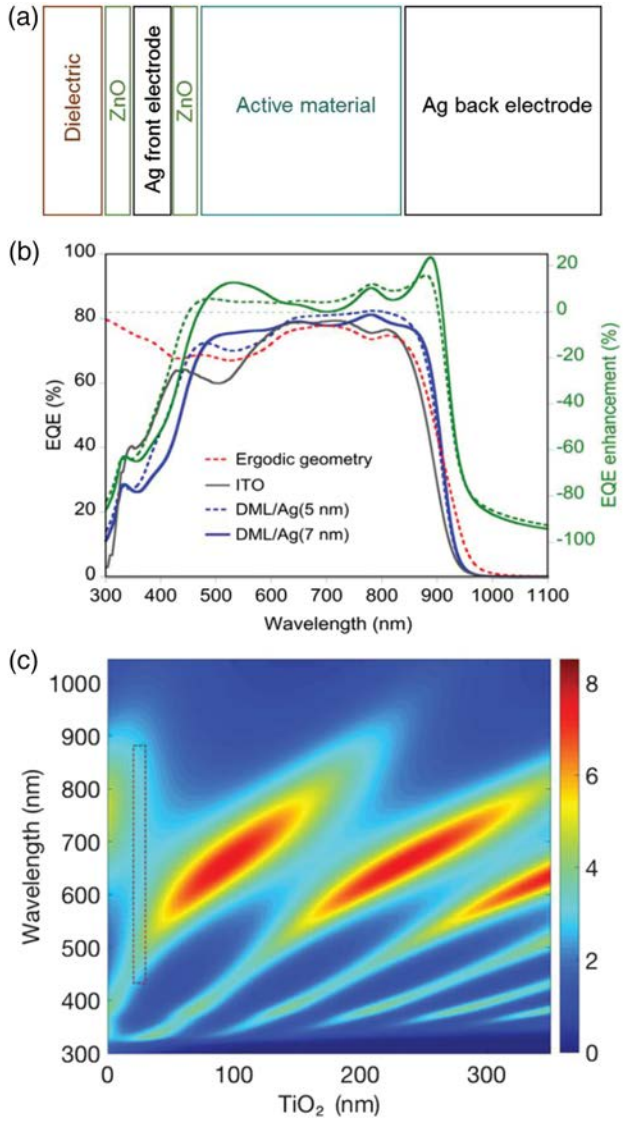

Fig. 14 Optical cavity inverse design. (a) Schematic representation of the dielectric/metal (DML) layer optical cavity. (b) Left axis: Computed EQEs for devices with a standard ITO cell configuration (solid grey line), the DML cell configuration with an Ag front electrode of 7 nm (solid blue line), and 5 nm Ag (dashed blue line), an optical ergodic geometry configuration with a 99% wave-length independent reflectivity back mirror (dashed red line). Right axis: EQE percentage enhancement for DML cells with a 7 nm (solid green line) and a 5 nm (dashed green line) Ag front electrode relative to the optical ergodic geometry configuration. (c) Energy storing capacity (vertical axis) of the DML cavity configuration as a function of the wavelength and dielectric layer (TiO2) thickness. A dashed rectangle indicates the broadband energy storage region. Reproduced by permission from Liu et al., Ref. 189.

electrode and optical absorber,[194,202] and with metallic nanoparticles[208] inserted in the different layers of the OPV devices.[209] Both near field and far field effects due to metal nanoparticles could be used to modify the generation of excited states in OPV materials; for small nanoparticles (2-20 nm), theory predicts that the near field enhancement can be sizable also without plasmonic coupling[210]; for large particles light scattering can lead to redistribution of light into the optical absorber in devices. The topic is reviewed in,[211] which concludes that the plasmonic effects are considerable, though the balance between enhanced absorption due to plasmons, light scattering and modified recombination/generation/transport can have many different results. The inevitable loss of energy of the incoming light in exciting the electrons in the metal always has to be compensated by improved exciton/charge generation.

Light scattering from inhomogenous polymeric films and dielectric nanoparticles are (almost) lossless processes. Dielectric scatterer based on titania can be used to redirect light in stacked homo-[212] and hetero-[213]tandem devices based on semitransparent[212–215] OPV devices, converting the semitransparent OPV to an opaque OPV. With white paper[216] or nanoporous polymers,[217] as well as a microstructured retroreflector,[218] light harvesting is improved.

7 Dye-Sensitized Solar Cells: Current Progress and Challenges

Section Author: Marina Freitag (Newcastle University)

Dye-sensitized solar cells (DSSCs) represent a promising PV technology due to their economic feasibility and potential for high conversion efficiencies. (DSSC device structure and principles may be seen in Fig. 15.) Recent advancements in the sector have explored improvements in the areas of device structure, redox shuttle alternatives, solid-state hole conductors, TiO2 photoelectrodes, catalyst materials, and novel sealing techniques, all contributing to the development of new monolithic cell designs.[219] Unique attributes include their high conversion efficiencies and commendable performance under diffused light and high temperatures, where traditional technologies struggle. Current research predicts future DSSCs to demonstrate up to 20% power conversion efficiencies (PCE) under sunlight and an astounding 45% for ambient light.[220]

Challenges in the path towards commercial scalability of DSSCs primarily revolve around the issue of charge recombination,[221–223] which currently serves as a major cause of efficiency loss in DSSCs. The intricate system dynamics involved in DSSC operation mean that modifications to one component—dye, redox shuttle, or semiconductor[224]—can yield impacts across the entire system, potentially boosting or diminishing the overall performance. Future developments must therefore maintain a holistic perspective when introducing new materials, ensuring that the system is adapted to accommodate such changes.

Currently, DSSCs are breaking new ground in several domains. Promising developments include use in ambient and IoT applications with PCE up to 40%,[225,226] as transparent solar cells[227,228] and photochromic in BIPV applications,[229] and in agrivoltaics for greenhouses and vertical gardening applications.[227,230] A fascinating area of exploration is "zombie solar cells" using copper coordination complexes and polymers as hole transport materials.[231–233] Meanwhile, innovative dyes are being developed that are non-toxic, low cost, and sustainable. Pre-adsorbing a hydroxamic acid derivative on the TiO_2 surface has shown to improve dye packing and PV performance, enabling record PCE up to 15.2% under standard sunlight.[234] With the prospect of PCEs reaching up to 20% under sunlight and 45% under ambient light conditions, the

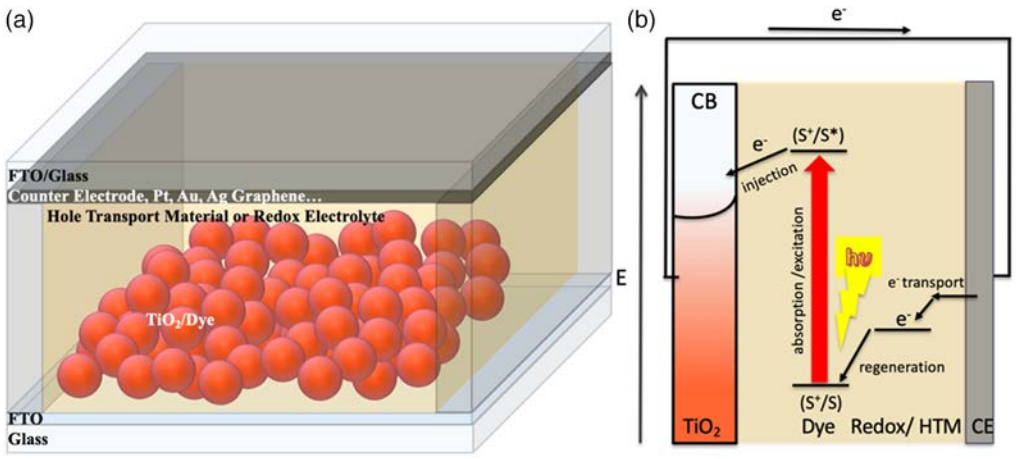

Fig. 15 (a) DSSC device structure; (b) DSSC working principles.

future of DSSCs appears promising. However, the complexity of DSSC devices necessitates a nuanced approach to their improvement, considering the potential impacts of any modifications on the overall system performance.[219]

Furthermore, the field of photocapacitors, which store energy photochemically in a reversible manner, also offer potential synergies with DSSCs. The integration of DSSCs with photocapacitors can result in a hybrid system that harnesses solar energy and efficiently stores it, offering the potential to meet peak demand times or function during periods of low solar irradiation.[235] This would further extend the utility of DSSCs, enabling more consistent energy supply and overcoming one of the key limitations of solar power.

8 Applications and Commercialization of Emerging PV

8.1 Indoor PV

Section Author: Lethy Krishnan Jagadamma (University of St Andrews)

One of the most emerging and thriving areas of PV is indoor light harvesting.[236–238] This advancement of indoor PV is spurred by the rapid development of the internet of things (IoT) and the urge to make this technology more sustainable and robust.[239] The main difference between indoor PV and outdoor solar cells lies in the properties of the incident illumination spectra. The illumination spectra of indoor artificial light sources are in the visible spectra range of 400-700 nm with an irradiance of ~0.05 to 0.35 mW/cm^2 whereas the sun's spectra range from UV to infrared with an irradiance of 100 mW/cm^2. The extremely low light intensity and higher photon energy for indoor PV demand new design guidelines in terms of the material chemistry (not only in the photoactive layer but also the functional charge extraction layers) and the device physics. The optimum bandgap is ~1.9 eV, and the theoretical power conversion efficiency (PCE) can be as high as 50-57% for indoor PV depending on whether the illumination source is a fluorescent lamp or a white LED.[240,241]

The most promising PV materials so far for efficient indoor light harvesting, are amorphous silicon, dye-sensitized solar cells (DSSCs), organic PV, and halide perovskites. Compared to DSSCs, the latter two possess higher prospects of commercialization due to their large area solution processibility, tuneable of bandgap, flexibility, and light weight. The latest reported champion power conversion efficiency (for 900-1000 lux indoor illumination) for these PV are respectively 36 % (a-Si: H),[242] 25 % (DSSC),[243] 30 % (OPV)[244] and 40.1 % (from the halide perovskites).[245] Despite these impressive PCEs, the gap between the theoretical and lab based PCE is still >20%.

To further advance the indoor PV field and its commercialization, the existing challenges need to be overcome. Presently, the field lacks a standardized illumination source. Considering the different indoor illumination levels (200 to 1500 lux), and artificial lights of white LEDs and fluorescent lamps, standardisation is not straightforward. However, reporting colour temperature, irradiance spectrum and irradiance of the indoor light source will make the comparison of the power conversion efficiency values from different research labs more meaningful. Validation of the measured short circuit current density (J_{sc}) with that from the external quantum efficiency (EQE) measurement should also be encouraged for indoor PV. In the case of hybrid perovskite-based indoor PV, along with the J-V curves in both scan directions, reporting steady-state power conversion efficiency would enhance the reliability of measurements. To close the gap between the theoretical and experimental efficiency values, an overall improvement in all the PV performance parameters is necessary.[246] However, the V_{oc}, loss needs immediate attention. Despite the large bandgap (1.8 to 2.0 eV) of the photoactive material, most of the reported indoor PV have a V_{oc} of ~0.8V only (loss of more than 1V). Though compared to normal outdoor solar cells, indoor PV may require less stringent stability testing protocols, many are yet to be formulated. In the coming years, research on indoor PV is expected to be focused on, maximising its PCE, developing the stability protocols, integrating with the energy storage units and implementing them in real IoT applications (see Fig. 16).

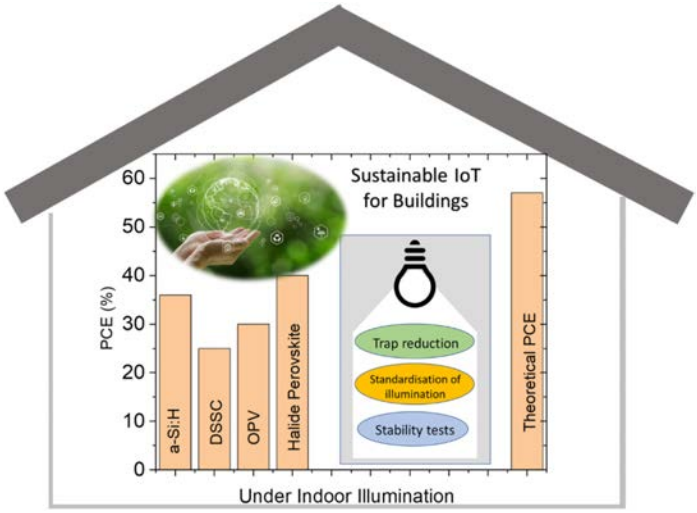

Fig. 16 Sustainable IoT for buildings.

8.2 Commercialization of Organic PV

Section Author: Stephan Kube (Heliatek GmbH)

Heliatek is the technology leader in organic PV, founded 2006 out of research in the field of organic electronics from TU Dresden and the University of Ulm. Researchers had developed a new generation of semiconductor materials built on carbon-based molecules from organic chemistry. With this new generation of materials, Heliatek was able to develop an innovative new solar technology called "organic photovoltaics" (OPV). Since 2006, Heliatek has developed new materials, new product concepts, and a proprietary "Roll-to-Roll" vacuum evaporation production process.

In 2022, Heliatek started to produce and sell its first commercial product HeliaSol. HeliaSol is an ultralight, flexible, and ultrathin solar film that can be easily glued to various building surfaces such as metal, glass, or concrete with the integrated backside adhesive. This makes HeliaSol the perfect choice for all applications where conventional solar modules reach their limits due to weight or surface restrictions (e.g., curved shapes). With a carbon footprint of less than 10 g CO_2e/kWh, HeliaSol is based on the greenest of all solar technologies and is amongst the greenest of all electricity generation technologies. The reasons for this ultralow carbon footprint mainly come from the few materials required to manufacture solar films and the abundance of toxic heavy metals (such as cadmium or lead) and rare earths. The films only use 1 g of organic material per film and the films weigh in total less than 2 kg.

The solar films are produced in an innovative roll-to-roll evaporation production process, where Heliatek processes coils with a length of up to 2.6 km and a width of up to 1.3 meter. This allows us to produce different product dimensions. The first HeliaSol that Heliatek is producing has a dimension of 2 m length and 0.44 cm width, which has a compact and easy to handle format. These films have a power between 50 and 60 W.

Heliatek has already proven the versatile applications possibilities in projects around the world, where its façade solutions, building rooftop applications, or special projects like a wind turbine tower in Spain, show that with lightweight, flexible solar films, Heliatek is able to transfer surfaces into active green electricity generators.

Heliatek is funded by the Free State of Saxony, the Federal Republic of Germany, and the European Union. The company has more than 250 employees at the headquarters in Dresden and the research location in Ulm. Figure 17 shows the diverse applications of the company's products globally.

Fig. 17 Clockwise from top left: HeliaSol solar film (rolled), production of solar films in Roll-to-Roll manufacturing process, façade installation in Korea, wind turbine tower in Spain, and biogas plant in Germany. Images courtesy of Heliatek, Samsung, Acciona, and RWE.

8.3 Agrivoltaics: Status, Land Use Conflicts and Synergy with Organic Photovoltaics

Section Author: Harald Hoppe (Friedrich Schiller University Jena, CEEC Jena, and IOMC)

With the current expansion of renewable energy supply in large parts of the world, primarily through wind energy, energy crop cultivation, and PV, the land use required for this is also increasing inexorably.[247–249] Not in all regions can land that is otherwise unusable be used for this purpose, and thus resistance to such projects is also growing.[250,251] In western countries, for example, this has led to increased state regulation with the associated extensive bureaucracy for the realization of new regenerative power plants, which makes further expansion considerably more difficult. On the other hand, there are now not only competitive situations with traditional agriculture, but also land use conflicts between energy crop cultivation and photovoltaics in particular have become a priority problem, for example in Germany.[252]

However, a solution to these land use conflicts could be found in a dual use of the available land through agrivoltaics,[253] a coexisting agriculture with PV installations, providing a solution to the water-food-energy nexus.[254] Typical agrivoltaic system installation parameter considerations (presented in Fig. 18) include crop type, PV module installation angle, distance, and overlap on the crops, and the transparency of the modules. At present, more than 15 GW of installed capacity have already been realized worldwide, for which subsidy programs have even been set up in some countries.[255]

The majority of agrivoltaic systems are currently being based on the use of silicon solar cells, which is accompanied by an increased installation effort compared to classical PV installations. However, there are already first projects for the use of organic solar cells, respectively organic PV.[256–258]

Organic solar cells have distinct advantages such as light weight and ease of integration, as well as the potential for very high average visible transmittance (AVT) due to their unique property of limited absorption bands within a spectral interval,[259–261] which potentially eliminates competition between PV and plant light use in greenhouses.[262,263] More research and development is needed,[264,265] however, in order to synthesis and mass-produce novel organic semiconductors that preferentially use the infrared (IR) section of the sun spectrum.

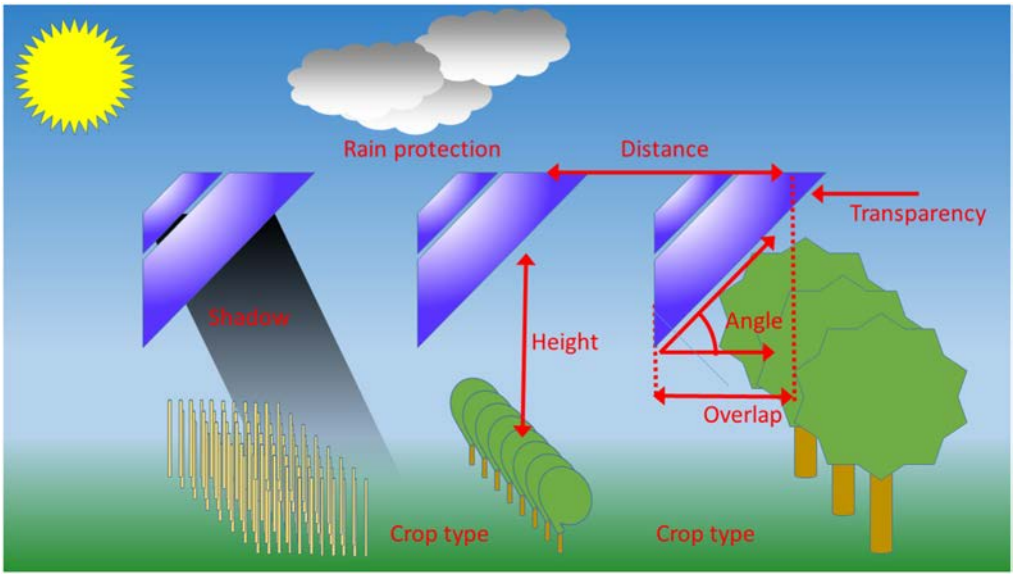

Fig. 18 The schematic shows the most important parameters of agrivoltaic installations. The crop type and its handling impacts, e.g., on the distance and height of installations. The angle, distance, and overlap determine the shadow or rain protection, while the transparency modulates the shadowing.

8.4 Perovskites for Space PV Applications

Section Authors: Duong Nguyen Minh (National Renewable Energy Laboratory) and Joseph M. Luther (National Renewable Energy Laboratory)

While the prospects of new PV technologies are growing rapidly for terrestrial terawatt-scale electricity generation,[266] PV was first marketed as technology to power spacecraft such as satellites, and emerging PV technologies could provide substantial cost reductions for the emerging space market.[267] The satellite industry is rapidly expanding due to the commercialization of launch opportunities (SpaceX and others). More than 10x the historical number of satellites are planned to launch in the upcoming 5 years.[268] Traditionally, III-V, multijunction solar cells make up the bulk of space PV market because of their higher efficiency, improved radiation tolerance, and improved temperature characteristics compared to Si albeit at much higher cost. Thus, the goal for new PV technologies, like perovskites would be to provide low cost options (equivalent to terrestrial Si) that may match or improve upon the radiation tolerance and temperature characteristics of III-V technologies.[269,270] Perovskite fabrication advantages enable flexible roll-out solar arrays and furthermore, the potential to even manufacture solar cells in space.[267,270]

Perovskites for space PV has already shown promising results.[271,272] Although the early demonstrations also reported the surprising high radiation tolerance of perovskites, the testing conditions are widely different.[273] Part of the rapid increase in interest of perovskites globally was because they are shown to tolerate a higher density of defects (while retaining high efficiency) than other PV technologies.[273] This is further beneficial because not only can they tolerate higher defect densities, the radiation produces less defects in perovskites from particles of relevant energy as shown by the slightly lower non-ionizing energy loss and slightly higher stopping range plotted in Figs. 19(a)–19(b). This property is ideally suited for radiation tolerance in space where interactions with charged particles can lead to atomic displacements or vacancies within the absorber layer. The future development of perovskite PV for space applications would benefit from a consistent ground-based radiation testing convention to accelerate the optimization of perovskite PV designs, because radiation tolerance may not only be an inherent property, but it may also be a design criterion to optimize with interfacial engineering and contact decisions. However, the well-developed radiation-testing protocol for conventional space PV technology may not be equally suitable for testing perovskite solar cells due to their

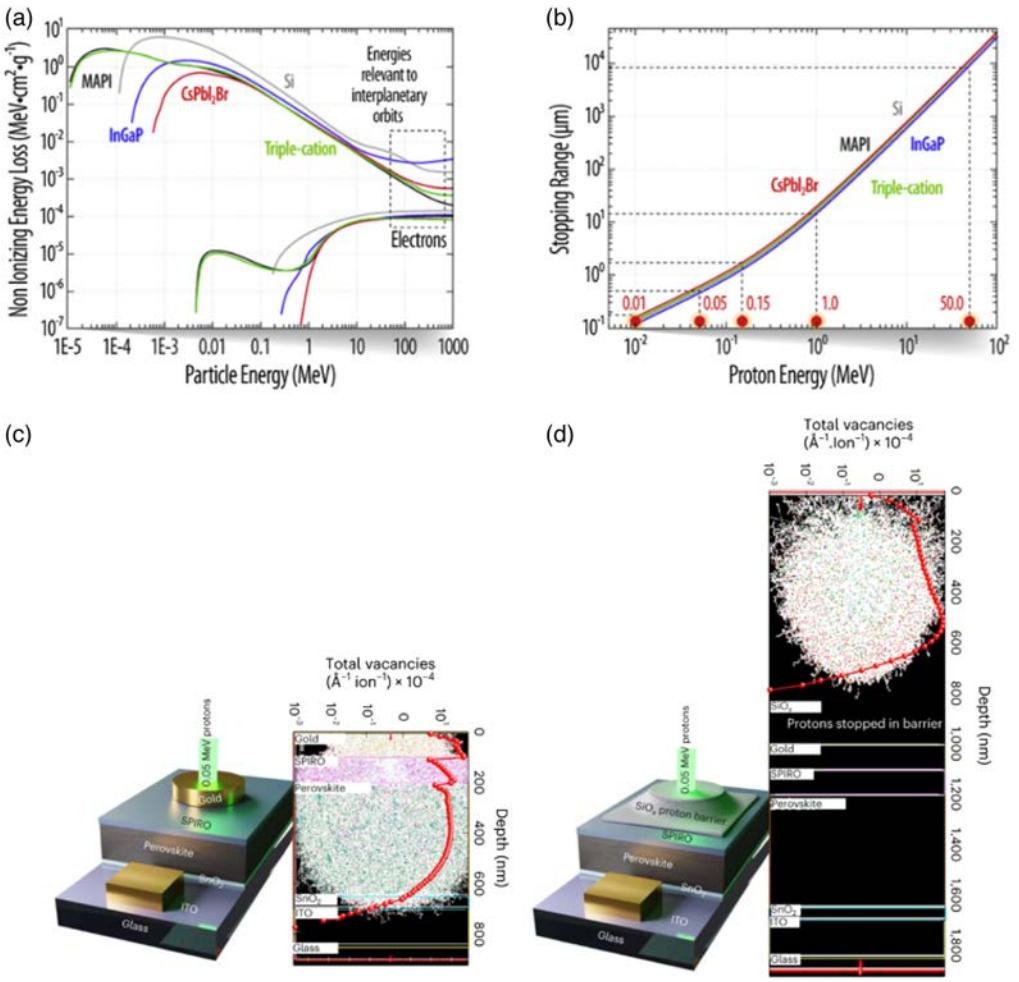

Fig. 19 Development of perovskite solar cells for space applications. a-b) Fresh protocol testing for perovskite solar cells. a) Comparison of irradiation interaction to Si, InGaP, and perovskite PV technology. b) stopping ranges of protons for various absorbers. c-d) Development of encapsulation for perovskite solar cells. c) Simulated proton interaction with perovskite devices. d) SiO_x barriers block proton irradiation to perovskites solar cells. Figure adapted with permission from Refs. 271 and 274.

soft lattices, thermal properties, and markedly different device architectures. Currently, the low-energy protons of 0.05-0.15 MeV were reported to cause atomic displacements and vacancies in unencapsulated devices,[273] which effective probe the radiation interactions in perovskite solar cells.

However, there are still many hurdles to overcome for perovskites in space regarding thermal properties.[267] Some orbits require aggressive thermal cycling tests (thousands of times more aggressive than IEC standards, and at wider and faster temperature swings), while other orbits may require constant operation indefinitely (no diurnal cycle), where the cells must be built to endure the temperature without convective heat transfer.

For either case (terrestrial or space), perovskites will need to be well-protected/packaged.[275] While polymers and sealants encapsulation are likely to decompose under harsh radiations because of the weakening carbon bonds, the use of traditional cover glass could also be challenged for weight and cost savings.[267,275] Comparatively thin (1 μm) SiOx encapsulation (lighter than 99% of conventional barriers) was recently shown to protect perovskites against the various key critical stressors in both terrestrial and space environments, including protons [as shown in Figs. 19(c)–19(d)], alpha particles, atomic oxygen, and moisture, and provides a good starting point for more complete packaging ideas.[274]

9 Strategies for Exceeding the Detailed Balance Limit

9.1 Progress towards the Hot Carrier Solar Cell

Section Authors: Ian R. Sellers (University at Buffalo), Vincent R. Whiteside (University of Oklahoma), and David K. Ferry (Arizona State University)

Since the pioneering work of Ross & Nozik,[276] the hot carrier solar cell has been considered a potential protocol to circumvent the single gap limit.[277] This limit suggests that practical losses due to transmission (of low energy photons) and thermalization (due to absorption of high energy photons) limit conventional semiconductor solar cells to ~30% power conversion efficiency.

The proposal in Ref. 276 suggests that solar cells operating in excess of 60% might be realized, without the need for multijunction architectures.[278] One scenario for the operation of a hot carrier solar cell will occur when carrier-carrier interactions have generated a steady state Maxwellian "hot carrier" distribution whose temperature is in excess of the lattice. Generally, this requires inhibiting the thermalization of high energy photogenerated carriers, then extracting these carriers at their higher energy.

Since its original inception in 1982,[276] the hot carrier solar has received significant attention with much of the work related to inhibited carrier-phonon interaction or the creation of a so-called hot phonon bottleneck[279,280] in low-dimensional structures such as quantum wells. Alternative approaches involve the investigation of materials with large phononic band gaps[281] that may inhibit hot LO phonon dissipation such as InN,[282] AlAsSb,[283] and/or HfN,[284] amongst others. In addition to these, recent approaches seek to control carrier-phonon interactions by design in type-II superlattice structures.[285,286]

While many of the early works in this area focused on spectroscopic analysis in both the CW[287–289] and ultrafast[290–292] regimes, recently hot carrier effects have also been observed in devices. Recent device results have shown: the presence of PV carrier extraction,[293,294] extremely high non-equilibrium carrier temperatures in quantum well devices,[295] and selective hot carrier extraction in metallic absorbers.[296] While these demonstrations show significant practical progress towards the realization, decoupling electron-phonon mediated heat generation remains challenging.

Recently, an alternative protocol has been proposed in which intervalley scattering is used to transfer high energy photogenerated carriers into the satellite valleys of the absorber layer of heterostructure solar cells.[297,298] In such valley PV solar cells, it is proposed that intervalley phonon scattering is harnessed to inhibit hot carrier-LO phonon interactions in a semiconductor. This process allows the transfer and stabilization of hot carriers via the efficient transfer of photogenerated carriers to the upper valleys in the absorber, a process by which radiative recombination is exponentially reduced. A schematic of this process in comparison to the typical operation of a single gap solar cell is shown in Fig. 20. Initial work in this area has shown proof

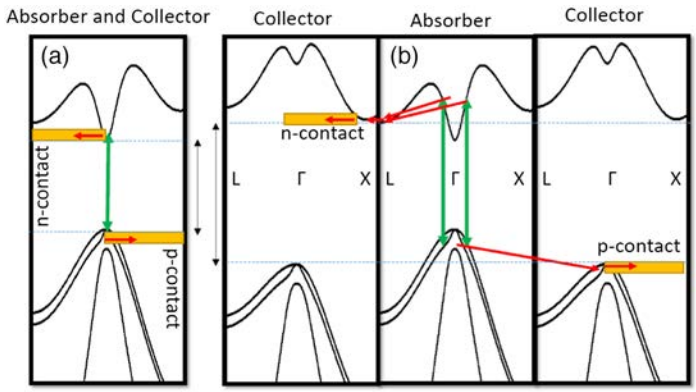

Fig. 20 (a) Schematic of the typical extraction energy/voltage in a single gap solar cell. (b) Protocol for hot carrier operation using IV scattering. Hot carriers are rapidly transferred to satellite valleys then extracted via an energy matched collector at $V > V_{oc}$. Figure created by Stephen J. Polly (RIT).

of principle operation and efficient carrier scattering in the InGaAs/AlInAs system,[297,298] with work now focused on efficient carrier extraction across the absorber/barrier interface. Efficient upper valley extraction would support photo-voltages in excess of the absorber band gap and power conversion efficiencies[299] well above that of the single gap limit.

10 Light Management

10.1 Luminescent Solar Concentrator PV: Performance

Section Authors: Angèle Reinders (Eindhoven University of Technology), Xitong Zhu (Eindhoven University of Technology), Wilfried van Sark (Utrecht University), and Michael G. Debije (Eindhoven University of Technology)

Luminescent solar concentrator photovoltaics (LSC-PV) act as spectral converters, optimizing spectral matching between the irradiance spectrum and peak of the response of PV cells.[300,301] An LSC-PV normally consists of a transparent optical lightguide (usually glass or a polymer such as poly [methyl methacrylate] [PMMA], polycarbonate [PC], or polydimethylsiloxane [PDMS][302]) with embedded luminophores which redirects absorbed light as downshifted emission toward the edge(s) where it may be used to illuminate attached PV cells;[303–305] see Fig. 21 (top and middle). Spectral conversion and (in larger lightguides) total internal reflection (TIR) are used to improve the LSC-PV device's efficiency.[306,307]

The concept of LSC-PV was introduced four decades ago,[308–310] initially to reduce the high cost of PV modules,[311] but now these colorful, transparent, visually appealing solar devices could contribute to the general acceptance of solar technologies in the built environment, even with modest efficiency, thanks to their greater design flexibility than conventional flat, rectangular PV modules; see Fig. 21 (bottom).

LSC-PV perform well under various irradiance conditions, particularly under diffuse light.[312] Color (from purple to red hues)[313] is determined by the luminophores employed and may comprise organic dyes,[314–317] quantum dots (QDs),[305,318–322] and/or rare-earth ions.[323–325] The optimal dye has broad spectral absorption,[326,327] high photoluminescence quantum yield (PLQY),[328–330] large Stokes shift,[331,332] good solubility in the host matrix material,[333,334] and good spectral overlap of the luminophore emission s and the spectral response of the PV.[335–337]

The performance of LSC-PV devices is limited by several loss mechanisms, including attenuation by the lightguide material, scattering, escape cone losses,[338] and reabsorption during the lightguiding process.[339,340] Several methods have been proposed to minimize loss mechanisms in lightguides and enhance the internal efficiency (η_{int}) and power conversion efficiencies (η_{PCE}).[319,341–343] Further proposed designs include using different lightguide materials, geometric shapes (e.g., rectangular,[344] square,[345,346] cylindrical,[347,348] and bent[346]), and different dimensions (from $1.5\,\text{cm} \times 1.5\,\text{cm} \times 0.1$ cm,[331] to $100\,\text{cm} \times 150\,\text{cm} \times 0.6$ cm,[349]) to numerous edge-mounted and or bottom-mounted PV cell technologies, including, GaInP,[350] GaAs,[321] CdTe,[350] CIGS,[350] mc-Si,[351] c-Si,[352] a-Si,[353–355] p-Si,[356] DSSC,[357] and perovskite.[358]

Reported LSC-PV devices have shown various efficiencies.[340,343] The most frequently reported world record of $\eta_{LSC-PV} = 7.1\%$ applies to a small-sized device ($5\,\text{cm} \times 5\,\text{cm} \times 0.5$ cm) with high efficiency GaAs solar cells edge attached to a PMMA containing a mixture of two organic dyes.[359] However, most LSC-PV devices have modest efficiencies in the range of 1-5%. The average efficiency of LSC-PV devices has increased from 2.5% (1980–1985) to 5% (2005–2021); Fig. 22 summarizes LSC-PV devices with variety in host matrix, luminescent materials, solar cell technology, lightguide dimension, PV cell size, geometric gain (Gg), internal efficiency (η_{int}), power conversion efficiency (η_{PCE}), and other design configurations.

Note the efficiencies reported in Fig. 22 were not obtained using the same metrics or measurement procedures, as comprehensive standard protocols for performance reporting have only recently been introduced.[360,361] As such, previously reported LSC-PV device efficiencies were overly positive, ignoring transparency of the LSC, and cannot be used for comparisons of other efficiencies obtained under STCs.[362]

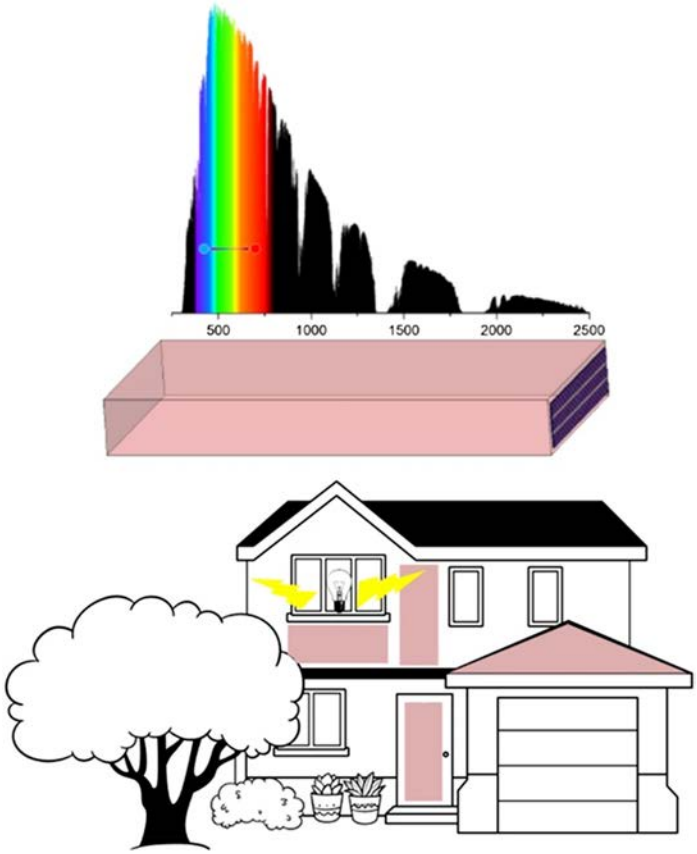

Fig. 21 (Top) Solar irradiance spectrum with an indication of conversion of a blue photon to the red part of the spectrum, (middle) a lightguide with a solar cell attached to one of its edges, (bottom) in pink, possible locations of application of LSC-PV devices in a dwelling.

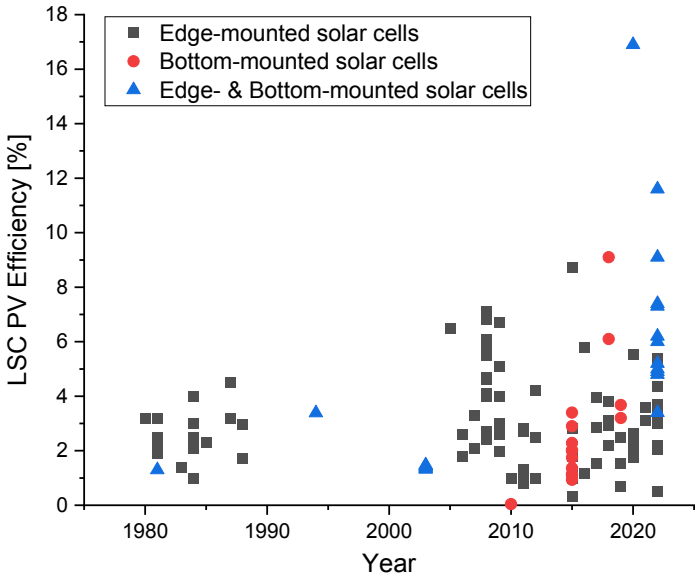

Fig. 22 Reported power conversion efficiencies of luminescent solar concentrator PV (LSC-PV) devices over the past 43 years with edge-attached (black squares), bottom-attached (red circles), and both edge- and bottom-attached solar cells (blue triangles).

10.2 Luminescent Solar Concentrator PV: Technology Status

Section Author: Vivian E. Ferry (University of Minnesota)

Luminescent solar concentrators (LSCs) have been proposed for PV applications for more than 40 years.[309] LSCs are attractive devices for integration of solar panels into the built environment: composed of luminescent materials (dyes, colloidal quantum dots) embedded in a polymer matrix, their colorful/semi-transparent nature and ability to capture and concentrate diffuse sunlight makes them excellent candidate architectural materials.[341] Diffuse sunlight is absorbed and emitted by the luminophore, and directed onto an adjacent solar cell by total internal reflection. Historically, performance has been limited by significant optical losses, and especially re-absorption in large-area devices, since every absorption/emission event is an opportunity for losses from the non-unity quantum yield or the imperfect waveguide (escape cone, scattering); see Fig. 23.

The past 15 years have seen considerable new interest in LSCs, driven by new advances in light-emitting materials.[364] For efficient operation, the luminophores must strongly absorb incident sunlight, have high quantum yields, and large Stokes shifts to avoid re-absorption of the luminescent light, and have low toxicity/earth-abundancy for large-scale application. Colloidal nanocrystals, such as II-VI particles,[351,352,365,366] Si,[331,367–369] carbon dots,[370] perovskites,[371–374] and ternary alloys,[300,375] and metal-halide nanoclusters[376] have all emerged as candidate materials,[363] offering highly tunable and advantageous optical properties. However, these new materials must be dispersed in polymer matrices and waveguide materials[370,377] without significant degradation of optical properties, light scattering, or absorption losses by the matrix material, and large-scale, cost-effective synthesis and fabrication methods are needed.[367] Additionally, as the quality of the luminophores improves, other aspects of optical design become increasingly important to the overall efficiency, such as photonic structures that trap and direct luminescence toward the PV cell.[351,377–381] Recent calls to standardize efficiency metrics for LSCs should also be noted.[382]

There are other intriguing new developments in the LSC community, including the implementation of downconverting/upconverting materials, as opposed to the downshifting mechanism of a traditional LSC architecture. New application spaces for LSCs with PV are emerging,[383] including the use of LSCs in greenhouses where the tailored transmission spectrum benefits crop growth.[384–387]

Large-area and scalable fabrication remains an important challenge for LSCs. Techniques such as doctor blade coating[367,388] or spray coating[389] are important for production, but may require materials advances for luminophore compatibility, as well as understanding of the process to create high quality, low haze materials. Similarly, photonic structures that assist in light-guiding must be manufacturable. Lifetime is critical to commercial applications, requiring luminescent composites that are stable against oxygen and moisture. Sustainable luminescent materials with low toxicity but excellent optical properties in the composite continue to need development.[390] Commercialization may also require different form factors or design modifications to integrate with application-specific components, i.e. architectural glazing or displays.[391]

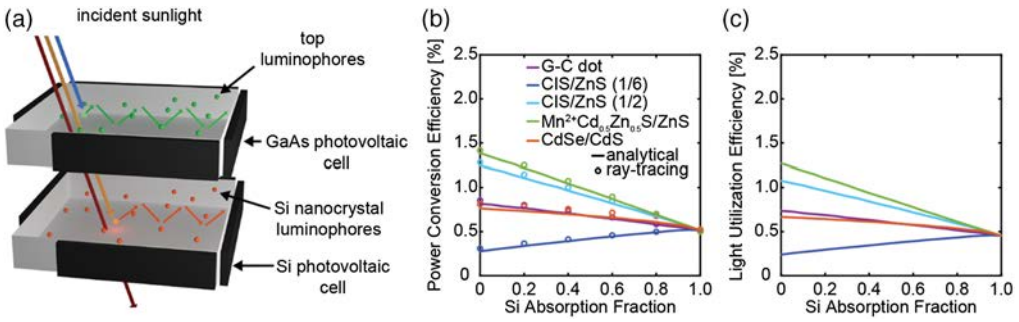

Fig. 23 Estimated power conversion efficiency and light utilization efficiency for a tandem LSC (a) with various candidate top luminophores, and [(b),(c)] constant overall absorption of 10%. Figure adapted from Ref. 363.

Given the large number of design variables (shape, luminophore, concentration, matrix material, use of photonic structures, environment for implementation, and others), there is an opportunity to understand the design rules for LSCs from the perspective of the commercial application, i.e., accounting for sustainability, scalability, and the operating environment from the start, rather than designing for small-scale laboratory tests. Computational methods that accelerate this design process will likely play an essential role in both understanding and optimizing these future generations of LSCs.

10.3 Spectrum Splitting PV Systems

Section Authors: Raymond K. Kostuk (University of Arizona) and Benjamin Chrysler (Amazon Lab)

High efficiency PV systems have many operational and financial advantages. High efficiency allows less land usage for the same electrical power generation and the ability to generate significant power in constrained areas. According to the detailed balance condition, high efficiency PV conversion can only be achieved by using multiple energy bandgap PV cells within the range of the solar energy illumination spectrum.[277,392] The most common way of doing this has been to stack multijunction cells in tandem with the topmost cell converting shorter wavelengths and the bottom most cell the longer wavelengths. This approach requires precise lattice matching between different bandgap materials, current matching, and is restricted to compatible materials. These factors increase cost and require high concentration optics for economic viability. An alternative approach is spectrum splitting in which an optical element separates the spectrum of the incident solar illumination and directs spectral components to an array of single junction cells that have high responsivity to different spectral bands [Fig. 24(b)]. In spectrum splitting systems the emphasis of the design shifts from the stacked multijunction cell to the design and fabrication of the optics that perform the spectral separation of the incident solar illumination. The concept of spectrum splitting PV systems is not new (dating back to 1955)[393] and comprehensive reviews have been given by Imenes and Mills[394] and Mojiri et al.[395]

During the past ten years, a variety of methods have been proposed for implementing spectrum splitting optics. These approaches include: cascaded dichroic reflection filters,[396,397] filter-mirror combinations, [398–400] optimized surface relief diffraction gratings,[401,402] hologram-lens combinations,[403] and volume holographic lenses.[404–406] All spectrum splitting systems require at least single axis tracking, however, single axis tracking is being used with many more efficient types of silicon cell modules and is therefore not considered a major impediment. The most robust and compact optical approaches are surface relief diffraction gratings (SRDGs)

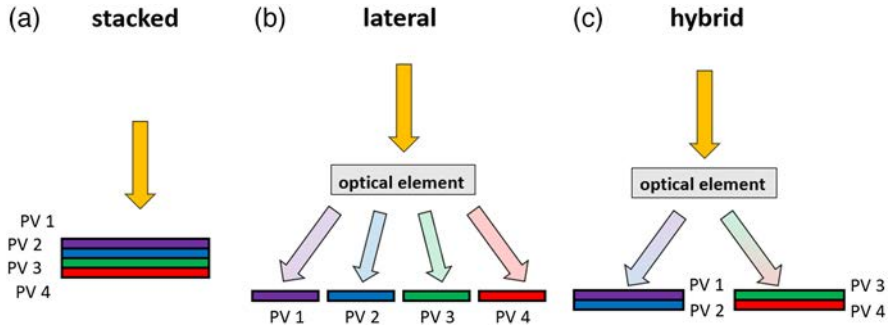

Fig. 24 (a) Stacked, (b) lateral, and (c) hybrid configurations for spectrum-splitting PV modules. In stacked modules, PV cells are placed on top of each other either. Upper cells in the stack convert shorter wavelength light and pass longer wavelength light to the lower cells. The stack can be implemented as a monolithic multijunction cell or a set of mechanically stacked single-junction cells. In a lateral configuration, an optical element sends different parts of the solar spectrum to single-junction PV cells located in different areas of the module. In a hybrid configuration, an optical element sends different parts of the solar spectrum to different cell stacks where the solar spectrum is further subdivided. In general, cells can be connected in series, series-parallel combinations, or electrically independent configurations.

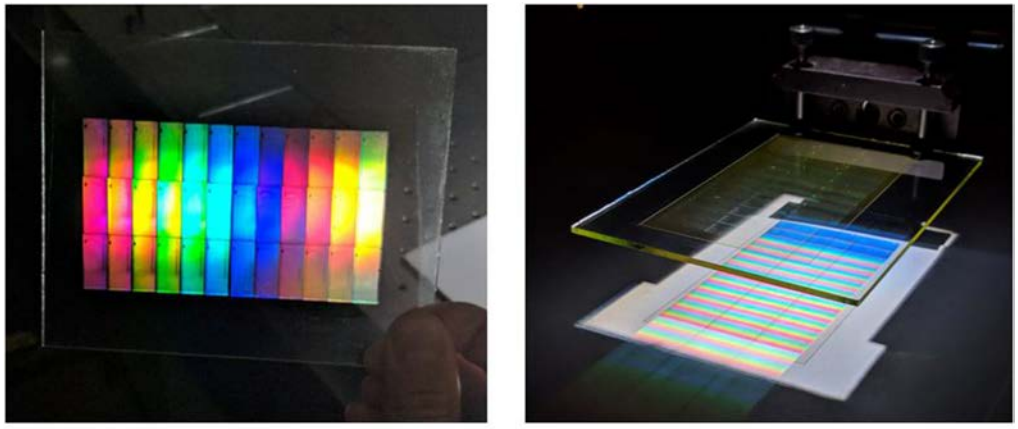

Fig. 25 (a) An array of volume holographic lenses fabricated using a replication system.[414] (b) Spectral band separation using the VHL array shown in (a).

and volume holographic lenses (VHLs). Ultimate use of either of these techniques will depend on fabrication cost and durability. Volume holographic elements have been successfully incorporated into traditional PV module packages that have passed accelerated life testing for 25 years or more and provide some support for the viability of this technique. In addition, methods for replicating volume holographic elements and lenses have also been demonstrated (Fig. 25).[407,408]

Recent work on spectrum splitting has led to an interesting result for optimal cell configurations.[409] Figure 24 shows cell types: stacked multijunction, lateral separated single junction, and hybrid cells. A stacked multijunction PV cell is a form of absorption spectral filtering where each cell in the stack filters and converts a different spectral band of the incident sunlight to electrical power. The laterally separated cells completely rely on optics for achieving spectral separation, while the hybrid cell uses a combination of absorption and optical spatial spectral separation mechanisms. It was found that the hybrid approach incurs less overall system loss. This approach can also take advantage of recent perovskite-silicon tandem cell development.[410]

Another emerging applications is for combined PV conversion and bio-growth (agrivoltaics[411]) where a volume holographic element filters part of the spectrum to match the photosynthesis active region of the spectrum (PAR)[412] and the remainder for electrical conversion.[413] The irradiance at the crop area can also be modified to further enhance plant growth. This approach can be applied to both open fields and greenhouse crops and provides dual use of much more land area with synergistic benefits for crop production.

11 PV Sustainability and Environmental Impact

Section Authors: Annick Anctil (Michigan State University) and Preeti Nain (Michigan State University)

To evaluate the benefit or identify potential concerns of solar PV, one must consider all the stages of the PV industry, from raw material extraction to end-of-life. With the forecasted rapid increase in new PV installations and dismantling of older modules in the upcoming decade, research and development efforts need to 1) minimize the environmental footprint of PV manufacturing and 2) plan for PV recycling and waste management globally.

This update focuses on two areas: PV manufacturing and end-of-life. Over the last decade, the global PV supply chain has moved from Europe, Japan, and the US, to China, which accounts for more than 80% of worldwide production.[415] The combination of policy incentives to support domestic production in North America and restrictions or tariffs on Chinese PV modules and components are responsible for many recent announcements of US PV manufacturing.[416] Carbon

footprint is a criterion for project selection in France and South Korea[417] and other countries will likely follow. Changing the manufacturing location along the supply chain affects the carbon footprint. Manufacturing PV in the US should have a lower carbon footprint than in China, but the difference is decreasing due to grid decarbonization in both countries.[418] In addition to electricity, manufacturing improvements and reduced material usage have led to a lower carbon footprint of PV modules over time.[419,420]

One other concern for PV modules is end-of-life management. Recycling methods for CdTe were established many years ago due to the scarcity of tellurium and toxicity of cadmium[421] but are not as commonly used for silicon. Standard waste characterization methods (i.e., Toxicity Characteristic Leaching Procedure, Waste Extraction Test, etc.) are used to evaluate the toxicity of PV. Copper, iron, aluminum, and lead can leach from PV modules when tested, but their concentration would not exceed the hazardous waste limit.[422] PV end-of-life management is required in Europe and a few states in the US. Still, additional efforts are needed globally to ensure that PV waste is recycled, and environmental impacts are minimized if landfilling is the only option.

A circular economy for PV has become one primary objective for long-term sustainability.[423,424] For manufacturers, low-carbon solar modules are becoming a competitive advantage, and being able to conduct LCA rapidly would facilitate product certification. Changes in material intensity and manufacturing process need to be incorporated in LCA databases to ensure a reduction of the environmental footprint of PV manufacturing with new module technologies.

For recycling, cost remains a challenge for closed-loop recycling of PV modules. Until sufficient modules wastes are produced, a centralized PV recycling scheme would ship wastes over long distances unless waste can be incorporated into the existing waste stream.[421] Another issue is forecasting the volume and value of future waste stream to plan for recycling facilities.[425] Regulations and incentives for recycling are required in addition to inexpensive and effective recycling methods. Figure 26 summarizes the areas of research needs for sustainable PV

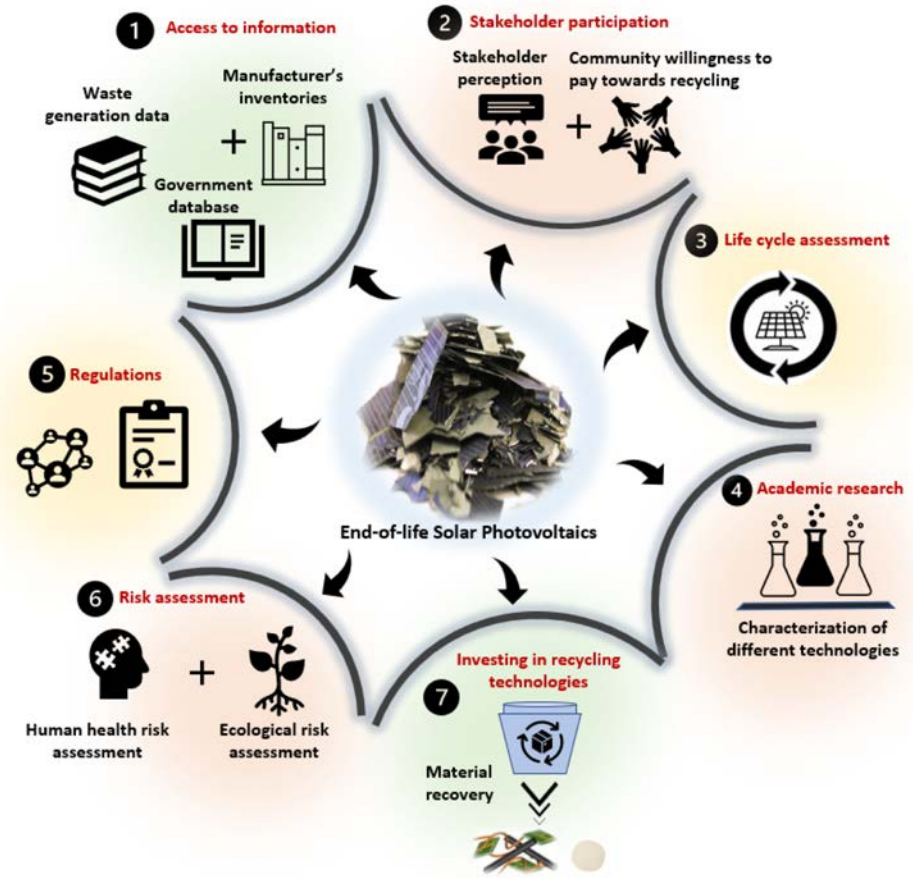

Fig. 26 Framework for sustainable PV management.

management. Overall, manufacturers could improve PV life cycle assessment and end-of-life management with a bill of material disclosure or through third-party certification. Solar technology is considered a green technology, and a holistic approach considering the environmental impact throughout its life-cycle is required to minimize adverse environmental impacts.

12 Conclusions and Perspectives

12.1 Common Themes and Challenges

The diverse contributions to this report demonstrate the remarkable range of emerging PV technologies as well as developments in their applications. They also describe some of the challenges to widespread deployment. Some of these challenges are specific to particular technologies—for example, finding materials for lattice matching for III-V solar cells. However, it is interesting to see that there are also challenges that arise across many (or all) solar technologies. One of these recurring themes is translating lab solar cell performance to modules and on to the production line. This includes challenges of scaling up of coating, module design, and developing appropriate manufacturing tools and processes. It applies not only to solar cells themselves but also to ways of enhancing their efficiency—for example, through light management and photonic structures.

Manufacture is also closely associated with related issues of cost, energy of manufacture and environmental impact. Whilst cost has been recognised for a long time as crucial for determining extent of deployment, the articles show increasing attention being paid to energy payback time, i.e., the time for a solar cell to generate energy equal to that required for its manufacture. There is also growing concern to develop clean manufacturing processes—for example, by using "green" solvents, and to consider the environmental impact of both the process and the materials used. There is increasing awareness of the importance of life cycle analysis. Indeed, to become truly sustainable it will be necessary to develop a circular economy for PV.

Progress in stability is needed for many solar technologies, especially perovskites, organics, and dye-sensitized solar cells, with a 25-year lifetime in the field being desirable. There are grounds for optimism as in related fields, such as organic light-emitting diodes (OLEDs), tremendous progress in stability has been made and the best lifetimes of OLED pixels are much longer than 25 years. Aspects of advancing stability include understanding degradation mechanisms and developing appropriate encapsulation and packaging. The impact of shading also needs to be considered as a shaded solar cell can experience a substantial reverse bias due to its neighbours.

The exciting applications emerging bring their own challenges that need to be addressed. One such issue is developing appropriate testing protocols as the intensity, spectrum and temperature may differ greatly from the standard test conditions developed for silicon solar cells. For example, indoor applications use light that is at shorter wavelength and much less intense than most of the solar spectrum. Stability testing protocols will also need tailoring to the application. Particular applications place their own requirements on solar cells—for example, some large warehouses have flimsy roofs that would only be able to support lightweight solar cells. For agriphotovoltaics and building integration, the transmission (and reflection) spectrum of the solar cells is important.

Finally, the authors share a spirit of optimism regarding the future of PV technology, despite varying perspectives on the priorities and challenges involved (see Sec. 12.2). Overall, this report provides an overview of emerging PV approaches that show potential in helping to achieve the development of new materials, device concepts, and light management strategies to enable higher efficiencies and more scalable and sustainable manufacturing.

12.2 Author Survey and Perspectives

As a way to gain a broader perspective on the field of emerging PV, the authors of this article were asked to complete an anonymous informal survey regarding their projections for the future directions of the field. 19 responses were received. Below is a list of the questions and summary of responses:

Q1: What do you think are the most near-term promising applications of emerging PV technology?
Responses (rank-ordered %): Agriculture (22%), PV-integrated parking structures (14%), Non-III-V in space (12%), IOT (12%), Automotive/mobile (12%), Semitransparent PV windows (10%), Indoor (8%), Other (8%)

Q2: When do you predict perovskites (all perovskite tandem or tandem with other materials) will reach commercialization at the level of 1 MW installation?
Responses (%): 1 - 3 years (26%), 3 - 10 years (47%), 10+ year (0%), Never (11%), No idea (16%)

Q3: When do you predict OPVs of any form will reach commercialization at the level of 1 MW installation?
Responses (%): 1 - 3 years (5%), 3 - 10 years (42%), 10+ year (32%), Never (11%), No idea (11%)

Q4: When do you predict DSSCs will reach commercialization at the level of 1 MW installation?
Responses (%): 1 - 3 years (5%), 3 - 10 years (11%), 10+ year (0%), Never (68%), No idea (16%)

Q5: Which of the "exotic" mechanisms for breaking the detailed balance limit will most likely be commercialized someday?
Responses (rank-ordered %): Photon up/down conversion (32%), Spectrum splitting (24%), Multiexciton generation (11%), None (11%), Hot carrier solar cells (8%), Intermediate band solar cells (5%), 2D absorbers (5%), Singlet fission (3%))

Q6: What PV materials are understudied and deserve more attention?
Responses (alphabetical order): Chalcogenides, Dilute nitrides, Inorganic semiconductors, Lead- and tin-free perovskites, Low bandgap materials, Mismatched materials, Non-toxic earth-abundant Inorganic materials, OPV, Solar concentrators, Thermophotovoltaics, Quantum dots

Q7: Which are the most pressing environmental and sustainability concerns of solar PV, which the community should focus on as technologies are being developed? Please rank the following 5 concerns.
Responses (rank, number): Recyclable solar cells (1^{st}, 4; 2^{nd}, 5; 3^{rd}, 3; 4^{th}, 5; 5^{th}, 2), Lifecycle analysis (1^{st}, 4; 2^{nd}, 1; 3^{rd}, 9; 4^{th}, 4; 1), Elemental availability (1^{st}, 5; 2^{nd}, 3; 3^{rd}, 2; 4^{th}, 5; 5^{th}, 3), Green chemistry for fabrication (1^{st}, 2; 2^{nd}, 7; 3^{rd}, 4; 4^{th}, 3; 5^{th}, 2), Land usage for sustainability (1^{st}, 4; 2^{nd}, 2; 3^{rd}, 1; 4^{th}, 1; 5^{th}, 11)

12.2.1 *Write-in responses*

The authors were also asked to share any final thoughts about the future of PV technologies as write-in responses. Several key responses are quoted below, anonymously.

"It is difficult to predict the future however I dare to say that PV technologies will be widely applied, in various environments, at a terrawatt level, meaning that PV waste management will be one of the greatest challenges for truly sustainable terrestrial and space PV applications."

"I imagine a broadening application space, solar integration and power transfer beyond today's technology."

"Perovskites will be important only if their lifetimes can be made comparable to silicon, CdTe, or CIGS."

"Spectrum splitting will become important if a low-cost wide bandgap material become available."

"Even though I ranked it last, land use is definitely important. I worry when I see articles about different environmental groups on opposite sides of a solar debate."

"PV technologies share in our power generation infrastructure will continue to grow. PV will always be part of the solution for renewable clean energy generation, however, not necessarily the only solution."

12.2.2 *Survey summary and conclusions*

Several speculative conclusions can be drawn from the survey results. In response to the first question, "What do you think are the most near-term promising applications of emerging PV technology," agriculture was the clear winner. This speaks to potential advantages and effectiveness of applying emerging technologies to the agricultural space as well as the importance of the food-energy nexus in global systems. Additionally, one author submitted as a write-in response "Extension of PV installations geographically further north" as a promising near-term application. This statement illustrates how much the PV industry has grown in recent years such that development in regions of the world with sub-optimal solar insolation should be expanded. It also hints at the opportunities for "geographically tailored" PV whose spectral and temperature responses, stability characteristics, and testing protocols are designed for more polar conditions.

In response to questions 2–4, regarding at which time in the future particular technologies will be commercialized at the level of 1 MW installation (an arbitrary value chosen for the purpose of this informal survey), authors were generally optimistic about the development of perovskites (all perovskite or tandems with other materials), with nearly 75% of authors predicting it will occur in less than ten years. OPV were also viewed optimistically with 47% predicting the target will be reached in that timeframe. Dye-sensitized solar cells were generally not viewed optimistically with 68% concluding that they will never reach 1 MW commercialization. However, it is important to note that this was an informal survey given to a statistically small number of researchers in the field. The results should not be considered as well-researched technoeconomic analysis, nor are they intended as guidance for researchers or policy makers in the field.

For question 5, on what mechanisms for breaking the detailed balance limit will most likely be commercialized someday (with no timeframe provided), photon up/down conversion and spectrum splitting received the most responses, with 32% and 12%, respectively. Multiple exciton generation and hot carrier solar cells garnered the third and fourth-highest number of votes. Four authors responded that none of the mechanisms listed would ever be commercialized. The same caveat as mentioned in the previous question also applies to this topic.

In the final question in the survey, on the question about the most pressing environmental and sustainability concerns of solar PV, the authors chose nearly evenly among the listed topics of recyclable solar cells, lifecycle analysis, elemental availability, green chemistry, and land usage. That no clear winner emerged from this question suggests that all these issues require deeper investigation and are critical for future PV implementation at global scale. Overall, the results suggest that researchers and educators in the physical sciences and engineering fields would do well to broaden their knowledge base and research efforts to encompass more aspects of sustainability.

Code and Data Availability

Data sharing is not applicable to this article, as no new data were created or analyzed.

Acknowledgments

This report was edited by Fatima Toor, Ifor D.W. Samuel, and Sean E. Shaheen. Annick Anctil acknowledges grant support from the US National Science Foundation (NSF) Division of Chemical, Bioengineering, Environmental and Transport Systems (CBET): Environmental Sustainability of Photovoltaics in the US (CAREER award no. 2044886). Raymond K. Kostuk and Benjamin D. Chrysler would like to acknowledge that the US NSF and DOE provided funding for the QESST Engineering Research Center (award no. EEC-1041895) for support of their research. Benjamin D. Chrysler would like to acknowledge support from the NSF Graduate Research Fellowship Program (award no. DGE-1143953). Hele Savin and Ville Vähänissi would like to acknowledge the provision of facilities and technical support by Micronova Nanofabrication Centre in Espoo, Finland, within the OtaNano research infrastructure at Aalto University. Hele Savin and Ville Vähänissi would also like to acknowledge funding provided by the Flagship on Photonics Research and Innovation "PREIN" (#346529) funded by the Research Council of Finland. This work was authored in part by the National Renewable Energy Laboratory (NREL), operated by Alliance for Sustainable Energy, LLC, for the US DOE under contract no. DE-AC36-08GO28308. Funding provided by the US DOE Office of Energy Efficiency and the Renewable Energy Solar Energy Technologies Office under award nos. 38257 and 38266. NREL

authors Duong Nguyen Minh and Joseph M. Luther also acknowledge support from the Operational Energy Capability Improvement Fund of the US Department of Defense. The views expressed in the article do not necessarily represent the views of the DOE or the US Government (USG). The USG retains and the publisher, by accepting the article for publication, acknowledges that the USG retains a nonexclusive, paid-up, irrevocable, worldwide license to publish or reproduce the published form of this work, or allow others to do so, for USG purposes.

References

1. L. Fernández, "Share of electricity generation from solar energy worldwide from 2010 to 2022," data from ember-climate.org (accessed July 2023).
2. E. J. Mitchel, "Photovoltaic power systems programme annual report," 2022, https://iea-pvps.org/wp-content/uploads/2023/04/PVPS_Annual_Report_2022_v7-1.pdf.
3. N. M. Haegel et al., "Photovoltaics at multi-terawatt scale: waiting is not an option," *Science* **380**(6640), 39–42 (2023).
4. T. S. Liang et al., "A review of crystalline silicon bifacial photovoltaic performance characterisation and simulation," *Energy Environ. Sci.* **12**(1), 116–148 (2019).
5. J. Trube and P. Baliozian, *International Technology Roadmap for Photovoltaic (ITRPV) 2022 Results*, 14th ed., VDMA e.V. (2023).
6. A. Blakers, "Development of the PERC solar cell," *IEEE J. Photovoltaics* **9**(3), 629–635 (2019).
7. J. Zhao et al., "24% efficient perl silicon solar cell: recent improvements in high efficiency silicon cell research," *Sol. Energy Mater. Sol. Cells* **41**, 87–99 (1996).
8. J. Zhao, A. Wang, and M. A. Green, "24.5% efficiency PERT silicon solar cells on SEH MCZ substrates and cell performance on other SEH CZ and FZ substrates," *Sol. Energy Mater. Sol. Cells* **66**(1), 27–36 (2001).
9. D. K. Ghosh et al., "Fundamentals, present status and future perspective of TOPCon solar cells: a comprehensive review," *Surf. Interfaces* **30**, 101917 (2022).
10. J. S. Stein, "Bifacial PV Project - PV Performance Modeling Collaborative (PVPMC)," 2023, https://pvpmc.sandia.gov/pv-research/bifacial-pv-project/ (accessed July 2023).
11. G. J. Ward, "The RADIANCE lighting simulation and rendering system," in *SIGGRAPH '94: Proc. 21st Annu. Conf. Comput. Graphics and Interact. Tech.*, pp. 459–472 (1994).
12. A. Asgharzadeh et al., "A sensitivity study of the impact of installation parameters and system configuration on the performance of bifacial PV arrays," *IEEE J. Photovoltaics* **8**(3), 798–805 (2018).
13. A. Asgharzadeh et al., "A comparison study of the performance of south/north-facing vs east/west-facing bifacial modules under shading condition," in *IEEE 7th World Conf. Photovoltaics Energy Convers. (WCPEC) (Joint Conf. of 45th IEEE PVSC, 28th PVSEC & 34th EU PVSEC)*, pp. 1730–1734 (2018).
14. J. S. Stein et al., "Outdoor field performance from bifacial photovoltaic modules and systems," in *IEEE 44th Photovoltaics Spec. Conf. (PVSC)*, pp. 3184–3189 (2017).
15. D. Riley et al., "A performance model for bifacial PV modules," in *IEEE 44th Photovoltaics Spec. Conf. (PVSC)*, pp. 3348–3353 (2017).
16. B. Marion et al., "A practical irradiance model for bifacial PV modules," in *IEEE 44th Photovoltaics Spec. Conf. (PVSC)*, pp. 1537–1542 (2017).
17. C. W. Hansen et al., "Analysis of irradiance models for bifacial PV modules," in *IEEE 43rd Photovoltaics Spec. Conf. (PVSC)*, pp. 0138–0143 (2016).
18. C. W. Hansen et al., "A detailed model of rear-side irradiance for bifacial PV modules," in *IEEE 44th Photovoltaics Spec. Conf. (PVSC)*, pp. 1543–1548 (2017).
19. C. Deline et al., "Evaluation and field assessment of bifacial photovoltaic module power rating methodologies," in *IEEE 44th Photovoltaics Spec. Conf. (PVSC)*, pp. 3698–3703 (2017).
20. C. Deline et al., "Assessment of bifacial photovoltaic module power rating methodologies—inside and out," *IEEE J. Photovoltaics* **7**(2), 575–580 (2017).
21. "IEC 60904: photovoltaic devices – Part 1-2: measurement of current-voltage characteristics of bifacial photovoltaic (PV) devices (Draft A)," 2023, https://pvpmc.sandia.gov/app/uploads/sites/243/2022/11/IEC_60904-1-2_IV_Bifacial_draft_A_ver7_submitted.pdf.
22. T. Pasanen et al., "Industrial applicability of antireflection-coating-free black silicon on PERC solar cells and modules," in *35th Eur. Photovoltaics Solar Energy Conf. and Exhibit.*, pp. 552–556 (2018).
23. L. L. Ma et al., "Wide-band "black silicon" based on porous silicon," *Appl. Phys. Lett.* **88**(17), 171907 (2006).
24. C. C. Striemer and P. M. Fauchet, "Dynamic etching of silicon for broadband antireflection applications," *Appl. Phys. Lett.* **81**(16), 2980–2982 (2002).
25. H. K. Raut et al., "Anti-reflective coatings: a critical, in-depth review," *Energy Environ. Sci.* **4**(10), 3779 (2011).

26. M. Otto et al., "Black silicon photovoltaics," *Adv. Opt. Mater.* **3**(2), 147–164 (2015).
27. A. J. Bett et al., "Wave optical simulation of the light trapping properties of black silicon surface textures," *Opt. Express* **24**(6), A434 (2016).
28. A. Ingenito, O. Isabella, and M. Zeman, "Experimental demonstration of $4n^2$ classical absorption limit in nanotextured ultrathin solar cells with dielectric omnidirectional back reflector," *ACS Photonics* **1**(3), 270–278 (2014).
29. M. Garín et al., "Black ultra-thin crystalline silicon wafers reach the $4n^2$ absorption limit–Application to IBC Solar Cells," *Small* **19**(39), 2302250 (2023).
30. G. Dingemans and W. M. M. Kessels, "(Invited) Aluminum oxide and other ALD materials for Si surface passivation," *ECS Trans.* **41**(2), 293–301 (2011).
31. G. Dingemans and W. M. M. Kessels, "Status and prospects of Al_2O_3-based surface passivation schemes for silicon solar cells," *J. Vac. Sci. Technol. A: Vac. Surf. Films* **30**(4), 040802 (2012).
32. M. Otto et al., "Extremely low surface recombination velocities in black silicon passivated by atomic layer deposition," *Appl. Phys. Lett.* **100**(19), 191603 (2012).
33. P. Repo et al., "Effective passivation of black silicon surfaces by atomic layer deposition," *IEEE J. Photovoltaics* **3**(1), 90–94 (2013).
34. H. Savin et al., "Black silicon solar cells with interdigitated back-contacts achieve 22.1% efficiency," *Nat. Nanotechnol.* **10**(7), 624–628 (2015).
35. J. Oh, H.-C. Yuan, and H. M. Branz, "An 18.2%-efficient black-silicon solar cell achieved through control of carrier recombination in nanostructures," *Nat. Nanotechnol.* **7**(11), 743–748 (2012).
36. S. Zhong et al., "Influence of the texturing structure on the properties of black silicon solar cell," *Sol. Energy Mater. Sol. Cells* **108**, 200–204 (2013).
37. P. Li et al., "Effective optimization of emitters and surface passivation for nanostructured silicon solar cells," *RSC Adv.* **6**(106), 104073–104081 (2016).
38. B. Kafle et al., "On the emitter formation in nanotextured silicon solar cells to achieve improved electrical performances," *Sol. Energy Mater. Sol. Cells* **152**, 94–102 (2016).
39. J. Benick et al., "High-efficiency n-Type HP mc silicon solar cells," *IEEE J. Photovoltaics* **7**(5), 1171–1175 (2017).
40. X. Dai et al., "The influence of surface structure on diffusion and passivation in multicrystalline silicon solar cells textured by metal assisted chemical etching (MACE) method," *Sol. Energy Mater. Sol. Cells* **186**, 42–49 (2018).
41. T. H. Fung et al., "Improved emitter performance of RIE black silicon through the application of in-situ oxidation during POCl3 diffusion," *Sol. Energy Mater. Sol. Cells* **210**, 110480 (2020).
42. G. Scardera et al., "On the enhanced phosphorus doping of nanotextured black silicon," *IEEE J. Photovoltaics* **11**(2), 298–305 (2021).
43. G. Von Gastrow et al., "Recombination processes in passivated boron-implanted black silicon emitters," *J. Appl. Phys.* **121**(18), 185706 (2017).
44. K. Chen et al., "Harnessing carrier multiplication in silicon solar cells using UV photons," *IEEE Photonics Technol. Lett.* **33**(24), 1415–1418 (2021).
45. L. Sainiemi et al., "Non-reflecting silicon and polymer surfaces by plasma etching and replication," *Adv. Mater.* **23**(1), 122–126 (2011).
46. M. M. Plakhotnyuk et al., "Low surface damage dry etched black silicon," *J. Appl. Phys.* **122**(14), 143101 (2017).
47. B. Iandolo et al., "Black silicon with ultra-low surface recombination velocity fabricated by inductively coupled power plasma," *Physica Status Solidi (RRL) – Rapid Res. Lett.* **13**(2), 1800477 (2019).
48. X. Li and P. W. Bohn, "Metal-assisted chemical etching in HF/H_2O_2 produces porous silicon," *Appl. Phys. Lett.* **77**(16), 2572–2574 (2000).
49. Z. Huang et al., "Metal-assisted chemical etching of silicon: a review: in memory of Prof. Ulrich Gösele," *Adv. Mater.* **23**(2), 285–308 (2011).
50. F. Toor et al., "Nanostructured silicon via metal assisted catalyzed etch (MACE): chemistry fundamentals and pattern engineering," *Nanotechnology* **27**(41), 412003 (2016).
51. F. Toor et al., "Metal assisted catalyzed etched (MACE) black Si: optics and device physics," *Nanoscale* **8**(34), 15448–15466 (2016).
52. Y.-T. Lu and A. R. Barron, "Nanopore-type black silicon anti-reflection layers fabricated by a one-step silver-assisted chemical etching," *Phys. Chem. Chem. Phys.* **15**(24), 9862 (2013).
53. Y. Matsui and S. Adachi, "Optical properties of "black silicon" formed by catalytic etching of Au/Si(100) wafers," *J. Appl. Phys.* **113**(17), 173502 (2013).
54. D. T. Cao et al., "Effect of $AgNO_3$ concentration on structure of aligned silicon nanowire arrays fabricated via silver-assisted chemical etching," *Int. J. Nanotechnol.* **10**(3/4), 343 (2013).
55. K. Chen et al., "MACE nano-texture process applicable for both single- and multi-crystalline diamond-wire sawn Si solar cells," *Sol. Energy Mater. Sol. Cells* **191**, 1–8 (2019).

56. S. K. Sundaram and E. Mazur, "Inducing and probing non-thermal transitions in semiconductors using femtosecond laser pulses," *Nat. Mater.* **1**(4), 217–224 (2002).
57. M. Huang et al., "The morphological and optical characteristics of femtosecond laser-induced large-area micro/nanostructures on GaAs, Si, and brass," *Opt. Express* **18**(S4), A600 (2010).
58. C. H. Crouch et al., "Infrared absorption by sulfur-doped silicon formed by femtosecond laser irradiation," *Appl. Phys. A* **79**(7), 1635–1641 (2004).
59. Y. Peng et al., "Optimal proportional relation between laser power and pulse number for the fabrication of surface-microstructured silicon," *Appl. Opt.* **50**(24), 4765 (2011).
60. B. Radfar, F. Es, and R. Turan, "Effects of different laser modified surface morphologies and post-texturing cleanings on c-Si solar cell performance," *Renew. Energy* **145**, 2707–2714 (2020).
61. B. Radfar et al., "Optoelectronic properties of black silicon fabricated by femtosecond laser in ambient air: exploring a large parameter space," *Opt. Lett.* **48**(5), 1224 (2023).
62. T. P. Pasanen et al., "Impact of black silicon on light- and elevated temperature-induced degradation in industrial passivated emitter and rear cells," *Prog. Photovoltaics Res. Appl.* **27**(11), 918–925 (2019).
63. T. P. Pasanen et al., "Black silicon significantly enhances phosphorus diffusion gettering," *Sci. Rep.* **8**(1), 1991 (2018).
64. M. U. Khan et al., "The role of metal-catalyzed chemical etching black silicon in the reduction of light- and elevated temperature-induced degradation in P-type multicrystalline wafers," *IEEE J. Photovoltaics* **11**(3), 627–633 (2021).
65. P. Ortega et al., "Black silicon back-contact module with wide light acceptance angle," *Prog. Photovoltaics Res. Appl.* **28**(3), 210–216 (2020).
66. "Best research-cell efficiency chart," 2023, https://www.nrel.gov/pv/cell-efficiency.html.
67. H. M. Wikoff, S. B. Reese, and M. O. Reese, "Embodied energy and carbon from the manufacture of cadmium telluride and silicon photovoltaics," *Joule* **6**(7), 1710–1725 (2022).
68. V. Bermudez and A. Perez-Rodriguez, "Understanding the cell-to-module efficiency gap in Cu(In,Ga)(S,Se) 2 photovoltaics scale-up," *Nat. Energy* **3**(6), 466–475 (2018).
69. T. Song, A. Kanevce, and J. R. Sites, "Emitter/absorber interface of CdTe solar cells," *J. Appl. Phys.* **119**(23), 233104 (2016).
70. M. A. Green et al., "Solar cell efficiency tables (Version 61)," *Prog. Photovoltaics Res. Appl.* **31**(1), 3–16 (2023).
71. T. Ablekim et al., "Exceeding 200 ns lifetimes in polycrystalline CdTe solar cells," *Solar RRL* **5**(8), 2100173 (2021).
72. J. M. Kephart et al., "Sputter-deposited oxides for interface passivation of CdTe photovoltaics," *IEEE J. Photovoltaics* **8**(2), 587–593 (2018).
73. J. M. Burst et al., "CdTe solar cells with open-circuit voltage breaking the 1 V barrier," *Nat. Energy* **1**(3), 16015 (2016).
74. J. M. Burst et al., "Carrier density and lifetime for different dopants in single-crystal and polycrystalline CdTe," *APL Mater.* **4**(11), 116102 (2016).
75. D. Krasikov et al., "Comparative study of As and Cu doping stability in CdSeTe absorbers," *Sol. Energy Mater. Sol. Cells* **224**, 111012 (2021).
76. A. Kanevce et al., "The roles of carrier concentration and interface, bulk, and grain-boundary recombination for 25% efficient CdTe solar cells," *J. Appl. Phys.* **121**(21), (2017).
77. J. Moseley et al., "Impact of dopant-induced optoelectronic tails on open-circuit voltage in arsenic-doped Cd(Se)Te solar cells," *J. Appl. Phys.* **128**(10), 103105 (2020).
78. R. Mallick et al., "Arsenic-doped CdSeTe solar cells achieve world record 22.3% efficiency," *IEEE J. Photovoltaics* **13**, 510–515 (2023).
79. G. Xiong and W. Metzger, *Thin Film Cadmium Telluride Photovoltaics*, Elsevier (2022).
80. W. K. Metzger et al., "Exceeding 20% efficiency with in situ group V doping in polycrystalline CdTe solar cells," *Nat. Energy* **4**(10), 837–845 (2019).
81. W. K. Metzger et al., "As-doped CdSeTe solar cells achieving 22% efficiency with −0.23%/°C temperature coefficient," *IEEE J. Photovoltaics* **12**(6), 1435–1438 (2022).
82. K. K. Subedi et al., "Enabling bifacial thin film devices by developing a back surface field using CuxAlOy," *Nano Energy* **83**, 105827 (2021).
83. A. W. Walker et al., "The effects of absorption and recombination on quantum dot multijunction solar cell efficiency," *IEEE J. Photovoltaics* **3**(3), 1118–1124 (2013).
84. R. M. France et al., "Triple-junction solar cells with 39.5% terrestrial and 34.2% space efficiency enabled by thick quantum well superlattices," *Joule* **6**(5), 1121–1135 (2022).
85. P. Schygulla et al., "Wafer-bonded two-terminal III–V//Si triple-junction solar cell with power conversion efficiency of 36.1% at AM1.5g," presented at 40th EU PVSEC, Lisbon 2DO.9 (2023); submitted to *Prog. Photovoltaics Res. Appl.*.
86. F. Dimroth et al., "Four-junction wafer-bonded concentrator solar cells," *IEEE J. Photovoltaics*, **6**(1), 343–349 (2016).

87. R. Cariou et al., "III–V-on-silicon solar cells reaching 33% photoconversion efficiency in two-terminal configuration," *Nat. Energy* **3**(4), 326–333 (2018).
88. T. J. Grassman et al., "$GaAs_{0.75}P_{0.25}$/Si dual-junction solar cells grown by MBE and MOCVD," *IEEE J. Photovoltaics* **6**(1), 326–331 (2016).
89. J. F. Geisz et al., "Building a six-junction inverted metamorphic concentrator solar cell," *IEEE J. Photovoltaics* **8**(2), 626–632 (2018).
90. R. M. France et al., "Metamorphic epitaxy for multijunction solar cells," *MRS Bull.* **41**(3), 202–209 (2016).
91. M. A. Green et al., "Solar cell efficiency tables (version 54)," *Prog. Photovoltaics Res. Appl.* **27**(7), 565–575 (2019).
92. K. T. VanSant, A. C. Tamboli, and E. L. Warren, "III-V-on-Si tandem solar cells," *Joule* **5**(3), 514–518 (2021).
93. K. Makita et al., "III-V//$Cu_xIn_{1-y}Ga_ySe_2$ multijunction solar cells with 27.2% efficiency fabricated using modified smart stack technology with Pd nanoparticle array and adhesive material," *Prog. Photovoltaics Res. Appl.* **29**(8), 887–898 (2021).
94. S. Essig et al., "Raising the one-sun conversion efficiency of III–V/Si solar cells to 32.8% for two junctions and 35.9% for three junctions," *Nat. Energy* **2**(9), 17144 (2017).
95. M. A. Green et al., "Solar cell efficiency tables (version 50)," *Prog. Photovoltaics Res. Appl.* **25**(7), 668–676 (2017).
96. C. E. Valdivia and K. Hinzer, "Subcell segmentation for current matching and design flexibility in multi-junction solar cells," *IEEE J. Photovoltaics* **10**(5), 1329–1339 (2020).
97. M. M. Wilkins et al., "Ripple-free boost-mode power supply using photonic power conversion," *IEEE Trans. Power Electron.* **34**(2), 1054–1064 (2019).
98. S. Fafard et al., "Ultrahigh efficiencies in vertical epitaxial heterostructure architectures," *Appl. Phys. Lett.* **108**(7), 071101 (2016).
99. S. Fafard et al., "High-photovoltage GaAs vertical epitaxial monolithic heterostructures with 20 thin p/n junctions and a conversion efficiency of 60%," *Appl. Phys. Lett.* **109**(13), 131107 (2016).
100. S. Fafard and D. P. Masson, "High-efficiency and high-power multijunction InGaAs/InP photovoltaic laser power converters for 1470 nm," *Photonics* **9**(7), 438 (2022).
101. M. Feifel et al., "Epitaxial GaInP/GaAs/Si triple-junction solar cell with 25.9% AM1.5g efficiency enabled by transparent metamorphic $Al_xGa_{1-x}AsyP_{1-y}$ step-graded buffer structures," *Solar RRL* **5**, 2000763 (2021).
102. M. A. Green et al., "Solar cell efficiency tables (version 51)," *Prog. Photovoltaics Res. Appl.* **26**(1), 3–12 (2018).
103. M. A. Green et al., "Solar cell efficiency tables (version 56)," *Prog. Photovoltaics Res. Appl.* **28**(7), 629–638 (2020).
104. M. A. Green et al., "Solar cell efficiency tables (Version 53)," *Prog. Photovoltaics Res. Appl.* **27**(1), 3–12 (2019).
105. Sharp Corporation, "Press release: sharp develops concentrator solar cell with world's highest conversion efficiency of 43.5%," 2012, http://sharp-world.com/corporate/news/120531.html (accessed 2 Jan. 2023).
106. NREL, "News release: NREL demonstrates 45.7% efficiency for concentrator solar cell," NR-4514, 2014, https://www.nrel.gov/news/press/2014/15436.html (accessed 2 Jan. 2023).
107. I. Almansouri et al., "Supercharging silicon solar cell performance by means of multijunction concept," *IEEE J. Photovoltaics* **5**(3), 968–976 (2015).
108. M. Levinshtein, S. Rumyantsev, and M. Shur, *Handbook Series on Semiconductor Parameters: Volume 2: Ternary And Quaternary III-V Compounds*, World Scientific (1996).
109. J. M. Gee and G. F. Virshup, "A 31%-efficient GaAs/silicon mechanically stacked, multijunction concentrator solar cell," in *Conf. Rec. of the Twentieth IEEE Photovoltaics Spec. Conf.*, IEEE, Las Vegas, Nevada (1988).
110. S. Essig et al., "Boosting the efficiency of III-V/Si tandem solar cells," in *IEEE 43rd Photovoltaics Spec. Conf. (PVSC)*, IEEE, Portland, Oregon (2016).
111. M. Schnabel et al., "Three-terminal III–V/Si tandem solar cells enabled by a transparent conductive adhesive," *Sustain. Energy Fuels* **4**(2), 549–558 (2020).
112. H. Mizuno et al., "Integration of Si heterojunction solar cells with III–V solar cells by the Pd nanoparticle array-mediated "Smart Stack" approach," *ACS Appl. Mater. Interfaces* **14**(9), 11322–11329 (2022).
113. K. Tanabe, K. Watanabe, and Y. Arakawa, "III-V/Si hybrid photonic devices by direct fusion bonding," *Sci. Rep.* **2**(1), 349 (2012).
114. K. Derendorf et al., "Fabrication of GaInP/GaAs//Si solar cells by surface activated direct wafer bonding," *IEEE J. Photovoltaics* **3**(4), 1423–1428 (2013).
115. S. Fan et al., "Current-matched III–V/Si epitaxial tandem solar cells with 25.0% efficiency," *Cell Rep. Phys. Sci.* **1**(9), 100208 (2020).

116. B. Kunert et al., "How to control defect formation in monolithic III/V hetero-epitaxy on (100) Si? A critical review on current approaches," *Semicond. Sci. Technol.* **33**(9), 093002 (2018).
117. J. T. Boyer et al., "Correlation of early-stage growth process conditions with dislocation evolution in MOCVD-based GaP/Si heteroepitaxy," *J. Cryst. Growth* **571**, 126251 (2021).
118. R. D. Hool et al., "Challenges of relaxed *n*-type GaP on Si and strategies to enable low threading dislocation density," *J. Appl. Phys.* **130**(24), 243104 (2021).
119. S. Essig et al., "Fast atom beam-activated n-Si/n-GaAs wafer bonding with high interfacial transparency and electrical conductivity," *J. Appl. Phys.* **113**(20), 203512 (2013).
120. H. Liu et al., "A worldwide theoretical comparison of outdoor potential for various silicon-based tandem module architecture," *Cell Rep. Phys. Sci.* **1**(4), 100037 (2020).
121. M. Rienäcker et al., "Mechanically stacked dual-junction and triple-junction III-V/Si-IBC cells with efficiencies of 31.5 % and 35.4," in *33rd Eur. Photovoltaics Solar Energy Conf. and Exhibit.* (2017).
122. K. Makita et al., "III-V//Si multijunction solar cells with 30% efficiency using smart stack technology with Pd nanoparticle array," *Prog. Photovoltaics Res. Appl.* **28**(1), 16–24 (2020).
123. J. Simon et al., "III-V-based optoelectronics with low-cost dynamic hydride vapor phase epitaxy," *Crystals* **9**(1), 3 (2018).
124. J. Chen and C. E. Packard, "Controlled spalling-based mechanical substrate exfoliation for III-V solar cells: a review," *Sol. Energy Mater. Sol. Cells* **225**, 111018 (2021).
125. K. Schulte, *High-Efficiency, Low-Cost III-V Solar Cells by Dynamic Hydride Vapor Phase Epitaxy Coupled with Rapid, Polishing-Free Wafer Reuse through Orientation-Optimized (110) Spalling*. No. NREL/TP-5900-80411, National Renewable Energy Lab. (NREL), Golden, Colorado (2021).
126. K. A. Horowitz et al., *A Techno-Economic Analysis and Cost Reduction Roadmap for III-V Solar Cells* (2018).
127. A. R. Bowring et al., "Reverse bias behavior of halide perovskite solar cells," *Adv. Energy Mater.* **8**(8), 1702365 (2018).
128. D. Bogachuk et al., "Perovskite photovoltaic devices with carbon-based electrodes withstanding reverse-bias voltages up to –9 V and surpassing IEC 61215:2016 International Standard," *Solar RRL* **6**(3), 2100527 (2022).
129. L. Bertoluzzi et al., "Incorporating electrochemical halide oxidation into drift-diffusion models to explain performance losses in perovskite solar cells under prolonged reverse bias," *Adv. Energy Mater.* **11**(10), 2002614 (2021).
130. I. E. Gould et al., "In-operando characterization of P-I-N perovskite solar cells under reverse bias," in *IEEE 48th Photovoltaics Spec. Conf. (PVSC)*, pp. 1365–1367 (2021).
131. R. A. Z. Razera et al., "Instability of p–i–n perovskite solar cells under reverse bias," *J. Mater. Chem. A* **8**(1), 242–250 (2020).
132. W. Li et al., "Sparkling hot spots in perovskite solar cells under reverse bias," *ChemPhysMater* **1**(1), 71–76 (2022).
133. Z. Ni et al., "Evolution of defects during the degradation of metal halide perovskite solar cells under reverse bias and illumination," *Nat. Energy* **7**(1), 65–73 (2021).
134. J. Qian et al., "Destructive reverse bias pinning in perovskite/silicon tandem solar modules caused by perovskite hysteresis under dynamic shading," *Sustain. Energy Fuels* **4**(8), 4067–4075 (2020).
135. S. G. Motti et al., "Controlling competing photochemical reactions stabilizes perovskite solar cells," *Nat. Photonics* **13**(8), 532–539 (2019).
136. G. Y. Kim et al., "Photo-effect on ion transport in mixed cation and halide perovskites and implications for photo-demixing," *Angew. Chem.* **133**(2), 833–839 (2021).
137. S. Bitton and N. Tessler, "Perovskite ionics – elucidating degradation mechanisms in perovskite solar cells *via* device modelling and iodine chemistry," *Energy Environ. Sci.* **16**(6), 2621–2628 (2023).
138. Z. Xu et al., "Halogen redox shuttle explains voltage-induced halide redistribution in mixed-halide perovskite devices," *ACS Energy Lett.* **8**(1), 513–520 (2023).
139. E. J. Wolf et al., "Designing modules to prevent reverse bias degradation in perovskite solar cells when partial shading occurs," *Solar RRL* **6**(3), 2100239 (2022).
140. B. Chen et al., "Insights into the development of monolithic perovskite/silicon tandem solar cells," *Adv. Energy Mater.* **12**(4), 2003628 (2022).
141. L. A. Zafoschnig, S. Nold, and J. C. Goldschmidt, "The race for lowest costs of electricity production: techno-economic analysis of silicon, perovskite and tandem solar cells," *IEEE J. Photovoltaics* **10**(6), 1632–1641 (2020).
142. F. Fu et al., "Monolithic perovskite-silicon tandem solar cells: from the lab to fab?" *Adv. Mater.* **34**(24), 2106540 (2022).
143. J. P. Mailoa et al., "A 2-terminal perovskite/silicon multijunction solar cell enabled by a silicon tunnel junction," *Appl. Phys. Lett.* **106**(12), 121105 (2015).

144. C. D. Bailie et al., "Mechanically stacked and monolithically integrated perovskite/silicon tandems and the challenges for high efficiency," in *IEEE 42nd Photovoltaics Spec. Conf. (PVSC)*, IEEE, New Orleans, Louisiana (2015).
145. J. Liu et al., "Efficient and stable perovskite-silicon tandem solar cells through contact displacement by MgF_x," *Science* **377**(6603), 302–306 (2022).
146. F. Sahli et al., "Fully textured monolithic perovskite/silicon tandem solar cells with 25.2% power conversion efficiency," *Nat. Mater.* **17**(9), 820–826 (2018).
147. E. Aydin et al., "Interplay between temperature and bandgap energies on the outdoor performance of perovskite/silicon tandem solar cells," *Nat. Energy* **5**(11), 851–859 (2020).
148. Z. Song et al., "Wide-bandgap, low-bandgap, and tandem perovskite solar cells," *Semicond. Sci. Technol.* **34**(9), 093001 (2019).
149. F. Gota et al., "Energy yield modelling of textured perovskite/silicon tandem photovoltaics with thick perovskite top cells," *Opt. Express* **30**(9), 14172 (2022).
150. S. Akhil et al., "Review on perovskite silicon tandem solar cells: status and prospects 2T, 3T and 4T for real world conditions," *Mater. Des.* **211**, 110138 (2021).
151. Y. Huang et al., "Limitations and solutions for achieving high-performance perovskite tandem photovoltaics," *Nano Energy* **88**, 106219 (2021).
152. Y. Hou et al., "Efficient tandem solar cells with solution-processed perovskite on textured crystalline silicon," *Science* **367**(6482), 1135–1140 (2020).
153. P. Tockhorn et al., "Nano-optical designs for high-efficiency monolithic perovskite–silicon tandem solar cells," *Nat. Nanotechnol.* **17**, 1214–1221 (2022).
154. Interactive best research-cell efficiency chart, https://www.nrel.gov/pv/interactive-cell-efficiency.html (accessed 30 November 2023).
155. T. Duong et al., "Bulk incorporation with 4-methylphenethylammonium chloride for efficient and stable methylammonium-free perovskite and perovskite-silicon tandem solar cells," *Adv. Energy Mater.* **13**(9), 2203607 (2023).
156. H. Kanda et al., "Three-terminal perovskite/integrated back contact silicon tandem solar cells under low light intensity conditions," *Interdiscipl. Mater.* **1**(1), 148–156 (2022).
157. P. Tockhorn et al., "Three-terminal perovskite/silicon tandem solar cells with top and interdigitated rear contacts," *ACS Appl. Energy Mater.* **3**(2), 1381–1392 (2020).
158. C. Chen et al., "Perovskite solar cells based on screen-printed thin films," *Nature* **612**(7939), 266–271 (2022).
159. Z. Li et al., "Scalable fabrication of perovskite solar cells," *Nat. Rev. Mater.* **3**(4), 18017 (2018).
160. Y. Rong et al., "Toward industrial-scale production of perovskite solar cells: screen printing, slot-die coating, and emerging techniques," *J. Phys. Chem. Lett.* **9**(10), 2707–2713 (2018).
161. S. P. Dunfield et al., "From defects to degradation: a mechanistic understanding of degradation in perovskite solar cell devices and modules," *Adv. Energy Mater.* **10**(26), 1904054 (2020).
162. R. Azm et al., "Damp heat–stable perovskite solar cells with tailored-dimensionality 2D/3D heterojunctions," *Science* **376**(6588), 73–77 (2022).
163. H. Lin et al., "Silicon heterojunction solar cells with up to 26.81% efficiency achieved by electrically optimized nanocrystalline-silicon hole contact layers," *Nat. Energy*, **8**, 789–799 (2023).
164. T. Rößler et al., "Production of Full-size Perovskite Silicon Heterojunction Tandem PV Modules with more than 23% Efficiency and more than 430 Wp," 2022, Tandem PV Workshop, Freiburg, Germany (2022).
165. K. Chong et al., "Realizing 19.05% efficiency polymer solar cells by progressively improving charge extraction and suppressing charge recombination," *Adv. Mater.* **34**(13), 2109516 (2022).
166. C. He et al., "Manipulating the D:A interfacial energetics and intermolecular packing for 19.2% efficiency organic photovoltaics," *Energy Environ. Sci.* **15**(6), 2537–2544 (2022).
167. R. Sun et al., "Single-junction organic solar cells with 19.17% efficiency enabled by introducing one asymmetric guest acceptor," *Adv. Mater.* **34**(26), 2110147 (2022).
168. J. Yuan et al., "Single-junction organic solar cell with over 15% efficiency using fused-ring acceptor with electron-deficient core," *Joule* **3**(4), 1140–1151 (2019).
169. Y. Cui et al., "Over 16% efficiency organic photovoltaic cells enabled by a chlorinated acceptor with increased open-circuit voltages," *Nat. Commun.* **10**(1), 2515 (2019).
170. Z. Luo et al., "Fine-tuning energy levels via asymmetric end groups enables polymer solar cells with efficiencies over 17%," *Joule* **4**(6), 1236–1247 (2020).
171. L. Yan et al., "Regioisomer-free difluoro-monochloro terminal-based hexa-halogenated acceptor with optimized crystal packing for efficient binary organic solar cells," *Angew. Chem. Int. Ed.* **134**(46), e202209454 (2022).
172. D. Yuk et al., "Simplified Y6-based nonfullerene acceptors: in-depth study on molecular structure–property relation, molecular dynamics simulation, and charge dynamics," *Small* **19**(10), 2206547 (2023).

173. H. Yu et al., "A vinylene-linker-based polymer acceptor featuring a coplanar and rigid molecular conformation enables high-performance all-polymer solar cells with over 17% efficiency," *Adv. Mater.* **34**(27), 2200361 (2022).
174. C. Sun et al., "Dimerized small-molecule acceptors enable efficient and stable organic solar cells," *Joule* **7**(2), 416–430 (2023).
175. G. Wang et al., "Large-area organic solar cells: material requirements, modular designs, and printing methods," *Adv. Mater.* **31**(45), 1805089 (2019).
176. J. S. Park et al., "Material design and device fabrication strategies for stretchable organic solar cells," *Adv. Mater.* **34**(31), 2201623 (2022).
177. Y. Li et al., "Semitransparent organic photovoltaics for building-integrated photovoltaic applications," *Nat. Rev. Mater.* **8**(3), 186–201 (2022).
178. J. W. Lee et al., "Intrinsically stretchable and non-halogenated solvent processed polymer solar cells enabled by hydrophilic spacer-incorporated polymers," *Adv. Energy Mater.* **12**(46), 2202224 (2022).
179. F. Qi et al., "Dimer acceptor adopting a flexible linker for efficient and durable organic solar cells," *Angew. Chem. Int. Ed.* **62**(21), e202303066 (2023).
180. M. Niggemann et al., "Light trapping in organic solar cells: light trapping in organic solar cells," *Physica Status Solidi (A)* **205**(12), 2862–2874 (2008).
181. Z. Tang, W. Tress, and O. Inganäs, "Light trapping in thin film organic solar cells," *Mater. Today* **17**(8), 389–396 (2014).
182. Z. T. Olle Inganäs, J. Bergqvist, and K. Tvingstedt, *Organic Solar Cells: Fundamentals, Devices, and Upscaling*, B. P. Rand and H. Richter, Eds., CRC Press, Taylor and Francis Group, Boca Raton (2014).
183. Y. Firdaus et al., "Long-range exciton diffusion in molecular non-fullerene acceptors," *Nat. Commun.* **11**(1), 5220 (2020).
184. W. Yang et al., "Balancing the efficiency, stability, and cost potential for organic solar cells via a new figure of merit," *Joule* **5**(5), 1209–1230 (2021).
185. L. A. A. Pettersson, L. S. Roman, and O. Inganäs, "Modeling photocurrent action spectra of photovoltaic devices based on organic thin films," *J. Appl. Phys.* **86**(1), 487–496 (1999).
186. L. S. Roman et al., "High quantum efficiency polythiophene," *Adv. Mater.* **10**(10), 774–777 (1998).
187. P. Peumans, V. Bulović, and S. R. Forrest, "Efficient photon harvesting at high optical intensities in ultrathin organic double-heterostructure photovoltaic diodes," *Appl. Phys. Lett.* **76**(19), 2650–2652 (2000).
188. B. V. Andersson et al., "An optical spacer is no panacea for light collection in organic solar cells," *Appl. Phys. Lett.* **94**(4), 043302 (2009).
189. Q. Liu et al., "Inverse optical cavity design for ultrabroadband light absorption beyond the conventional limit in low-bandgap nonfullerene acceptor–based solar cells," *Adv. Energy Mater.* **9**(20), 1900463 (2019).
190. J. Wang et al., "A tandem organic photovoltaic cell with 19.6% efficiency enabled by light distribution control," *Adv. Mater.* **33**(39), 2102787 (2021).
191. L. Zuo et al., "Microcavity-enhanced light-trapping for highly efficient organic parallel tandem solar cells," *Adv. Mater.* **26**(39), 6778–6784 (2014).
192. B. Siegmund et al., "Organic narrowband near-infrared photodetectors based on intermolecular charge-transfer absorption," *Nat. Commun.* **8**(1), 15421 (2017).
193. B. V. Andersson, N.-K. Persson, and O. Inganäs, "Comparative study of organic thin film tandem solar cells in alternative geometries," *J. Appl. Phys.* **104**(12), 124508 (2008).
194. K. Tvingstedt et al., "Surface plasmon increase absorption in polymer photovoltaic cells," *Appl. Phys. Lett.* **91**(11), 113514 (2007).
195. Y. Zhou et al., "Multifolded polymer solar cells on flexible substrates," *Appl. Phys. Lett.* **93**(3), 033302 (2008).
196. S.-B. Rim et al., "An effective light trapping configuration for thin-film solar cells," *Appl. Phys. Lett.* **91**(24), 243501 (2007).
197. K. Tvingstedt et al., "Trapping light with micro lenses in thin film organic photovoltaic cells," *Opt. Express* **16**(26), 21608 (2008).
198. K. Tvingstedt, Z. Tang, and O. Inganäs, "Light trapping with total internal reflection and transparent electrodes in organic photovoltaic devices," *Appl. Phys. Lett.* **101**(16), 163902 (2012).
199. L. Stolz Roman et al., "Trapping light in polymer photodiodes with soft embossed gratings," *Adv. Mater.* **12**(3), 189–195 (2000).
200. M. Takakuwa et al., "Nanograting structured ultrathin substrate for ultraflexible organic photovoltaics," *Small Methods* **4**(3), 1900762 (2020).
201. B. Lipovsek, J. Krc, and M. Topic, "Optimization of microtextured light-management films for enhanced light trapping in organic solar cells under perpendicular and oblique illumination conditions," *IEEE J. Photovoltaics* **4**(2), 639–646 (2014).
202. B. Lipovsek, J. Krc, and M. Topic, "Microtextured light-management foils and their optimization for planar organic and perovskite solar cells," *IEEE J. Photovoltaics* **8**(3), 783–792 (2018).

203. J. A. Mayer et al., "Self-contained optical enhancement film for printed photovoltaics," *Sol. Energy Mater. Sol. Cells* **163**, 51–57 (2017).
204. J. A. Mayer et al., "Optical enhancement of a printed organic tandem solar cell using diffractive nanostructures," *Opt. Express* **26**(6), A240 (2018).
205. M. Merkel, J. Imbrock, and C. Denz, "Diffraction-optimized aperiodic surface structures for enhanced current density in organic solar cells," *Opt. Express* **30**(20), 36678 (2022).
206. M. Merkel, T. Schemme, and C. Denz, "Aperiodic biomimetic Vogel spirals as diffractive optical elements for tailored light distribution in functional polymer layers," *J. Opt.* **23**(6), 065401 (2021).
207. M. Parchine et al., "Large area colloidal photonic crystals for light trapping in flexible organic photovoltaic modules applied using a roll-to-roll Langmuir-Blodgett method," *Sol. Energy Mater. Sol. Cells* **185**, 158–165 (2018).
208. B. P. Rand, P. Peumans, and S. R. Forrest, "Long-range absorption enhancement in organic tandem thin-film solar cells containing silver nanoclusters," *J. Appl. Phys.* **96**(12), 7519–7526 (2004).
209. Y.-F. Li et al., "Plasmon-enhanced organic and perovskite solar cells with metal nanoparticles," *Nanophotonics* **9**(10), 3111–3133 (2020).
210. J.-Y. Lee and P. Peumans, "The origin of enhanced optical absorption in solar cells with metal nanoparticles embedded in the active layer," *Opt. Express* **18**(10), 10078 (2010).
211. S. Liu et al., "A review on plasmonic nanostructures for efficiency enhancement of organic solar cells," *Mater. Today Phys.* **24**, 100680 (2022).
212. Z. Tang et al., "Semi-transparent tandem organic solar cells with 90% internal quantum efficiency," *Adv. Energy Mater.* **2**(12), 1467–1476 (2012).
213. Z. Tang et al., "Light trapping with dielectric scatterers in single- and tandem-junction organic solar cells," *Adv. Energy Mater.* **3**(12), 1606–1613 (2013).
214. A. Gadisa et al., "Transparent polymer cathode for organic photovoltaic devices," *Synth. Met.* **156**(16–17), 1102–1107 (2006).
215. J.-Y. Lee et al., "Semitransparent organic photovoltaic cells with laminated top electrode," *Nano Lett.* **10**(4), 1276–1279 (2010).
216. Z. Tang et al., "Fully-solution-processed organic solar cells with a highly efficient paper-based light trapping element," *J. Mater. Chem. A* **3**(48), 24289–24296 (2015).
217. S. Yu et al., "Nanoporous polymer reflectors for organic solar cells," *Energy Technol.* **10**(2), 2100676 (2022).
218. S. Esiner et al., "Quantification and validation of the efficiency enhancement reached by application of a retroreflective light trapping texture on a polymer solar cell," *Adv. Energy Mater.* **3**(8), 1013–1017 (2013).
219. A. B. Muñoz-García et al., "Dye-sensitized solar cells strike back," *Chem. Soc. Rev.* **50**(22), 12450–12550 (2021).
220. J. Briscoe and S. Dunn, "Dye-sensitized solar cells: the future of using earth-abundant elements in counter electrodes for dye-sensitized solar cells (Adv. Mater. 20/2016)," *Adv. Mater.* **28**(20), 3976–3976 (2016).
221. C. Dong et al., "Controlling interfacial recombination in aqueous dye-sensitized solar cells by octadecyltrichlorosilane surface treatment," *Angew. Chem. Int. Ed.* **53**(27), 6933–6937 (2014).
222. F. Fabregat-Santiago et al., "Electron transport and recombination in solid-state dye solar cell with spiro-OMeTAD as hole conductor," *J. Am. Chem. Soc.* **131**(2), 558–562 (2009).
223. J. W. Ondersma and T. W. Hamann, "Recombination and redox couples in dye-sensitized solar cells," *Coord. Chem. Rev.* **257**(9–10), 1533–1543 (2013).
224. I. Benesperi et al., "Dynamic dimer copper coordination redox shuttles," *Chem* **8**(2), 439–449 (2022).
225. M. Freitag et al., "Dye-sensitized solar cells for efficient power generation under ambient lighting," *Nat. Photonics* **11**(6), 372–378 (2017).
226. H. Michaels et al., "Emerging indoor photovoltaics for self-powered and self-aware IoT towards sustainable energy management," *Chem. Sci.* **14**(20), 5350–5360 (2023).
227. A. Dessì et al., "Thiazolo[5,4-*d*]thiazole-based organic sensitizers with improved spectral properties for application in greenhouse-integrated dye-sensitized solar cells," *Sustain. Energy Fuels* **4**(5), 2309–2321 (2020).
228. F. Grifoni et al., "Toward sustainable, colorless, and transparent photovoltaics: state of the art and perspectives for the development of selective near-infrared dye-sensitized solar cells," *Adv. Energy Mater.* **11**(43), 2101598 (2021).
229. Q. Huaulmé et al., "Photochromic dye-sensitized solar cells with light-driven adjustable optical transmission and power conversion efficiency," *Nat. Energy* **5**(6), 468–477 (2020).
230. E. F. Fernández et al., "Global energy assessment of the potential of photovoltaics for greenhouse farming," *Appl. Energy* **309**, 118474 (2022).
231. H. Michaels et al., "Dye-sensitized solar cells under ambient light powering machine learning: towards autonomous smart sensors for the internet of things," *Chem. Sci.* **11**(11), 2895–2906 (2020).

232. G. H. Morritt, H. Michaels, and M. Freitag, "Coordination polymers for emerging molecular devices," *Chem. Phys. Rev.* **3**(1), 011306 (2022).
233. E. Tanaka et al., "Synergy of co-sensitizers in a copper bipyridyl redox system for efficient and cost-effective dye-sensitized solar cells in solar and ambient light," *J. Mater. Chem. A* **8**(3), 1279–1287 (2020).
234. Y. Ren et al., "Hydroxamic acid pre-adsorption raises the efficiency of cosensitized solar cells," *Nature* **613**(7942), 60–65 (2023).
235. N. Flores-Diaz et al., "Progress of photocapacitors," *Chem. Rev.* **123**(15), 9327–9355 (2023).
236. B. Li, B. Hou, and G. A. J. Amaratunga, "Indoor photovoltaics, *The Next Big Trend* in solution-processed solar cells," *InfoMat* **3**(5), 445–459 (2021).
237. B. T. Muhammad et al., "Halide perovskite-based indoor photovoltaics: recent development and challenges," *Mater. Today Energy* **23**, 100907 (2022).
238. B. Yan et al., "Indoor photovoltaics awaken the world's first solar cells," *Sci. Adv.* **8**(49), eadc9923 (2022).
239. V. Pecunia, L. G. Occhipinti, and R. L. Z. Hoye, "Emerging indoor photovoltaic technologies for sustainable internet of things," *Adv. Energy Mater.* **11**(29), 2100698 (2021).
240. M. Freunek, M. Freunek, and L. M. Reindl, "Maximum efficiencies of indoor photovoltaic devices," *IEEE J. Photovoltaics* **3**(1), 59–64 (2013).
241. J. K. W. Ho, H. Yin, and S. K. So, "From 33% to 57% – an elevated potential of efficiency limit for indoor photovoltaics," *J. Mater. Chem. A* **8**(4), 1717–1723 (2020).
242. G. Kim et al., "Transparent thin-film silicon solar cells for indoor light harvesting with conversion efficiencies of 36% without photodegradation," *ACS Appl. Mater. Interfaces* **12**(24), 27122–27130 (2020).
243. C. C. Chen et al., "Anthracene-bridged sensitizers for dye-sensitized solar cells with 37% efficiency under dim light (Adv. Energy Mater. 20/2022)," *Adv. Energy Mater.* **12**(20), 2270080 (2022).
244. C. Lee et al., "Over 30% efficient indoor organic photovoltaics enabled by morphological modification using two compatible non-fullerene acceptors," *Adv. Energy Mater.* **12**(22), 2200275 (2022).
245. X. He et al., "40.1% record low-light solar-cell efficiency by holistic trap-passivation using micrometer-thick perovskite film," *Adv. Mater.* **33**(27), 2100770 (2021).
246. B. H. Hamadani, "Understanding photovoltaic energy losses under indoor lighting conditions," *Appl. Phys. Lett.* **117**(4), 043904 (2020).
247. J. Lovering et al., "Land-use intensity of electricity production and tomorrow's energy landscape," *PLoS One* **17**(7), e0270155 (2022).
248. S. Nonhebel, "Renewable energy and food supply: will there be enough land?" *Renew. Sustain. Energy Rev.* **9**(2), 191–201 (2005).
249. M. Pogson, A. Hastings, and P. Smith, "How does bioenergy compare with other land-based renewable energy sources globally?" *GCB Bioenergy* **5**(5), 513–524 (2013).
250. H. Stevens, "We need an area the size of Texas for wind and solar. Here's how to halve it," *The Washington Post*, 10 May 2023, https://www.washingtonpost.com/climate-environment/interactive/2023/renewable-energy-land-use-wind-solar/ (accessed October 2023).
251. E. Rosen, "As demand for green energy grows, solar farms face local resistance," *The New York Times*, 2 November 2021, https://www.nytimes.com/2021/11/02/business/solar-farms-resistance.html (accessed October 2023).
252. M. Unger and T. Lakes, "Land use conflicts and synergies on agricultural land in Brandenburg, Germany," *Sustainability* **15**(5), 4546 (2023).
253. A. Goetzberger, "Kartoffeln unter dem Kollektor," *Sonnenenergie* **3**, 19–22 (1981).
254. M. Wagner et al., "Agrivoltaics: the environmental impacts of combining food crop cultivation and solar energy generation," *Agronomy* **13**(2), 299 (2023).
255. A. Klokov et al., "A mini-review of current activities and future trends in agrivoltaics," *Energies*, **16**(7), 3009 (2023).
256. L. La Notte et al., "Hybrid and organic photovoltaics for greenhouse applications," *Appl. Energy* **278**, 115582 (2020).
257. L. Lu et al., "Comprehensive review on the application of inorganic and organic photovoltaics as greenhouse shading materials," *Sustain. Energy Technol. Assess.* **52**, 102077 (2022).
258. R. Waller et al., "Evaluating the performance of flexible, semi-transparent large-area organic photovoltaic arrays deployed on a greenhouse," *AgriEngineering* **4**(4), 969–992 (2022).
259. M. Charles et al., "Emergent molecular traits of lettuce and tomato grown under wavelength-selective solar cells," *Front. Plant. Sci.* **14**, 1087707 (2023).
260. B. Park et al., "Synthesis of a halogenated low bandgap polymeric donor for semi-transparent and near-infrared organic solar cells," *Org. Electron.* **113**, 106717 (2023).
261. S. S. Dipta et al., "Estimating the potential for semitransparent organic solar cells in agrophotovoltaic greenhouses," *Appl. Energy* **328**, 120208 (2022).
262. R. Meitzner, U. S. Schubert, and H. Hoppe, "Agrivoltaics—the perfect fit for the future of organic photovoltaics," *Adv. Energy Mater.* **11**(1), 2002551 (2021).

263. E. Ravishankar et al., "Organic solar powered greenhouse performance optimization and global economic opportunity," *Energy Environ. Sci.* **15**(4), 1659–1671 (2022).
264. C. J. M. Emmott et al., "Organic photovoltaic greenhouses: a unique application for semi-transparent PV?" *Energy Environ. Sci.* **8**(4), 1317–1328 (2015).
265. X. Rodríguez-Martínez et al., "Laminated organic photovoltaic modules for agrivoltaics and beyond: an outdoor stability study of all-polymer and polymer: small molecule blends," *Adv. Funct. Mater.* **33**(10), 2213220 (2023).
266. R. E. Smalley, "Future global energy prosperity: the terawatt challenge," *MRS Bull.* **30**(6), 412–417 (2005).
267. V. Romano et al., "Advances in perovskites for photovoltaic applications in space," *ACS Energy Lett.* **7**(8), 2490–2514 (2022).
268. A. W. Y. Ho-Baillie et al., "Deployment opportunities for space photovoltaics and the prospects for perovskite solar cells," *Adv. Mater. Technol.* **7**(3), 2101059 (2022).
269. J. J. Berry et al., "Perovskite photovoltaics: the path to a printable terawatt-scale technology," *ACS Energy Lett.* **2**(11), 2540–2544 (2017).
270. L. McMillon-Brown, J. M. Luther, and T. J. Peshek, "What would it take to manufacture perovskite solar cells in space?" *ACS Energy Lett.* **7**(3), 1040–1042 (2022).
271. I. Cardinaletti et al., "Organic and perovskite solar cells for space applications," *Sol. Energy Mater. Sol. Cells* **182**, 121–127 (2018).
272. L. K. Reb et al., "Perovskite and organic solar cells on a rocket flight," *Joule* **4**(9), 1880–1892 (2020).
273. A. R. Kirmani et al., "Countdown to perovskite space launch: guidelines to performing relevant radiation-hardness experiments," *Joule* **6**(5), 1015–1031 (2022).
274. A. R. Kirmani et al., "Metal oxide barrier layers for terrestrial and space perovskite photovoltaics," *Nat. Energy* **8**(2), 191–202 (2023).
275. N. Y. Nia, "Barrier layer for space," *Nat. Energy* **8**(2), 117–118 (2023).
276. R. T. Ross and A. J. Nozik, "Efficiency of hot-carrier solar energy converters," *J. Appl. Phys.* **53**(5), 3813–3818 (1982).
277. W. Shockley and H. J. Queisser, "Detailed balance limit of efficiency of *p-n* junction solar cells," *J. Appl. Phys.* **32**(3), 510–519 (1961).
278. H. Cotal et al., "III–V multijunction solar cells for concentrating photovoltaics," *Energy Environ. Sci.* **2**(2), 174–192 (2009).
279. G. Conibeer et al., "Progress on hot carrier cells," *Sol. Energy Mater. Sol. Cells* **93**(6–7), 713–719 (2009).
280. P. Lugli and S. M. Goodnick, "Nonequilibrium longitudinal-optical phonon effects in GaAs-AlGaAs quantum wells," *Phys. Rev. Lett.* **59**(6), 716–719 (1987).
281. Y. Yao and D. König, "Comparison of bulk material candidates for hot carrier absorber," *Sol. Energy Mater. Sol. Cells* **140**, 422–427 (2015).
282. P. Aliberti et al., "Investigation of theoretical efficiency limit of hot carriers solar cells with a bulk indium nitride absorber," *J. Appl. Phys.* **108**(9), 094507 (2010).
283. L. Lindsay, D. A. Broido, and T. L. Reinecke, "*Ab initio* thermal transport in compound semiconductors," *Phys. Rev. B* **87**(16), 165201 (2013).
284. S. Chung et al., "Nanosecond long excited state lifetimes observed in hafnium nitride," *Sol. Energy Mater. Sol. Cells* **169**, 13–18 (2017).
285. H. Esmaielpour et al., "Hot carrier relaxation and inhibited thermalization in superlattice heterostructures: the potential for phonon management," *Appl. Phys. Lett.* **118**(21), 213902 (2021).
286. J. Garg and I. R. Sellers, "Phonon linewidths in InAs/AlSb superlattices derived from first-principles—application towards quantum well hot carrier solar cells," *Semicond. Sci. Technol.* **35**(4), 044001 (2020).
287. L. C. Hirst et al., "Hot carriers in quantum wells for photovoltaic efficiency enhancement," *IEEE J. Photovoltaics* **4**(1), 244–252 (2014).
288. A. Le Bris et al., "Thermalisation rate study of GaSb-based heterostructures by continuous wave photoluminescence and their potential as hot carrier solar cell absorbers," *Energy Environ. Sci.* **5**(3), 6225 (2012).
289. J. Tang et al., "Effects of localization on hot carriers in InAs/$AlAs_xSb_{1-x}$ quantum wells," *Appl. Phys. Lett.* **106**(6), 061902 (2015).
290. Y. Rosenwaks et al., "Hot-carrier cooling in GaAs: quantum wells versus bulk," *Phys. Rev. B* **48**(19), 14675–14678 (1993).
291. J. Shah, "Hot carriers in quasi-2-D polar semiconductors," *IEEE J. Quantum Electron.* **22**(9), 1728–1743 (1986).
292. J. Shah et al., "Energy-loss rates for hot electrons and holes in GaAs quantum wells," *Phys. Rev. Lett.* **54**(18), 2045–2048 (1985).
293. L. C. Hirst et al., "Experimental demonstration of hot-carrier photo-current in an InGaAs quantum well solar cell," *Appl. Phys. Lett.* **104**(23), 231115 (2014).

294. J. Rodière et al., "Experimental evidence of hot carriers solar cell operation in multi-quantum wells heterostructures," *Appl. Phys. Lett.* **106**(18), 183901 (2015).
295. D.-T. Nguyen et al., "Quantitative experimental assessment of hot carrier-enhanced solar cells at room temperature," *Nat. Energy* **3**(3), 236–242 (2018).
296. J. A. R. Dimmock et al., "Demonstration of a hot-carrier photovoltaic cell: demonstration of a hot-carrier photovoltaic cell," *Prog. Photovoltaics Res. Appl.* **22**(2), 151–160 (2014).
297. H. Esmaielpour et al., "Exploiting intervalley scattering to harness hot carriers in III–V solar cells," *Nat. Energy* **5**(4), 336–343 (2020).
298. V. R. Whiteside et al., "The role of intervalley phonons in hot carrier transfer and extraction in type-II InAs/AlAsSb quantum-well solar cells," *Semicond. Sci. Technol.* **34**(9), 094001 (2019).
299. D. K. Ferry, "In search of a true hot carrier solar cell," *Semicond. Sci. Technol.* **34**(4), 044001 (2019).
300. F. Meinardi et al., "Highly efficient large-area colourless luminescent solar concentrators using heavy-metal-free colloidal quantum dots," *Nat. Nanotechnol.* **10**(10), 878–885 (2015).
301. W. G. J. H. M. Van Sark, "Luminescent solar concentrators – a low cost photovoltaics alternative," *Renew. Energy* **49**, 207–210 (2013).
302. M. Buffa et al., "Dye-doped polysiloxane rubbers for luminescent solar concentrator systems," *Sol. Energy Mater. Sol. Cells* **103**, 114–118 (2012).
303. S. M. El-Bashir, "Enhanced fluorescence polarization of fluorescent polycarbonate/zirconia nanocomposites for second generation luminescent solar concentrators," *Renew. Energy* **115**, 269–275 (2018).
304. A. Reinders et al., "Luminescent solar concentrator photovoltaic designs," *Jpn. J. Appl. Phys.* **57**(8S3), 08RD10 (2018).
305. B. C. Rowan, L. R. Wilson, and B. S. Richards, "Advanced material concepts for luminescent solar concentrators," *IEEE J. Sel. Top. Quantum Electron.* **14**(5), 1312–1322 (2008).
306. *Third Generation Photovoltaics*, Springer Berlin Heidelberg (2006).
307. A. A Martí, *Next Generation Photovoltaics: High Efficiency through Full Spectrum Utilization*, 1st ed., CRC Press (2003).
308. A. Goetzberger, "Fluorescent solar energy collectors: operating conditions with diffuse light," *Appl. Phys.* **16**(4), 399–404 (1978).
309. W. H. Weber and J. Lambe, "Luminescent greenhouse collector for solar radiation," *Appl. Opt.* **15**(10), 2299 (1976).
310. E. Yablonovitch, "Thermodynamics of the fluorescent planar concentrator," *J. Opt. Soc. Am.* **70**(11), 1362 (1980).
311. X. Wang and A. Barnett, "The evolving value of photovoltaic module efficiency," *Appl. Sci.* **9**(6), 1227 (2019).
312. M. G. Debije and V. A. Rajkumar, "Direct versus indirect illumination of a prototype luminescent solar concentrator," *Sol. Energy* **122**, 334–340 (2015).
313. A. Reinders, *Designing with Photovoltaics*, CRC Press (2020).
314. P. Della Sala et al., "First demonstration of the use of very large Stokes shift cycloparaphenylenes as promising organic luminophores for transparent luminescent solar concentrators," *Chem. Commun.* **55**(21), 3160–3163 (2019).
315. Y. El Mouedden et al., "A cost-effective, long-lifetime efficient organic luminescent solar concentrator," *J. Appl. Phys.* **118**(1), 015502 (2015).
316. Y. Li et al., "A structurally modified perylene dye for efficient luminescent solar concentrators," *Sol. Energy* **136**, 668–674 (2016).
317. A. Sanguineti et al., "High stokes shift perylene dyes for luminescent solar concentrators," *Chem. Commun.* **49**(16), 1618 (2013).
318. V. I. Klimov et al., "Quality factor of luminescent solar concentrators and practical concentration limits attainable with semiconductor quantum dots," *ACS Photonics* **3**(6), 1138–1148 (2016).
319. P. Moraitis, R. E. I. Schropp, and W. G. J. H. M. Van Sark, "Nanoparticles for luminescent solar concentrators - a review," *Opt. Mater.* **84**, 636–645 (2018).
320. F. Purcell-Milton and Y. K. Gun'ko, "Quantum dots for luminescent solar concentrators," *J. Mater. Chem.* **22**(33), 16687 (2012).
321. K. Wu, H. Li, and V. I. Klimov, "Tandem luminescent solar concentrators based on engineered quantum dots," *Nat. Photonics* **12**(2), 105–110 (2018).
322. Y. Zhou et al., "Harnessing the properties of colloidal quantum dots in luminescent solar concentrators," *Chem. Soc. Rev.* **47**(15), 5866–5890 (2018).
323. V. T. Freitas et al., "Eu^{3+} -based bridged silsesquioxanes for transparent luminescent solar concentrators," *ACS Appl. Mater. Interfaces* **7**(16), 8770–8778 (2015).
324. A. Frias et al., "Transparent luminescent solar concentrators using Ln3+-based ionosilicas towards photovoltaic windows," *Energies* **12**(3), 451 (2019).

325. J. Liu et al., "Preparation of cerium modified titanium dioxide nanoparticles and investigation of their visible light photocatalytic performance," *Int. J. Photoenergy* **2014**, 695679 (2014).
326. G. V. Shcherbatyuk et al., "Viability of using near infrared PbS quantum dots as active materials in luminescent solar concentrators," *Appl. Phys. Lett.* **96**(19), 191901 (2010).
327. Y. Zhou et al., "Near infrared, highly efficient luminescent solar concentrators," *Adv. Energy Mater.* **6**(11), 1501913 (2016).
328. M. R. Bergren et al., "High-performance $CuInS_2$ quantum dot laminated glass luminescent solar concentrators for windows," *ACS Energy Lett.* **3**(3), 520–525 (2018).
329. K. E. Knowles et al., "Bright $CuInS_2$/CdS nanocrystal phosphors for high-gain full-spectrum luminescent solar concentrators," *Chem. Commun.* **51**(44), 9129–9132 (2015).
330. B. Zhang et al., "Aggregation-induced emission-mediated spectral downconversion in luminescent solar concentrators," *Mater. Chem. Front.* **2**(3), 615–619 (2018).
331. F. Meinardi et al., "Doped halide perovskite nanocrystals for reabsorption-free luminescent solar concentrators," *ACS Energy Lett.* **2**(10), 2368–2377 (2017).
332. O. M. Ten Kate, K. W. Krämer, and E. Van Der Kolk, "Efficient luminescent solar concentrators based on self-absorption free, Tm2+ doped halides," *Sol. Energy Mater. Sol. Cells* **140**, 115–120 (2015).
333. G. Griffini, "Host matrix materials for luminescent solar concentrators: recent achievements and forthcoming challenges," *Front. Mater.* **6**, 29 (2019).
334. M. J. Kastelijn, C. W. M. Bastiaansen, and M. G. Debije, "Influence of waveguide material on light emission in luminescent solar concentrators," *Opt. Mater.* **31**(11), 1720–1722 (2009).
335. W. Chen et al., "Heavy metal free nanocrystals with near infrared emission applying in luminescent solar concentrator," *Solar RRL* **1**(6), 1700041 (2017).
336. A. Reinders, M. G. Debije, and A. Rosemann, "Measured efficiency of a luminescent solar concentrator PV module called leaf roof," *IEEE J. Photovoltaics* **7**(6), 1663–1666 (2017).
337. A. Sanguineti et al., "NIR emitting ytterbium chelates for colourless luminescent solar concentrators," *Phys. Chem. Chem. Phys.* **14**(18), 6452 (2012).
338. M. G. Debije et al., "Measured surface loss from luminescent solar concentrator waveguides," *Appl. Opt.* **47**(36), 6763 (2008).
339. M. Kennedy et al., "Large Stokes shift downshifting Eu(III) films as efficiency enhancing UV blocking layers for dye sensitized solar cells: Eu(III) films as efficiency enhancing UV blocking layers for dye sensitized solar cells," *Physica Status Solidi (A)*, **212**(1), 203–210 (2015).
340. M. Rafiee et al., "An overview of various configurations of Luminescent Solar Concentrators for photovoltaic applications," *Opt. Mater.* **91**, 212–227 (2019).
341. M. G. Debije and P. P. C. Verbunt, "Thirty years of luminescent solar concentrator research: solar energy for the built environment," *Adv. Energy Mater.* **2**(1), 12–35 (2012).
342. J. C. Goldschmidt et al., "Increasing the efficiency of fluorescent concentrator systems," *Sol. Energy Mater. Sol. Cells* **93**(2), 176–182 (2009).
343. W. G. J. H. M. Van Sark et al., "Luminescent solar concentrators - a review of recent results," *Opt. Express* **16**(26), 21773 (2008).
344. M. Kanellis et al., "The solar noise barrier project: 1. Effect of incident light orientation on the performance of a large-scale luminescent solar concentrator noise barrier," *Renew. Energy* **103**, 647–652 (2017).
345. R. López-Martín and L. Valenzuela, "Optical efficiency measurement of solar receiver tubes: a testbed and case studies," *Case Stud. Thermal Eng.* **12**, 414–422 (2018).
346. B. Vishwanathan et al., "A comparison of performance of flat and bent photovoltaic luminescent solar concentrators," *Sol. Energy* **112**, 120–127 (2015).
347. R. H. Inman et al., "Cylindrical luminescent solar concentrators with near-infrared quantum dots," *Opt. Express* **19**(24), 24308 (2011).
348. J. J. H. Videira, E. Bilotti, and A. J. Chatten, "Cylindrical array luminescent solar concentrators: performance boosts by geometric effects," *Opt. Express* **24**(14), A1188 (2016).
349. N. Aste et al., "Performance analysis of a large-area luminescent solar concentrator module," *Renew. Energy* **76**, 330–337 (2015).
350. M. J. Currie et al., "High-efficiency organic solar concentrators for photovoltaics," *Science* **321**(5886), 226–228 (2008).
351. N. D. Bronstein et al., "Quantum dot luminescent concentrator cavity exhibiting 30-fold concentration," *ACS Photonics* **2**(11), 1576–1583 (2015).
352. I. Coropceanu and M. G. Bawendi, "Core/shell quantum dot based luminescent solar concentrators with reduced reabsorption and enhanced efficiency," *Nano Lett.* **14**(7), 4097–4101 (2014).
353. S. M. El-Bashir, F. M. Barakat, and M. S. AlSalhi, "Metal-enhanced fluorescence of mixed Coumarin dyes by silver and gold nanoparticles: towards plasmonic thin-film luminescent solar concentrator," *J. Lumin.* **143**, 43–49 (2013).

354. S. M. El-Bashir, F. M. Barakat, and M. S. AlSalhi, "Double layered plasmonic thin-film luminescent solar concentrators based on polycarbonate supports," *Renew. Energy* **63**, 642–649 (2014).
355. D. J. Farrell et al., "Using amorphous silicon solar cells to boost the viability of luminescent solar concentrators," *Physica Status Solidi C* **7**(3–4), 1045–1048 (2010).
356. C. Tummeltshammer et al., "On the ability of Förster resonance energy transfer to enhance luminescent solar concentrator efficiency," *Nano Energy* **32**, 263–270 (2017).
357. S.-J. Ha et al., "Upconversion-assisted dual-band luminescent solar concentrator coupled for high power conversion efficiency photovoltaic systems," *ACS Photonics* **5**(9), 3621–3627 (2018).
358. K. Kim et al., "Photon upconversion-assisted dual-band luminescence solar concentrators coupled with perovskite solar cells for highly efficient semi-transparent photovoltaic systems," *Nanoscale* **12**(23), 12426–12431 (2020).
359. L. H. Slooff et al., "A luminescent solar concentrator with 7.1% power conversion efficiency: carbon nanotube/epoxy resin composites using a block copolymer as a dispersing agent," *Physica Status Solidi (RRL) - Rapid Res. Lett.* **2**(6), 257–259 (2008).
360. M. G. Debije, R. C. Evans, and G. Griffini, "Laboratory protocols for measuring and reporting the performance of luminescent solar concentrators," *Energy Environ. Sci.* **14**(1), 293–301 (2021).
361. C. Yang, D. Liu, and R. R. Lunt, "How to accurately report transparent luminescent solar concentrators," *Joule* **3**(12), 2871–2876 (2019).
362. T. Warner, K. P. Ghiggino, and G. Rosengarten, "A critical analysis of luminescent solar concentrator terminology and efficiency results," *Sol. Energy* **246**, 119–140 (2022).
363. J. Keil et al., "Evaluating tandem luminscent solar concentrator performance based on luminophore selection," in *IEEE 48th Photovoltaics Spec. Conf. (PVSC)*, IEEE, Fort Lauderdale, Florida (2021).
364. R. Mazzaro and A. Vomiero, "The renaissance of luminescent solar concentrators: the role of inorganic nanomaterials," *Adv. Energy Mater.* **8**(33), 1801903 (2018).
365. L. R. Bradshaw et al., "Nanocrystals for luminescent solar concentrators," *Nano Lett.* **15**(2), 1315–1323 (2015).
366. N. D. Bronstein et al., "Luminescent solar concentration with semiconductor nanorods and transfer-printed micro-silicon solar cells," *ACS Nano* **8**(1), 44–53 (2014).
367. S. K. E. Hill et al., "Poly(methyl methacrylate) films with high concentrations of silicon quantum dots for visibly transparent luminescent solar concentrators," *ACS Appl. Mater. Interfaces* **12**(4), 4572–4578 (2020).
368. S. K. E. Hill et al., "Silicon quantum dot–poly(methyl methacrylate) nanocomposites with reduced light scattering for luminescent solar concentrators," *ACS Photonics* **6**(1), 170–180 (2019).
369. R. Mazzaro et al., "Hybrid Silicon nanocrystals for color-neutral and transparent luminescent solar concentrators," *ACS Photonics* **6**(9), 2303–2311 (2019).
370. Y. Li et al., "N-doped carbon-dots for luminescent solar concentrators," *J. Mater. Chem. A* **5**(40), 21452–21459 (2017).
371. F. Meinardi et al., "Highly efficient luminescent solar concentrators based on earth-abundant indirect-bandgap silicon quantum dots," *Nat. Photonics* **11**(3), 177–185 (2017).
372. S. Mirershadi and S. Ahmadi-Kandjani, "Efficient thin luminescent solar concentrator based on organo-metal halide perovskite," *Dyes Pigm.* **120**, 15–21 (2015).
373. K. Nikolaidou et al., "Hybrid perovskite thin films as highly efficient luminescent solar concentrators," *Adv. Opt. Mater.* **4**(12), 2126–2132 (2016).
374. H. Zhao et al., "Perovskite quantum dots integrated in large-area luminescent solar concentrators," *Nano Energy* **37**, 214–223 (2017).
375. C. Li et al., "Large Stokes shift and high efficiency luminescent solar concentrator incorporated with CuInS2/ZnS quantum dots," *Sci. Rep.* **5**(1), 17777 (2015).
376. Y. Zhao et al., "Near-infrared harvesting transparent luminescent solar concentrators," *Adv. Opt. Mater.* **2**(7), 606–611 (2014).
377. R. Connell et al., "CdSe/CdS–poly(cyclohexylethylene) thin film luminescent solar concentrators," *APL Mater.* **7**(10), 101123 (2019).
378. M. G. Debije et al., "Effect on the output of a luminescent solar concentrator on application of organic wavelength-selective mirrors," *Appl. Opt.* **49**(4), 745 (2010).
379. U. Rau, F. Einsele, and G. C. Glaeser, "Efficiency limits of photovoltaic fluorescent collectors," *Appl. Phys. Lett.* **87**(17), 171101 (2005).
380. R. Connell, C. Pinnell, and V. E. Ferry, "Designing spectrally-selective mirrors for use in luminescent solar concentrators," *J. Opt.* **20**(2), 024009 (2018).
381. P. P. C. Verbunt et al., "Increased efficiency of luminescent solar concentrators after application of organic wavelength selective mirrors," *Opt. Express* **20**(S5), A655 (2012).
382. C. Yang et al., "Consensus statement: standardized reporting of power-producing luminescent solar concentrator performance," *Joule* **6**(1), 8–15 (2022).

383. I. Papakonstantinou, M. Portnoi, and M. G. Debije, "The hidden potential of luminescent solar concentrators," *Adv. Energy Mater.* **11**(3), 2002883 (2021).
384. C. Corrado et al., "Power generation study of luminescent solar concentrator greenhouse," *J. Renew. Sustain. Energy* **8**(4), 043502 (2016).
385. D. Hebert et al., "Luminescent quantum dot films improve light use efficiency and crop quality in greenhouse horticulture," *Front. Chem.* **10**, 988227 (2022).
386. J. Keil et al., "Bilayer luminescent solar concentrators with enhanced absorption and efficiency for agrivoltaic applications," *ACS Appl. Energy Mater.* **4**(12), 14102–14110 (2021).
387. L. Shen et al., "Increasing greenhouse production by spectral-shifting and unidirectional light-extracting photonics," *Nat. Food* **2**(6), 434–441 (2021).
388. H. Li et al., "Doctor-blade deposition of quantum dots onto standard window glass for low-loss large-area luminescent solar concentrators," *Nat. Energy* **1**(12), 16157 (2016).
389. J. Wang et al., "Quantum dot-based luminescent solar concentrators fabricated through the ultrasonic spray-coating method," *ACS Appl. Mater. Interfaces* **14**(36), 41013–41021 (2022).
390. M. A. Hernández-Rodríguez et al., "A perspective on sustainable luminescent solar concentrators," *J. Appl. Phys.* **131**(14), 140901 (2022).
391. C. Yang et al., "Integration of near-infrared harvesting transparent luminescent solar concentrators onto arbitrary surfaces," *J. Lumin.* **210**, 239–246 (2019).
392. C. H. Henry, "Limiting efficiencies of ideal single and multiple energy gap terrestrial solar cells," *J. Appl. Phys.* **51**(8), 4494–4500 (1980).
393. E. D. Jackson, "Areas for improvement of the semiconductor solar energy converter," in *Trans. Conf. Use of Solar Energy*, Tucson, Arizona, p. 122 (1955).
394. A. G. Imenes and D. R. Mills, "Spectral beam splitting technology for increased conversion efficiency in solar concentrating systems: a review," *Sol. Energy Mater. Sol. Cells* **84**(1–4), 19–69 (2004).
395. A. Mojiri et al., "Spectral beam splitting for efficient conversion of solar energy—a review," *Renew. Sustain. Energy Rev.* **28**, 654–663 (2013).
396. J. D. McCambridge et al., "Compact spectrum splitting photovoltaic module with high efficiency," *Prog. Photovoltaics Res. Appl.* **19**(3), 352–360 (2011).
397. A. Polman and H. A. Atwater, "Photonic design principles for ultrahigh-efficiency photovoltaics," *Nat. Mater.* **11**(3), 174–177 (2012).
398. C. G. Stojanoff, "Engineering applications of HOEs manufactured with enhanced performance DCG films," *Proc. SPIE* **6316**, 613601 (2006).
399. D. Vincenzi et al., "Concentrating PV system based on spectral separation of solar radiation," *Physica Status Solidi (A)* **206**(2), 375–378 (2009).
400. Y. Wu et al., "Design of folded holographic spectrum-splitting photovoltaic system for direct and diffuse illumination conditions," *Proc. SPIE* **9175**, 91750G (2014).
401. N. Mohammad et al., "Enhancing photovoltaic output power by 3-band spectrum-splitting and concentration using a diffractive micro-optic," *Opt. Express* **22**(S6), A1519 (2014).
402. S. Vorndran et al., "Broadband Gerchberg-Saxton algorithm for freeform diffractive spectral filter design," *Opt. Express* **23**(24), A1512 (2015).
403. J. M. Russo et al., "Spectrum splitting metrics and effect of filter characteristics on photovoltaic system performance," *Opt. Express* **22**(S2), A528 (2014).
404. B. D. Chrysler, S. E. Shaheen, and R. K. Kostuk, "Lateral spectrum splitting system with perovskite photovoltaic cells," *J. Photonics Energy* **12**(2), 022206 (2022).
405. S. D. Vorndran et al., "Off-axis holographic lens spectrum-splitting photovoltaic system for direct and diffuse solar energy conversion," *Appl. Opt.* **55**(27), 7522 (2016).
406. D. Zhang et al., "Spectrum-splitting photovoltaic system using transmission holographic lenses," *J. Photonics Energy* **3**(1), 034597 (2013).
407. B. D. Chrysler and R. K. Kostuk, "Volume hologram replication system for spectrum-splitting photovoltaic applications," *Appl. Opt.* **57**(30), 8887 (2018).
408. A. D. Cronin et al., "Holographic CPV field tests at the Tucson Electric Power solar test yard," in *37th IEEE Photovoltaics Spec. Conf.*, IEEE, Seattle, Washington (2011).
409. B. D. Chrysler and R. K. Kostuk, "A comparison of spectrum-splitting configurations for high-efficiency photovoltaic systems with perovskite cells," *IEEE J. Photovoltaics* **12**(6), 1477–1486 (2022).
410. J. Werner, B. Niesen, and C. Ballif, "Perovskite/silicon tandem solar cells: marriage of convenience or true love story? – An overview," *Adv. Mater. Interfaces* **5**(1), 1700731 (2018).
411. G. A. Barron-Gafford et al., "Agrivoltaics provide mutual benefits across the food–energy–water nexus in drylands," *Nat. Sustain.* **2**(9), 848–855 (2019).
412. B. B. Jorgensen, Y. Cohen, and D. J. Des Marais, "Photosynthetic action spectra and adaptation to spectral light distribution in a benthic cyanobacterial mat," *Appl. Environ. Microbiol.* **53**(4), 879–886 (1987).

413. S. Vorndran et al., "Holographic diffraction-through-aperture spectrum splitting for increased hybrid solar energy conversion efficiency: holographic diffraction-through-aperture spectrum-splitting system," *Int. J. Energy Res.* **39**(3), 326–335 (2015).
414. SPIE, "Holograms increase solar energy yield," 2021, https://spie.org/news/holograms-increase-solar-energy-yield?SSO=1.
415. International Energy Agency (IEA), "The world needs more diverse solar panel supply chains to ensure a secure transition to net zero emissions," 2022, https://www.iea.org/news/the-world-needs-more-diverse-solar-panel-supply-chains-to-ensure-a-secure-transition-to-net-zero-emissions) (accessed 31 Jan. 2023).
416. DOE Solar Energy Technologies Office, *Federal Tax Credits for Solar Manufacturers* (2022).
417. Ultra Low-Carbon Solar Alliance, "South Korea is implementing carbon footprint assessment regulations for the PV market," 2021, https://ultralowcarbonsolar.org/blog/south-korea-implementing-carbon-footprint-assessment-regulations/.
418. A. Anctil, "Comparing the carbon footprint of monocrystalline silicon solar modules manufactured in China and the United States," in *IEEE 48th Photovoltaics Spec. Conf. (PVSC)*, IEEE, Fort Lauderdale, Florida (2021).
419. V. Fthenakis and E. Leccisi, "Updated sustainability status of crystalline silicon-based photovoltaic systems: life-cycle energy and environmental impact reduction trends," *Prog. Photovoltaics Res. Appl.* **29**(10), 1068–1077 (2021).
420. L. Yuan and A. Anctil, "Material use and life cycle impact of crystalline silicon PV modules over time," in *IEEE 49th Photovoltaics Spec. Conf. (PVSC)*, IEEE, Philadelphia (2022).
421. H. Zhang et al., "Green or not? Environmental challenges from photovoltaic technology," *Environ. Pollut.* **320**, 121066 (2023).
422. P. Nain and A. Kumar, "Understanding metal dissolution from solar photovoltaics in MSW leachate under standard waste characterization conditions for informing end-of-life photovoltaic waste management," *Waste Manage.* **123**, 97–110 (2021).
423. D. Sica et al., "Management of end-of-life photovoltaic panels as a step towards a circular economy," *Renew. Sustain. Energy Rev.* **82**, 2934–2945 (2018).
424. S. Mahmoudi, N. Huda, and M. Behnia, "Multi-levels of photovoltaic waste management: a holistic framework," *J. Cleaner Prod.* **294**, 126252 (2021).
425. L. Hocine and K. M. Samira, "Optimal PV panel's end-life assessment based on the supervision of their own aging evolution and waste management forecasting," *Sol. Energy* **191**, 227–234 (2019).

Annick Anctil is an associate professor in Civil and Environmental Engineering at Michigan State University (MSU), where she leads research on sustainable energy systems. She uses anticipatory lifecycle assessment to reduce the environmental impact of new technologies. She received an NSF CAREER award in 2021 to work on the impact of the solar photovoltaics industry in the US. At MSU, she teaches classes on sustainability and life cycle assessment of energy.

Meghan Beattie is a postdoctoral fellow with the SUNLAB in the School of Electrical Engineering and Computer Science at the University of Ottawa. She holds a PhD in Physics from the University of Ottawa (2021) and a BSc in Physics from Queen's University (2015). Her research interests include materials and devices for advanced photovoltaic energy conversion and the development of photovoltaic receivers for optical wireless and fiber power transmission.

Christopher Case began his career as Assistant Professor of Engineering at Brown University, followed by ten years at AT&T; Bell Laboratories. He also had ten years as Chief Technology and Scientific Officer with BOC, part of Linde, where he oversaw the global technology strategy and R&D; for the €8 billion business. He has helped companies large and small to manage their IP portfolios, broaden their scope of influence, and build successful and profitable businesses. Chris actively contributes to advancing the solar industry including serving as a board member of the European Solar Manufacturing Council and a Steering Committee member of the European Technology and Innovation Platform for Photovoltaics (ETIP-PV). Since 2021, he has been the President of the International Thin-Film Solar Industry Association (PVthin).

Aditya Chaudhary studied power engineering at National Power Training Institute, New Delhi, India, and graduated in 2014. Afterwards, he completed a master's degree in electrical sustainable energy from TU Delft, Delft, Netherlands, in 2017. His master thesis involved development of four terminal mechanically stacked a-SiOx/c-Si solar cells. From January 2018 to April 2022,

he worked at ISC Konstanz, Konstanz, Germany, as a PhD researcher. The topic of his work was screen-printed metallization of polysilicon/SiOx passivated contacts. After the completion of the project at ISC Konstanz he moved to ipv (University of Stuttgart), to work as a postdoc in the group headed by Dr. Stephanie Essig, developing perovskite/Silicon tandem solar cells.

Michael G. Debije is an associate professor in the Stimuli-responsive Functional Materials and Devices group at the TU Eindhoven. He has been working on the luminescent concentrator device for fifteen years as part of his research line of light control in the built environment. His other projects relate to the fabrication and study of environmentally responsive liquid crystal-based actuators for soft robotics.

Stephanie Essig is heading the high-efficiency solar cells group of Institute for Photovoltaics at the University of Stuttgart. Previously, she performed research on III-V/Si multi-junction, GaAs nanowire and CIGS thin-film solar cells at NREL in Colorado, EPFL in Switzerland, Sol Voltaics AB in Sweden, and ZSW in Germany. She holds an MPhys degree from Heriot-Watt University Edinburgh, a diploma in physics from Karlsruhe Institute of Technology, and a PhD from the University of Konstanz.

Vivian E. Ferry is an associate professor at the University of Minnesota in the Department of Chemical Engineering and Materials Science. She received her SB in chemistry from the University of Chicago, and her PhD from the California Institute of Technology, working with Prof. Harry Atwater. She was a postdoctoral fellow with Prof. Paul Alivisatos at Lawrence Berkeley National Laboratory. Her research interests include light management in photovoltaics, tunable metamaterials, and nanoscale chirality.

Karin Hinzer is a professor at the School of Electrical Engineering and Computer Science at the University of Ottawa and the University Research Chair in Photonic Devices for Energy. She has published >210 refereed papers, trained >190 highly qualified personnel, and her laboratory has spun-off three Canadian companies in the energy sector. Her research interests include new materials, high efficiency light sources and detectors, solar cells and modules, new electrical grid architectures and voltage converters.

Raymond K. Kostuk is a professor in the Department of Electrical and Computer Engineering and the Wyant College of Optical Sciences at the University of Arizona. He has published extensively on the application of holography and optics in PV systems and summarized many of these concepts in the SPIE Spotlight e-book Holographic Applications in Photovoltaic Energy-Conversion Processes. He is a fellow of Optica and SPIE.

Daniel Kirk completed his doctoral work in Oxford and working in industrial research at Dupont (metallization development) and Nexeon (Li-ion battery technology). He joined Oxford PV in 2014. Since 2015 he has been heavily involved in optimization of both perovskite and silicon cells for tandem applications. More recently he has focused on supporting the scaling up the technology to full-wafer scale at Oxford PV, as well as on optimization of the product for commercial realization in various markets.

Stephan Kube is Head of Marketing at Heliatek since 2019. He has more than ten years of experience in B2B marketing in the emerging international solar industry. Stephan has worked for the technology leaders Solar Frontier (CIGS) and now Heliatek (OPV), driving their brand awareness and business success.

Preeti Nain is a postdoctoral researcher in the Department of Civil and Environmental Engineering at Michigan State University. She received her PhD in Environmental Engineering from Indian Institute of Technology, Delhi, India. Her research focuses on different aspects of end-of-life solar photovoltaics. Her current interests include PFAS analysis in solar photovoltaics and life cycle assessment for PV repowering in the United States.

Angèle Reinders is a full professor in Design of Sustainable Energy Systems in the Energy Technology Group at the TU Eindhoven, and the Director of Solliance. She aims at an optimal integration of solar technologies in products, buildings and local infrastructures by design-driven research on these technologies. She simulates, prototypes and experimentally characterizes ,

among others, luminescent solar concentrator PV, BIPV and VIPV. She is a physicist with a track record in PV performance research.

Ifor D. W. Samuel is Professor of Physics at the University of St Andrews. He received his MA and PhD from the University of Cambridge, working on optical spectroscopy of organic semiconductors. In 2000, he moved to the University of St Andrews where he founded and leads the Organic Semiconductor Centre. His current work concerns the photophysics of organic semiconductor materials and devices. He is a fellow of the Royal Society of Edinburgh and of SPIE.

Wilfried van Sark is full professor "Integration of Photovoltaics" at the Copernicus Institute of Sustainable Development at Utrecht University. He is an experimental physicist by training (MSc/PhD), and has over 40 years of experience in photovoltaics. He worked on various material systems such as crystalline and thin film silicon and III-V solar cells, both experimentally and theoretically. Currently he focuses on building and grid integration focusing on luminescent solar concentrators and bidirectional charging of electric vehicles.

Hele Savin received the DSc (Tech) degree in semiconductor technology from the Helsinki University of Technology, Espoo, Finland, in 2005. She is currently a professor with the Department of Electronics and Nanoengineering, Aalto University, Espoo. Her current research interests focus on photonic devices, especially photon detection and solar cells, nanofabrication methods, and defect engineering in group-IV materials.

Sean E. Shaheen is a professor of electrical, computer, and energy engineering; professor by courtesy of physics; and fellow of the Renewable and Sustainable Energy Institute at the University of Colorado Boulder. He obtained his BS and PhD in physics from Carnegie Mellon University (1991) and the University of Arizona (1999), respectively. His research interests include organic and hybrid photovoltaics, photonics, and neuromorphic/bio-inspired computing. He is currently the editor-in-chief of the *Journal of Photonics for Energy.*

Fatima Toor is an endowed chair and associate professor in the Department of Electrical and Computer Engineering at the University of Iowa. She earned her PhD in electrical engineering from Princeton University in 2009 and was a postdoctoral researcher in the silicon PV group at NREL from 2010 to 2011. Her team's current research involves the development of semiconductor optoelectronic devices for applications in the health, environment, and energy industries. She is a senior member of SPIE.

Ville Vähänissi received the DSc (Tech) degree in semiconductor technology from Aalto University, Espoo, Finland, in 2016. He is currently working as a staff scientist at the Department of Electronics and Nanoengineering, School of Electrical Engineering, Aalto University. His research interests include defect engineering in silicon, especially photovoltaics, as well as atomic layer deposition and nanopatterning, and their various applications in semiconductor devices.

Emily L. Warren is a senior scientist and group manager at the National Renewable Energy Laboratory where she leads a core program on the development of high efficiency tandem solar cells. She received her PhD from the California Institute of Technology, an MPhil from the University of Cambridge in Engineering for Sustainable Development, and a BS in Chemical Engineering from Cornell University. Her research interests include the development and modeling of tandem solar cells and modules, photoelectrochemical production of solar fuels, and heteroepitaxy of III-V semiconductors.

Han Young Woo received his PhD degree in chemistry from the Korea Advanced Institute of Science and Technology (KAIST), Republic of Korea, in 1999. After postdoctoral training at the University of California, Santa Barbara (UCSB), USA, he joined the Pusan National University as an assistant professor. In 2015, he moved to Korea University where he is currently a professor in the Department of Chemistry. His current research focuses on conjugated polymers and polyelectrolytes for applications in organic optoelectronic devices.

Gang Xiong currently is the Director of First Solar California Technology Center, managing the site operation and research programs such as CdTe, perovskite, and tandem. He joined First Solar

in 2007 and has since worked on cell/module research and manufacturing implementation. Representing First Solar, Dr. Xiong also serves at a few industrial advisory boards (IABs), including as the IAB chair of US Manufacturing of Advanced Cadmium Telluride Photovoltaics, the former IAB chair of Solar Powered Future 2050 under the National Science Foundation, and the IAB member of US Manufacturing of Advanced Perovskite.

Xitong Zhu is a PhD candidate in the Energy Technology Group at TU Eindhoven. He has been focused on ray-tracing simulation of luminescent solar concentrator photovoltaics (LSC PV). Currently, he focuses on different geometry LSC PV devices and the application feasibility of LSCs for BIPV. He is devoted to research on the applications of sustainable energy.

Biographies of the other authors are not available.